Supporting Information

Homoleptic complexes of titanium(IV) fused with O^N^O Schiff Base derivatives: design, BSA-DNA interaction, molecular docking, DFT and cytotoxicity

Shivabasayya V Salimath[a], Kavita B Hiremath[a], Mahabarathi Subramaniyan[a], Arjita Ghosh[b], Evangeline Lawrence[b], Anbalagan Moorthy[b], Murugesh Shivashankar[a] and Madhvesh Pathak[a]*

[a]*Department of Chemistry, School of Advanced Sciences, Vellore Institute of Technology (VIT), Vellore, Tamil Nadu, India*

[b]*Department of Integrative Biology, School of Bioscience and Technology (SBST), Vellore Institute of Technology (VIT), Vellore, Tamil Nadu, India*

*Email: madhveshpathak@vit.ac.in   *ORCID iD: https://orcid.org/0000-0002-1567-6519

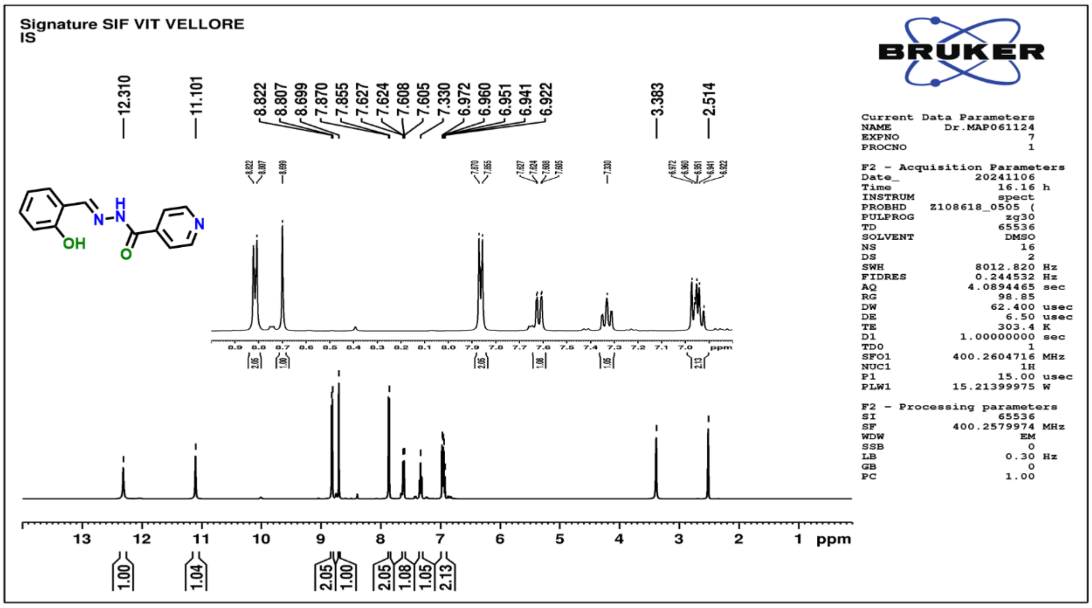

Figure.S1. ^{1}H NMR spectrum of ligand IS (400 MHz, DMSO-d_6)

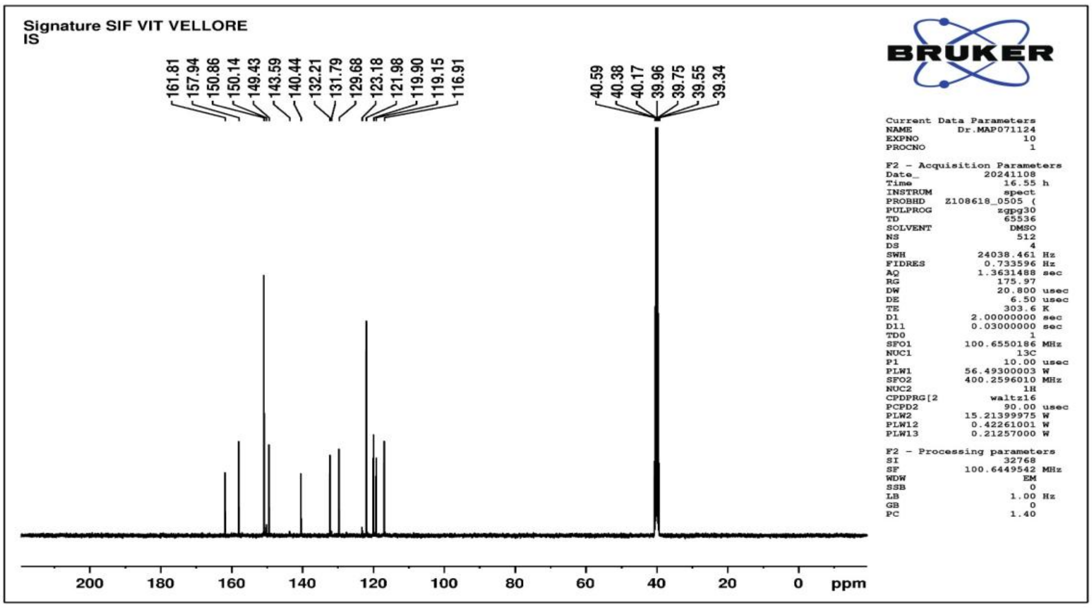

Figure.S2. ^{13}C NMR spectrum of ligand IS (400 MHz, DMSO-d_6)

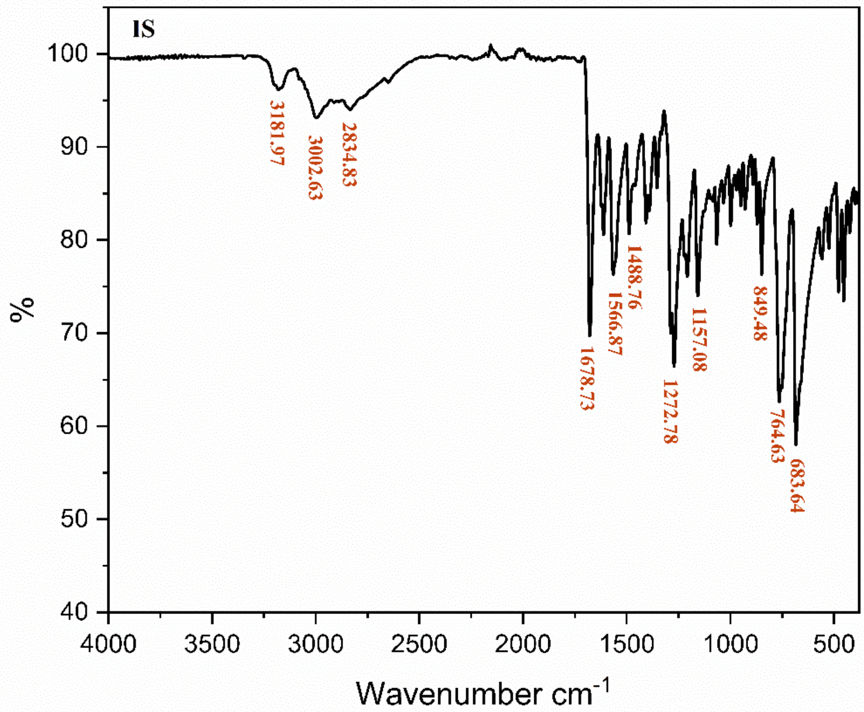

Figure.S3. FTIR spectrum of ligand IS (400 MHz, DMSO-d_6)

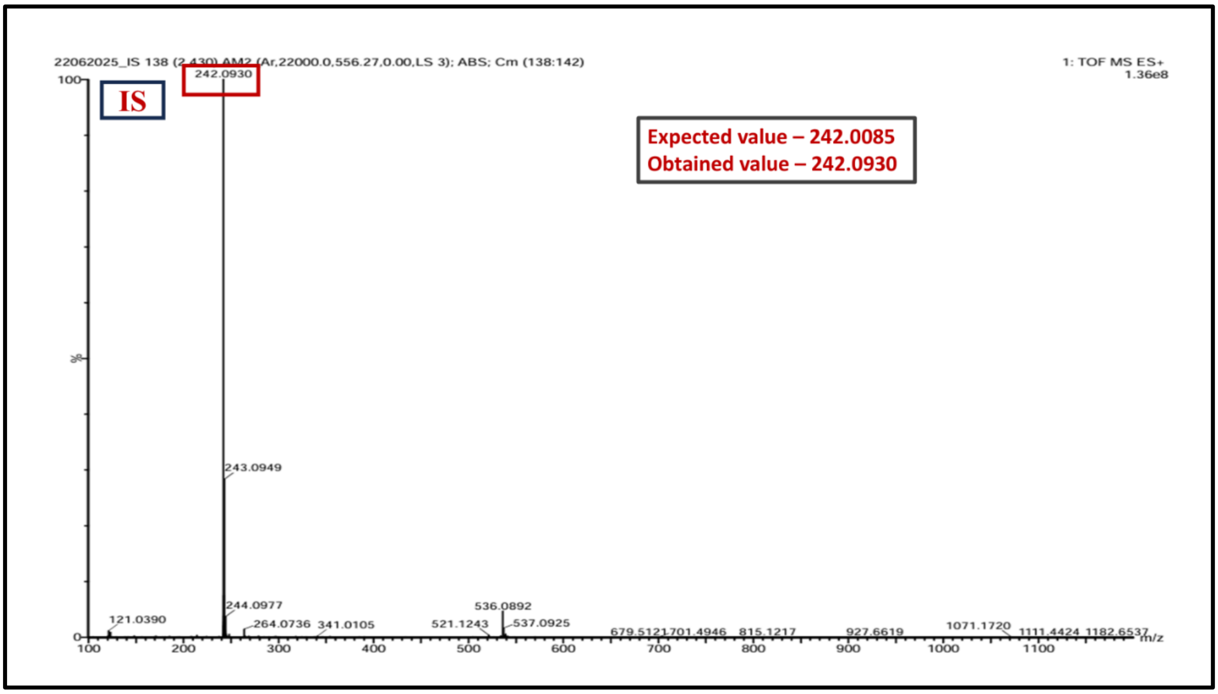

Figure.S4. ESI-MS spectrum of ligand IS

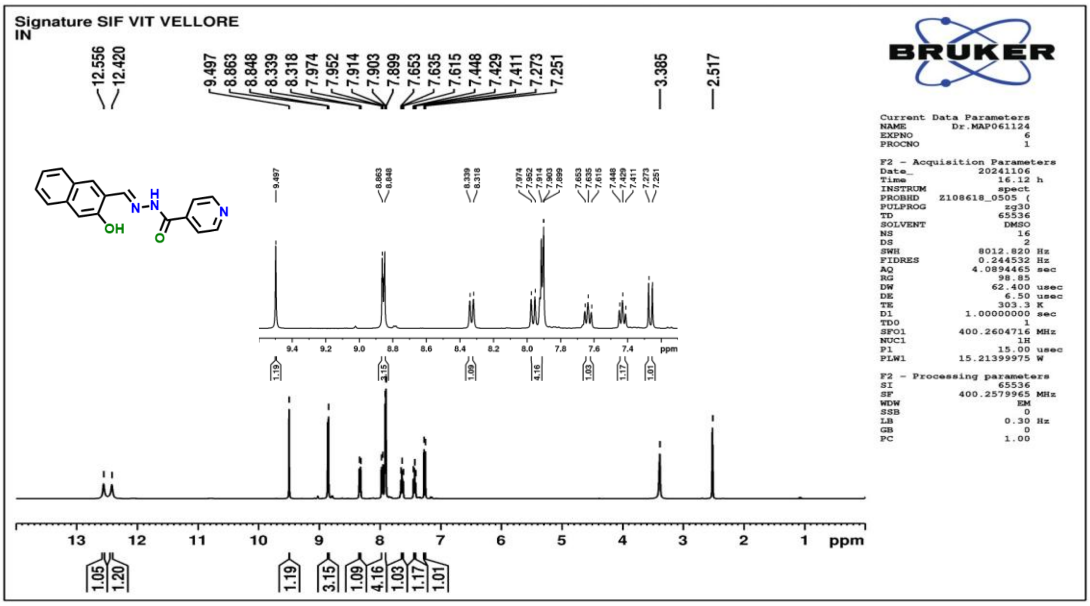

Figure.S5. ^{1}H NMR spectrum of ligand IN (400 MHz, DMSO-d$_6$)

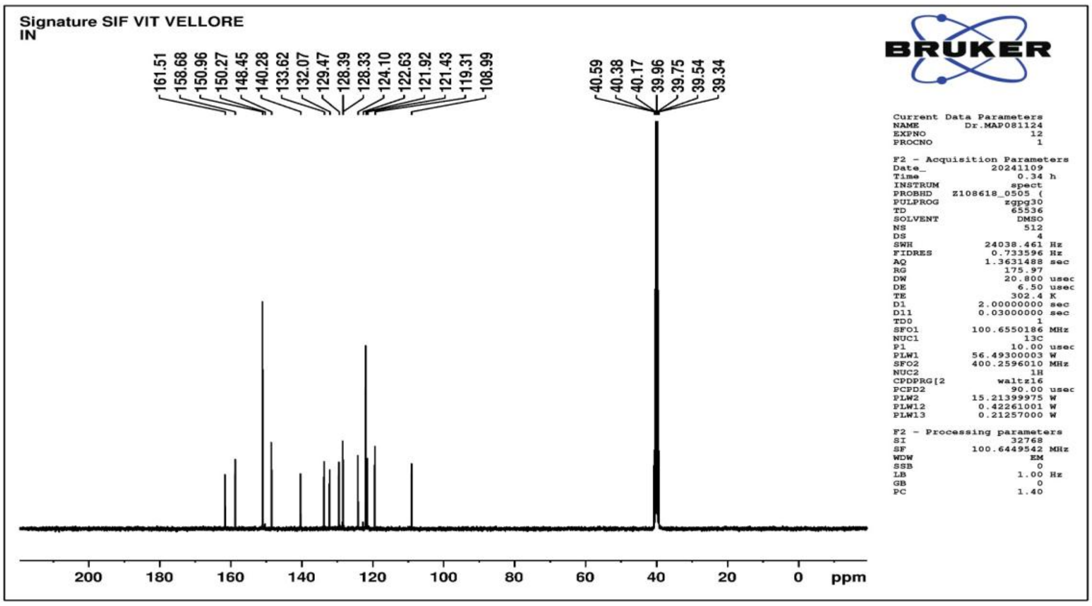

Figure.S6. ^{13}C NMR spectrum of ligand IN (400 MHz, DMSO-d$_6$)

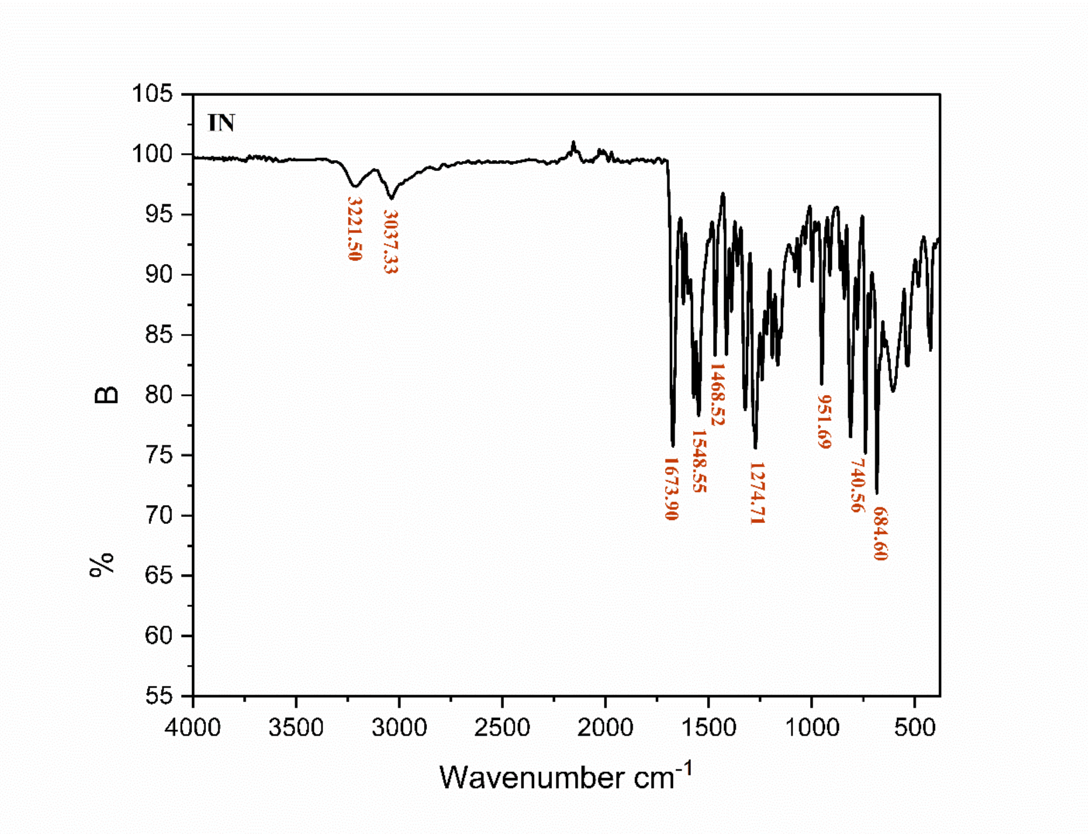

Figure.S7. FTIR spectrum of ligand IN (400 MHz, DMSO-d_6)

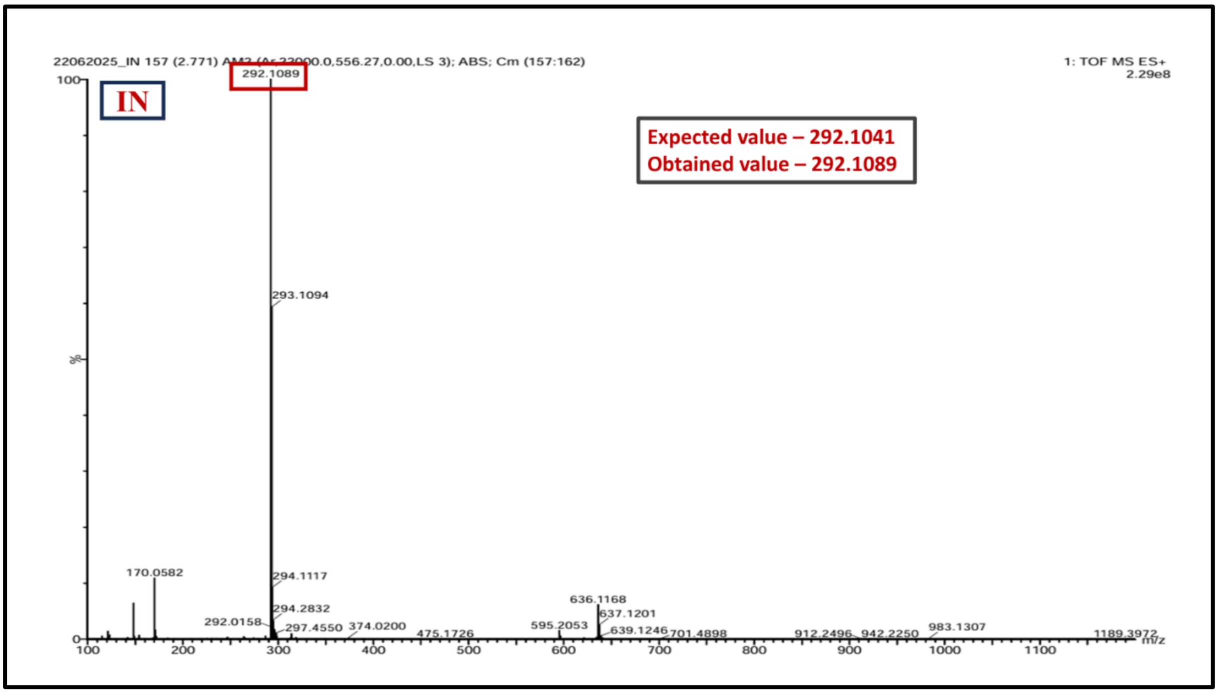

Figure.S8. ESI-MS spectrum of ligand IN

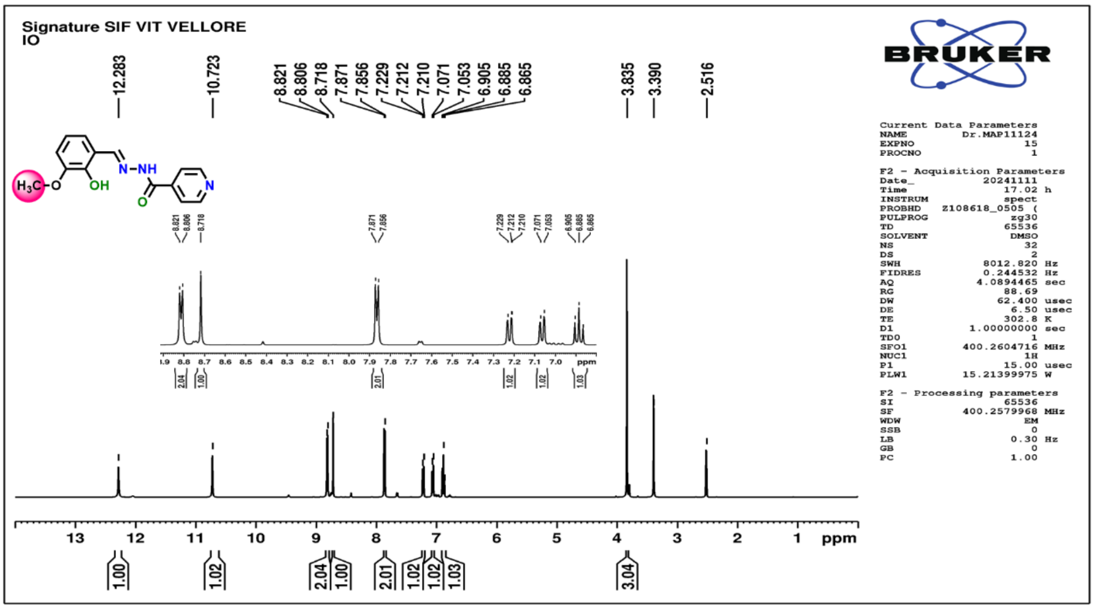

Figure.S9.[1]H NMR spectrum of ligand IO (400 MHz, DMSO-d_6)

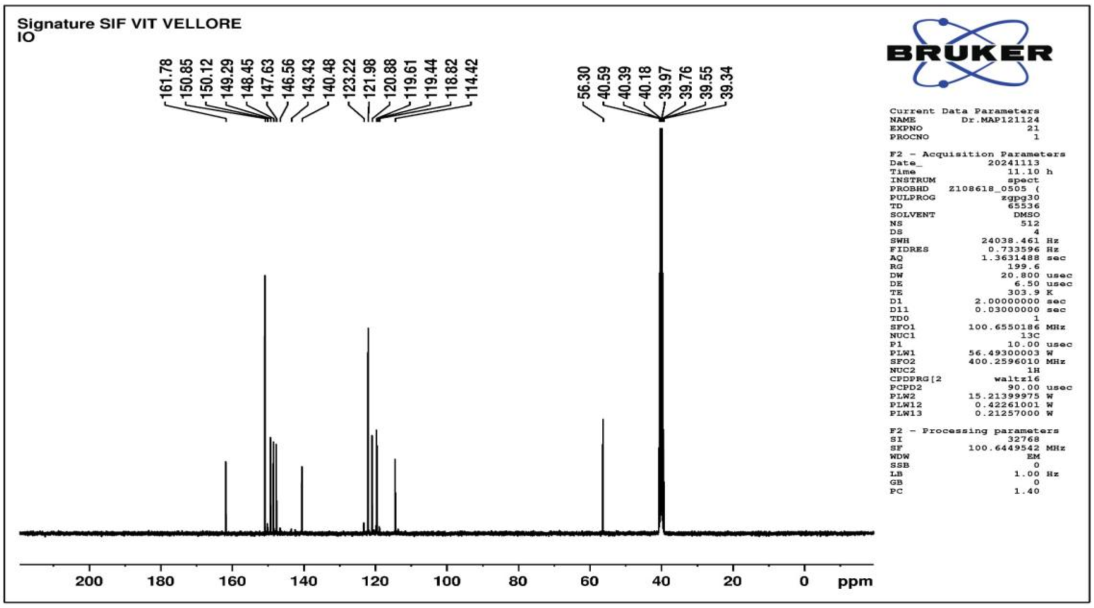

Figure.S10. [13]C NMR spectrum of ligand IO (400 MHz, DMSO-d_6)

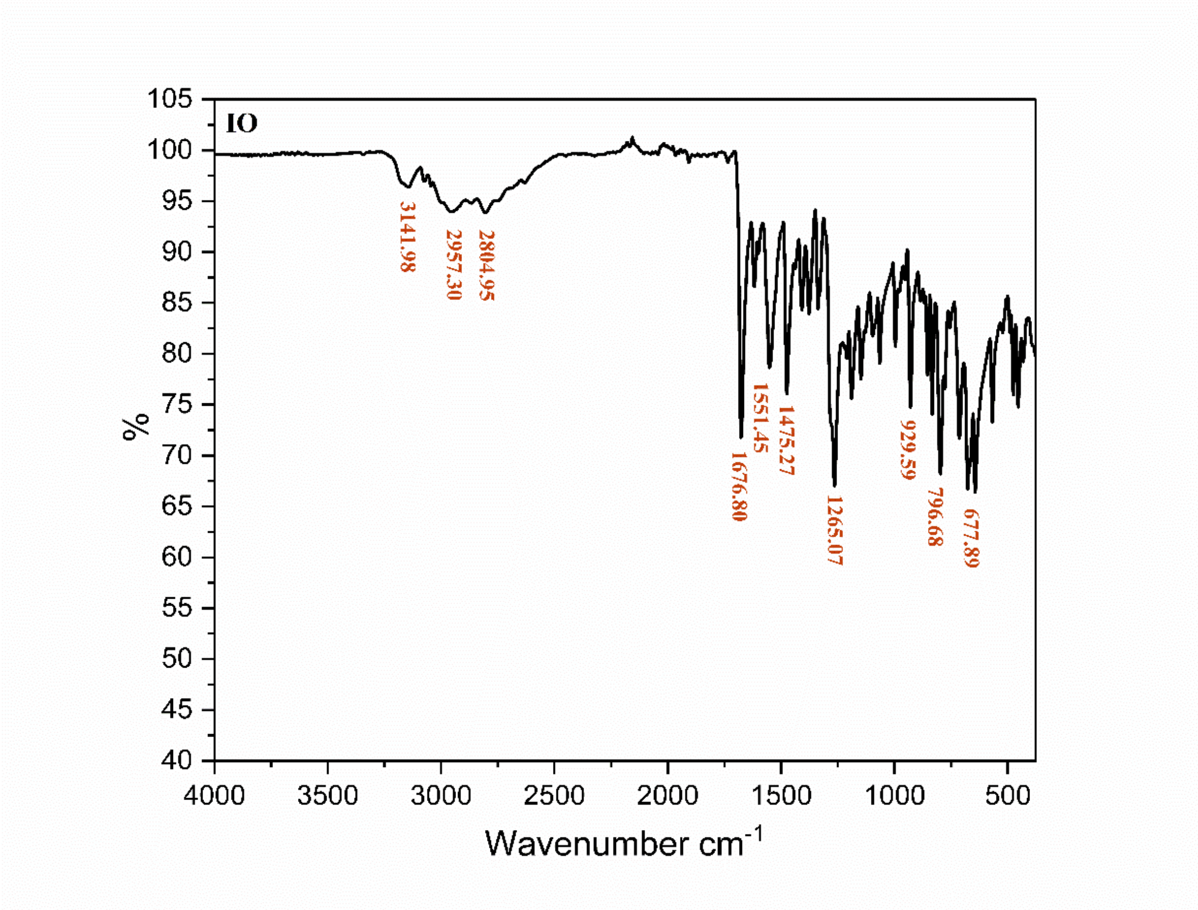

Figure.S11. FTIR spectrum of ligand IO

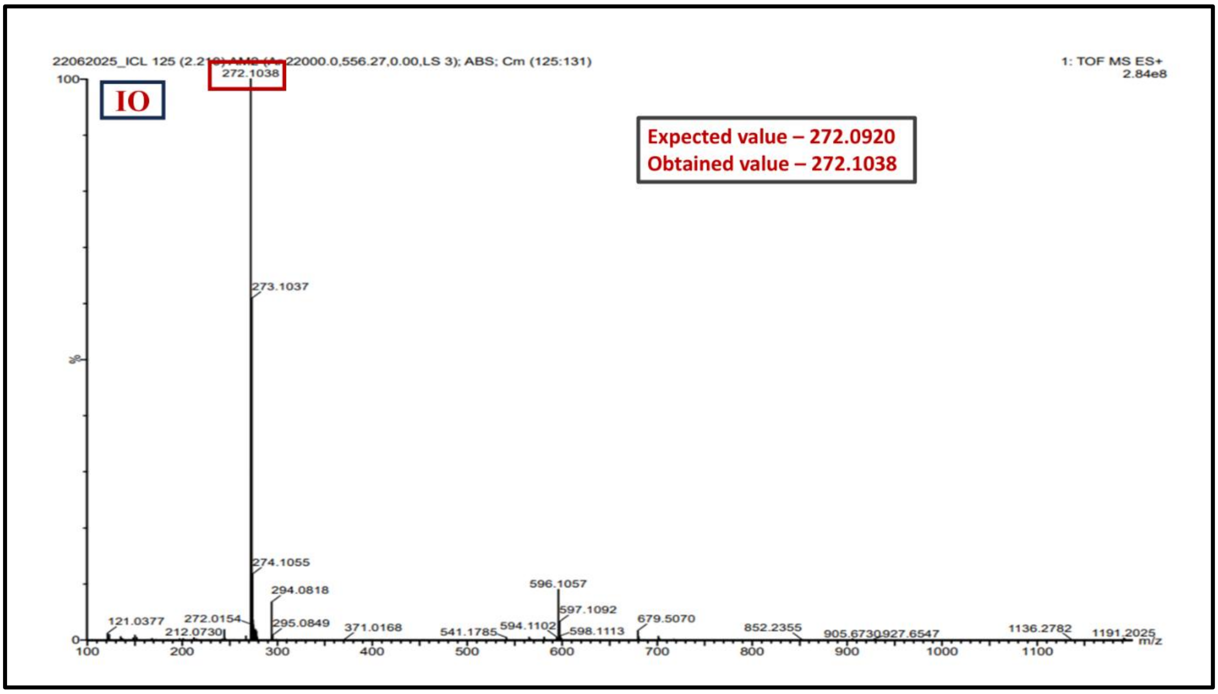

Figure.S12. ESI-MS spectrum of ligand IO

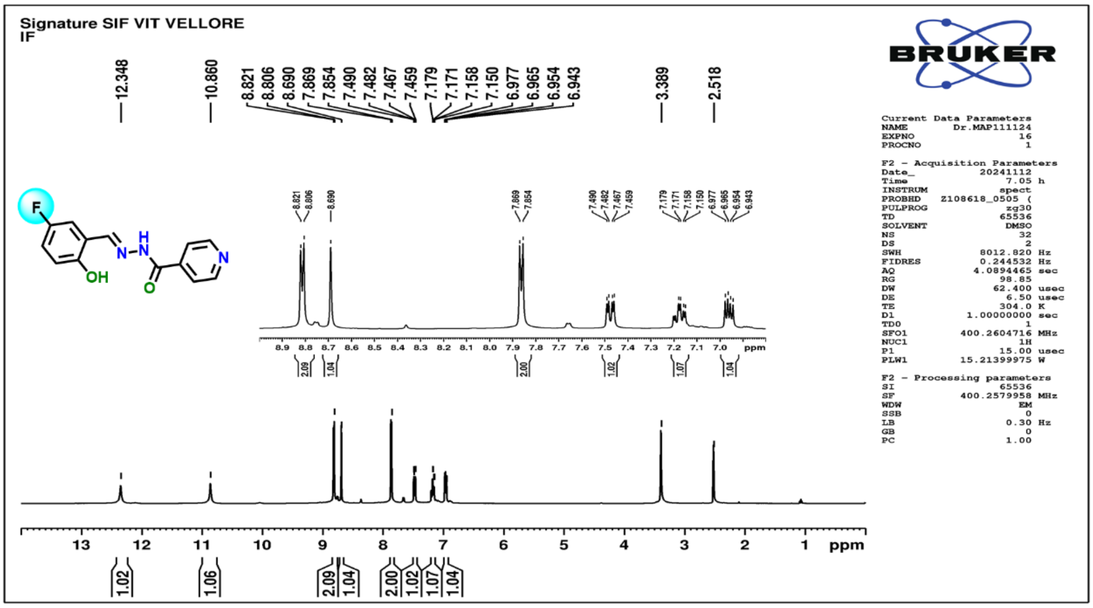

Figure.S13. ^{1}H NMR spectrum of ligand IF(400 MHz, DMSO-d_6)

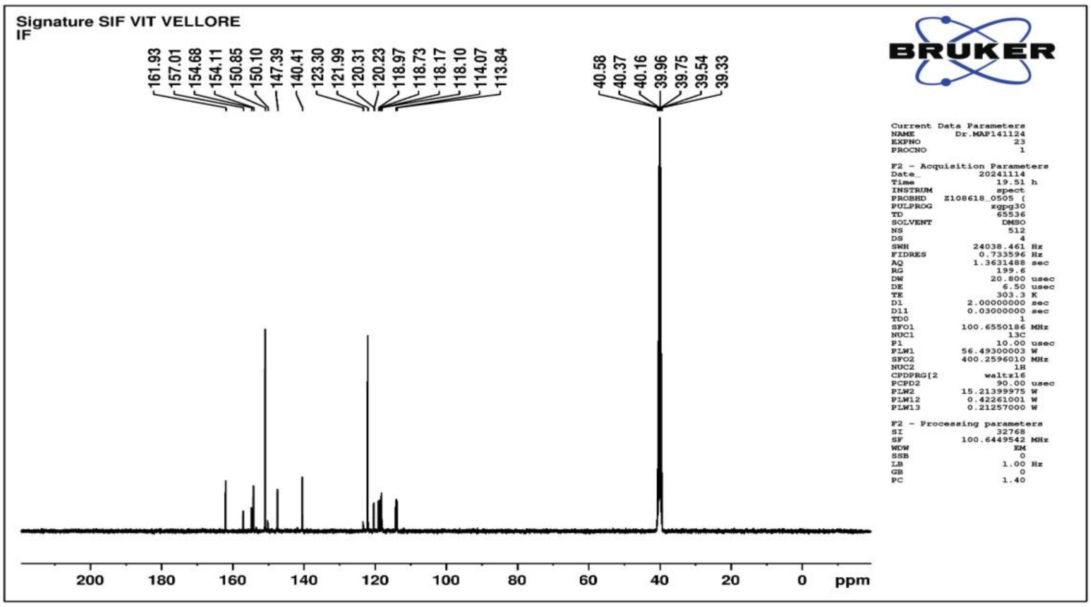

Figure.S14. ^{13}C NMR spectrum of ligand IF(400 MHz, DMSO-d_6)

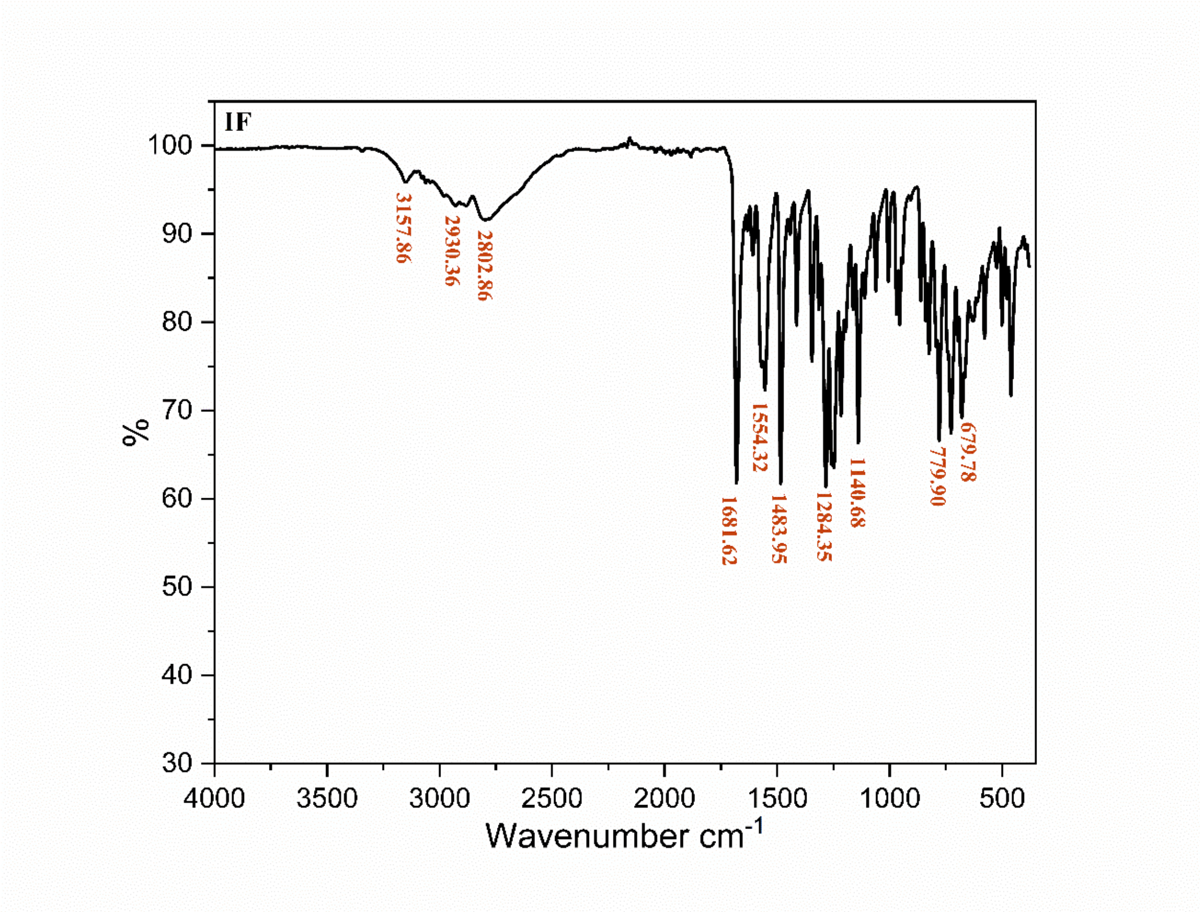

Figure.S15. FTIR spectrum of ligand IF (400 MHz, DMSO-d_6)

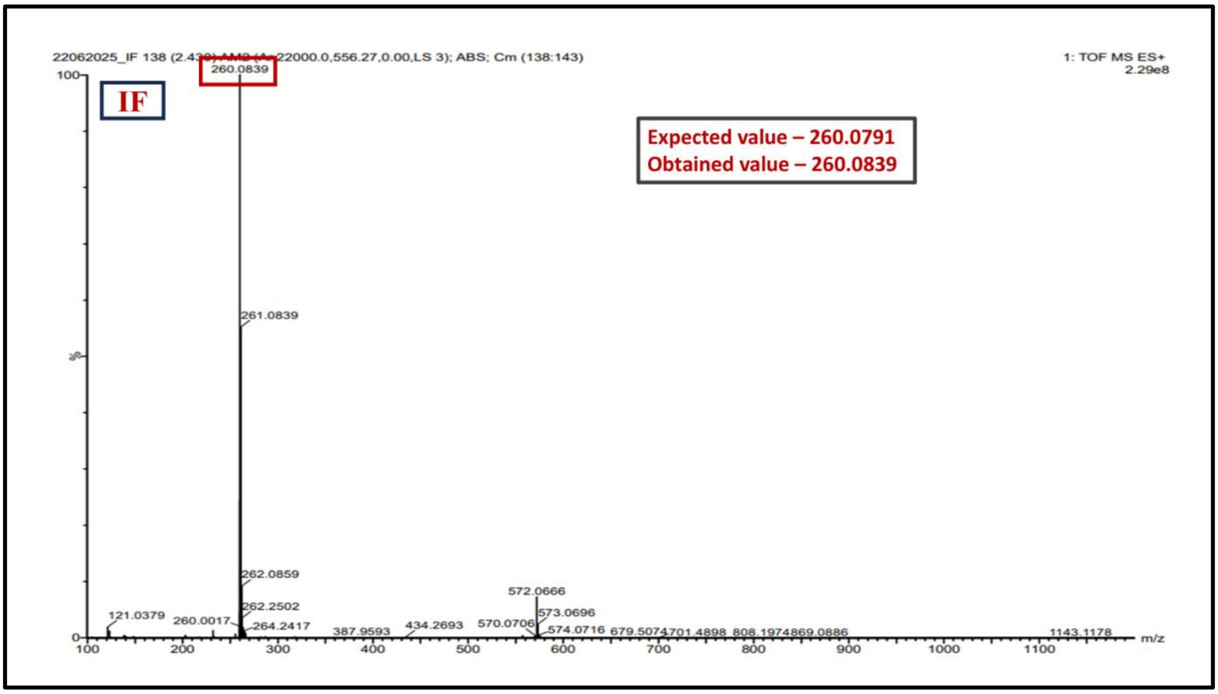

Figure.S16. ESI-MS spectrum of ligand IF

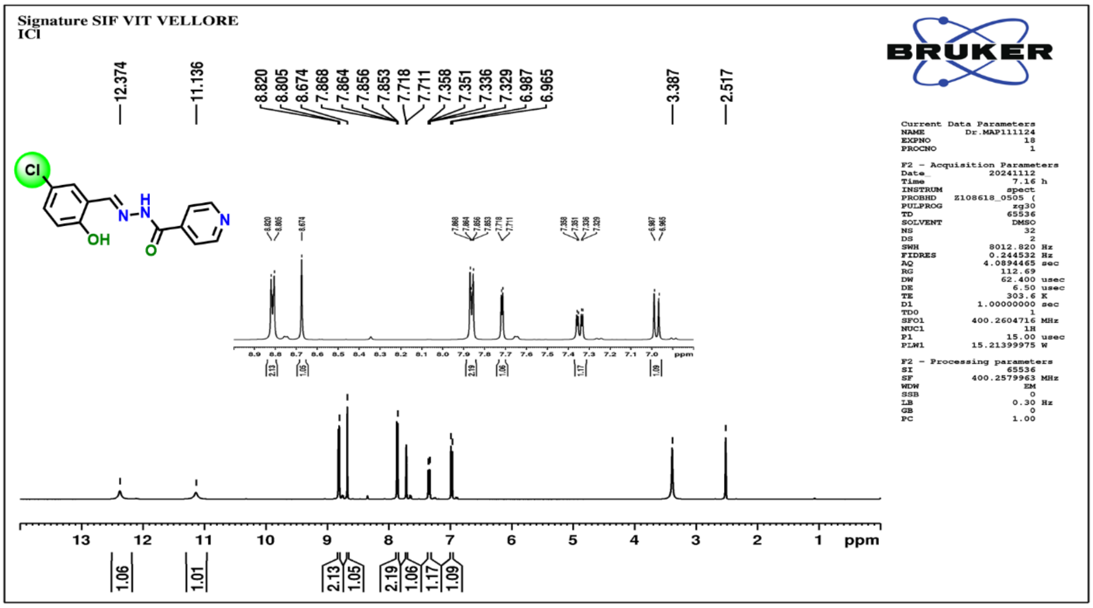

Figure.S17. ^{1}H NMR spectrum of ligand ICl (400 MHz, DMSO-d_6)

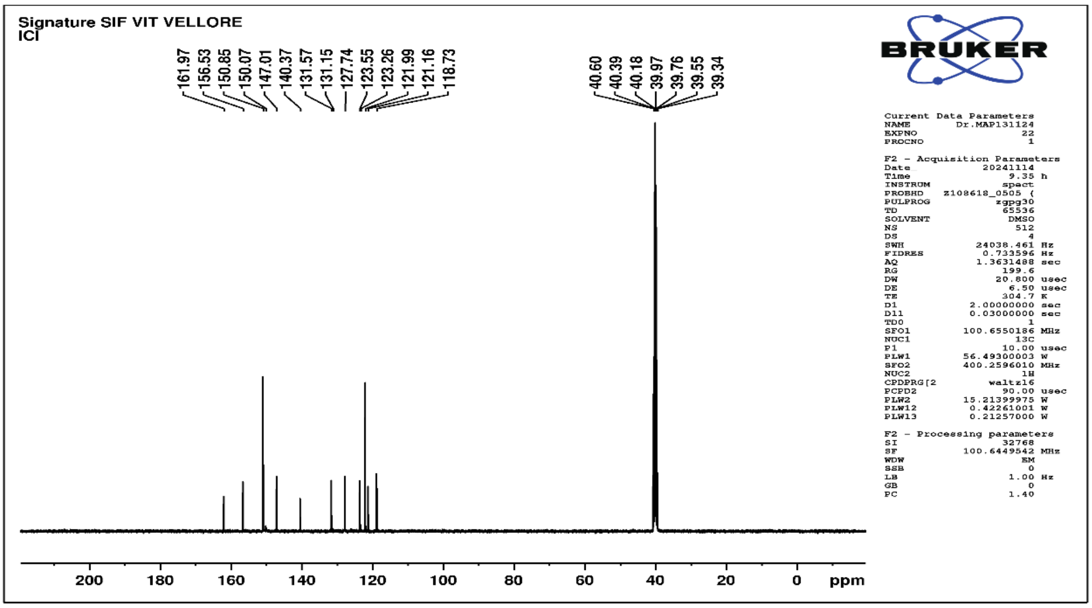

Figure.S18. ^{13}C NMR spectrum of ligand ICl (400 MHz, DMSO-d_6)

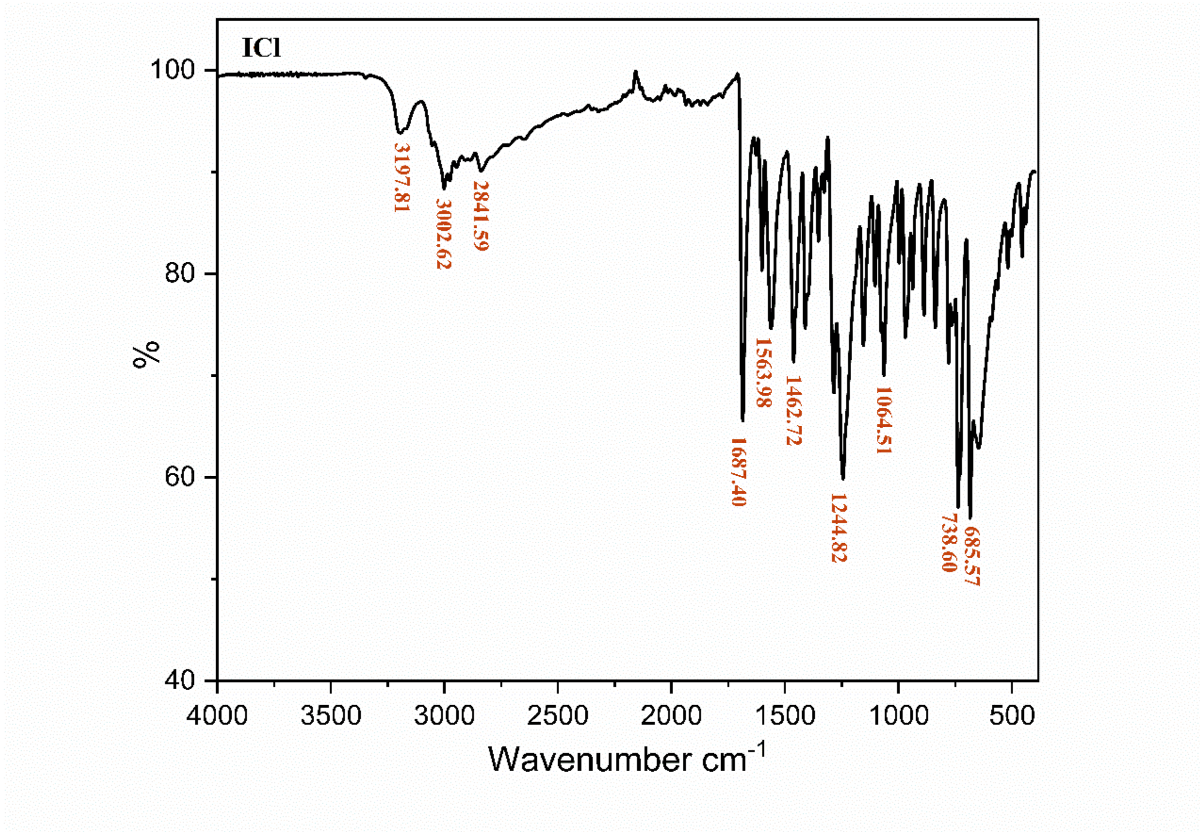

Figure.S19. FTIR spectrum of ligand ICl

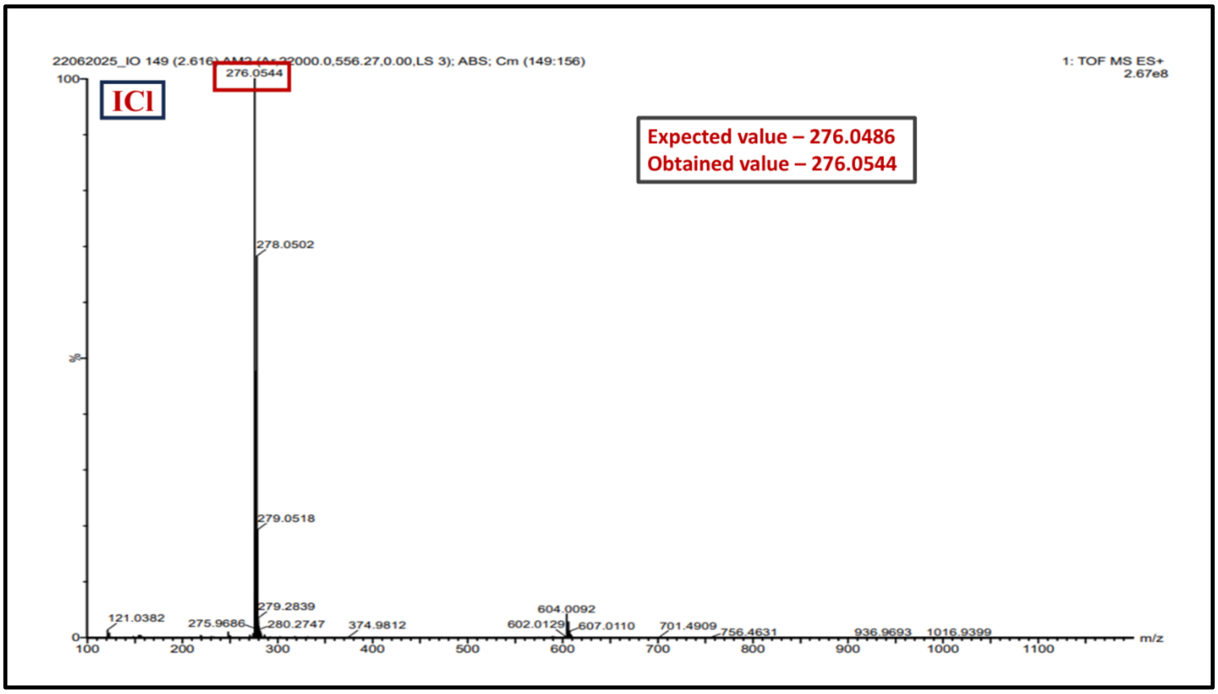

Figure.S20. ESI-MS spectrum of ligand ICl

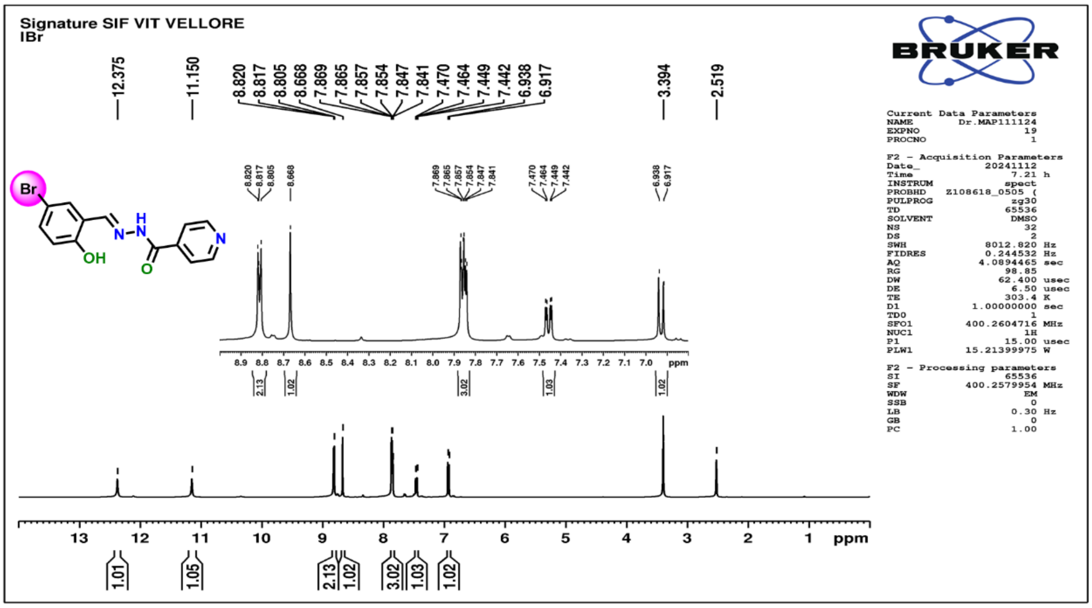

Figure.S21. ^{1}H NMR spectrum of ligand IBr (400 MHz, DMSO-d_6)

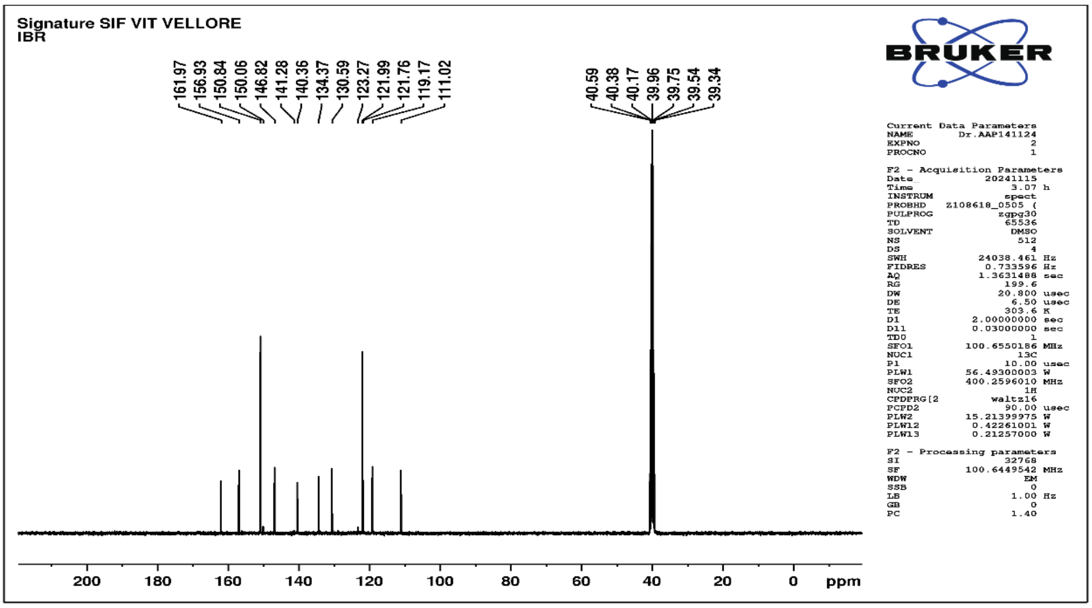

Figure.S22. ^{13}C NMR spectrum of ligand IBr (400 MHz, DMSO-d_6)

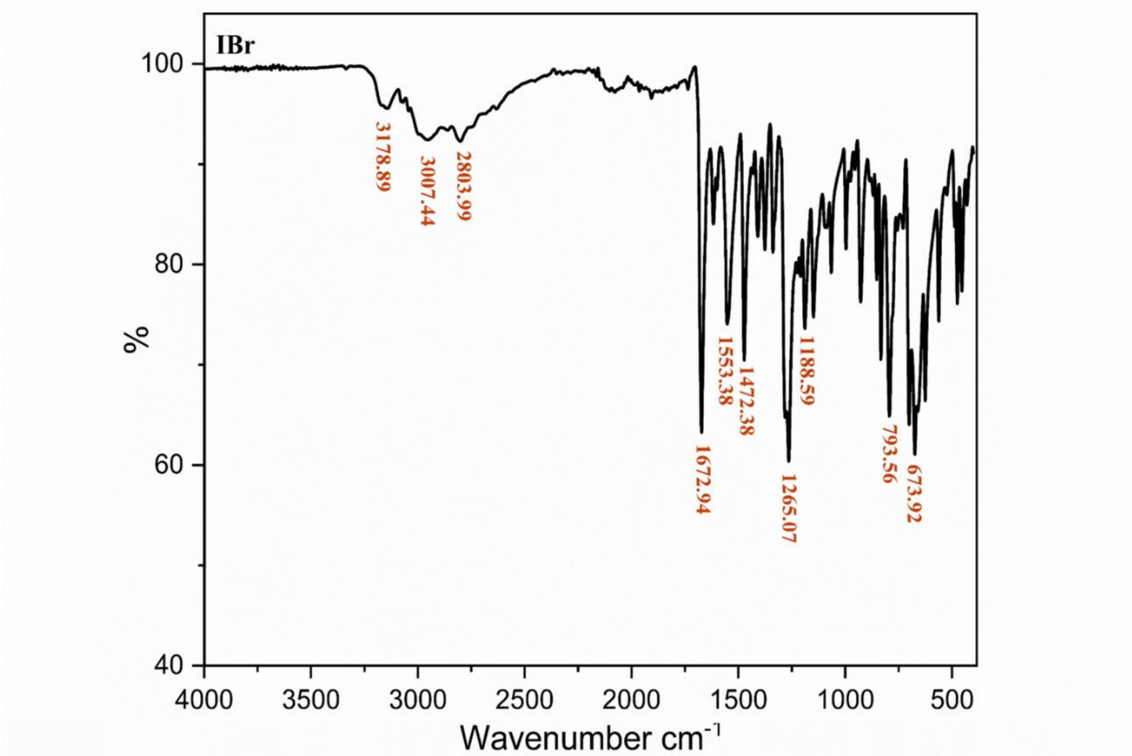

Figure.S23. FTIR spectrum of ligand IBr

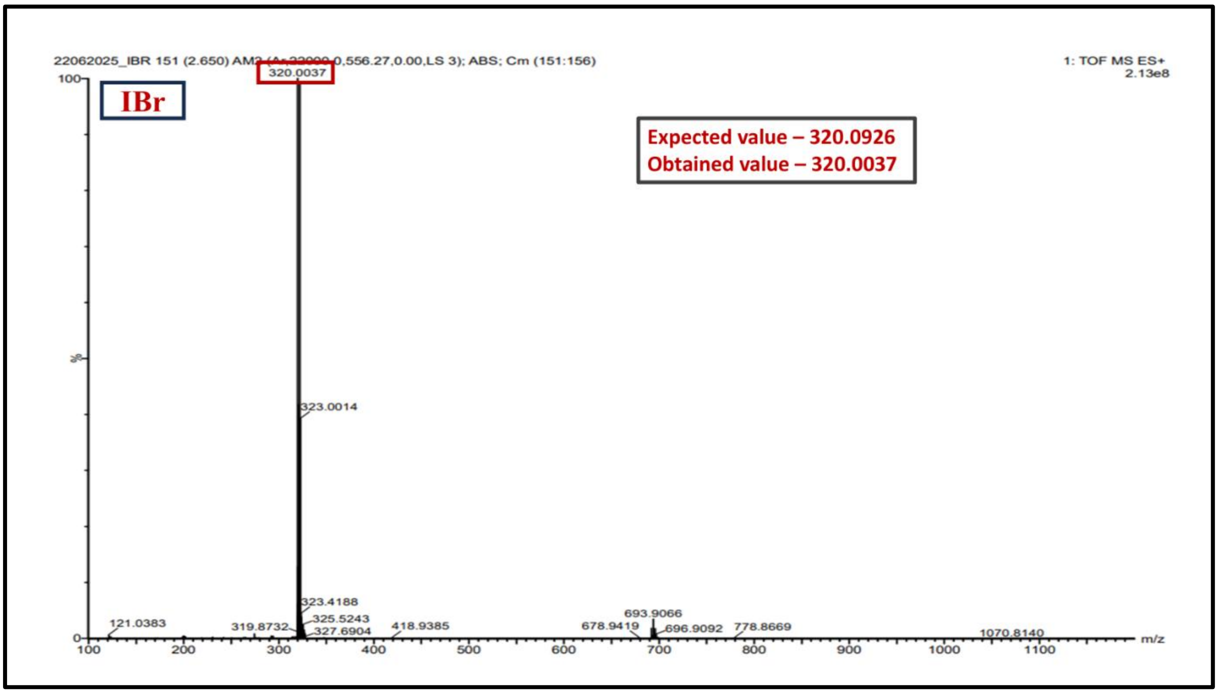

Figure.S24. ESI-MS spectrum of ligand IF

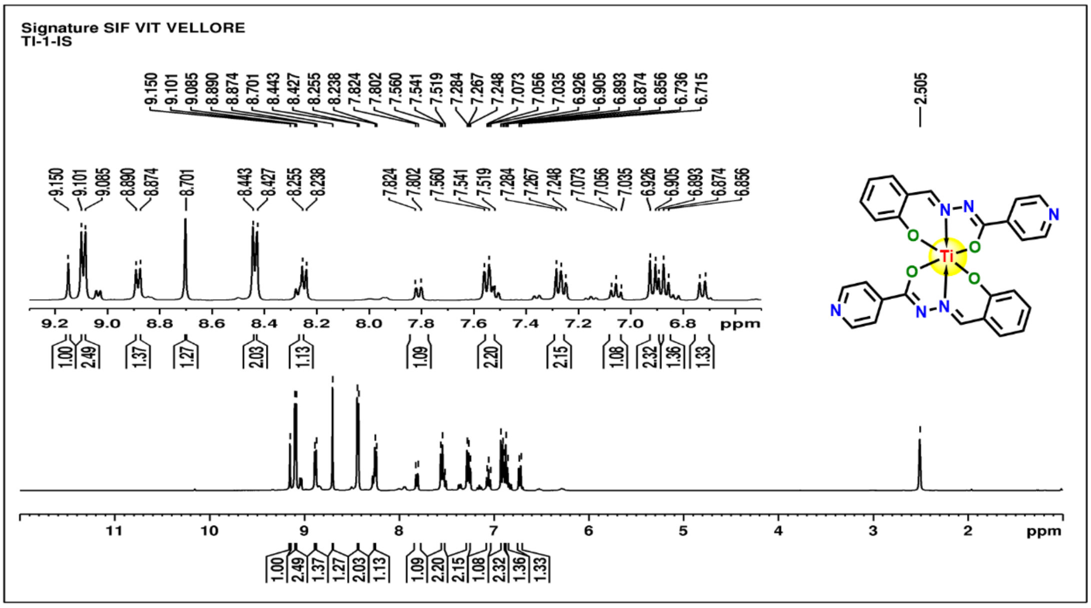

Figure.S25. ^{1}H NMR spectrum of complex Ti-1-IS (400 MHz, DMSO-d$_6$)

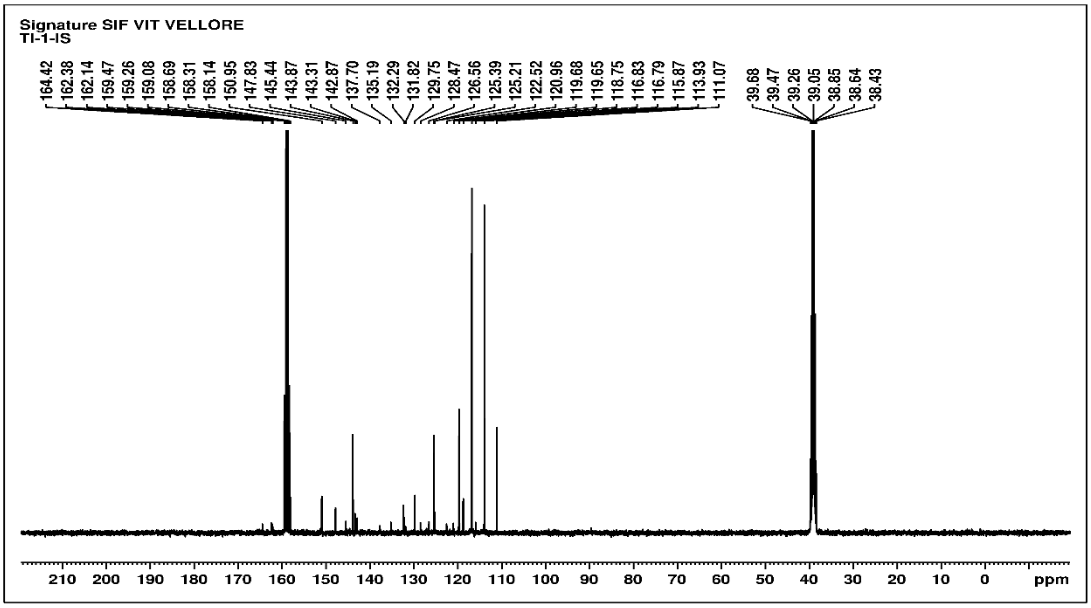

Figure.S26. ^{13}C NMR spectrum of complex Ti-1-IS (400 MHz, DMSO-d$_6$)

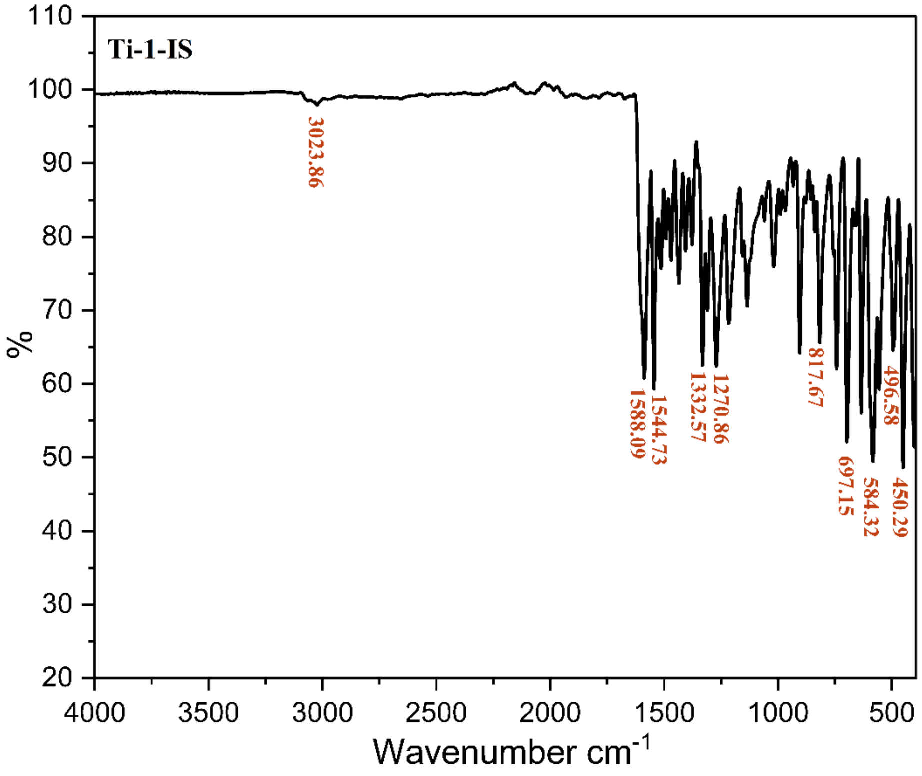

Figure.S27. FTIR spectrum of complex Ti-1-IS (400 MHz, DMSO-d_6)

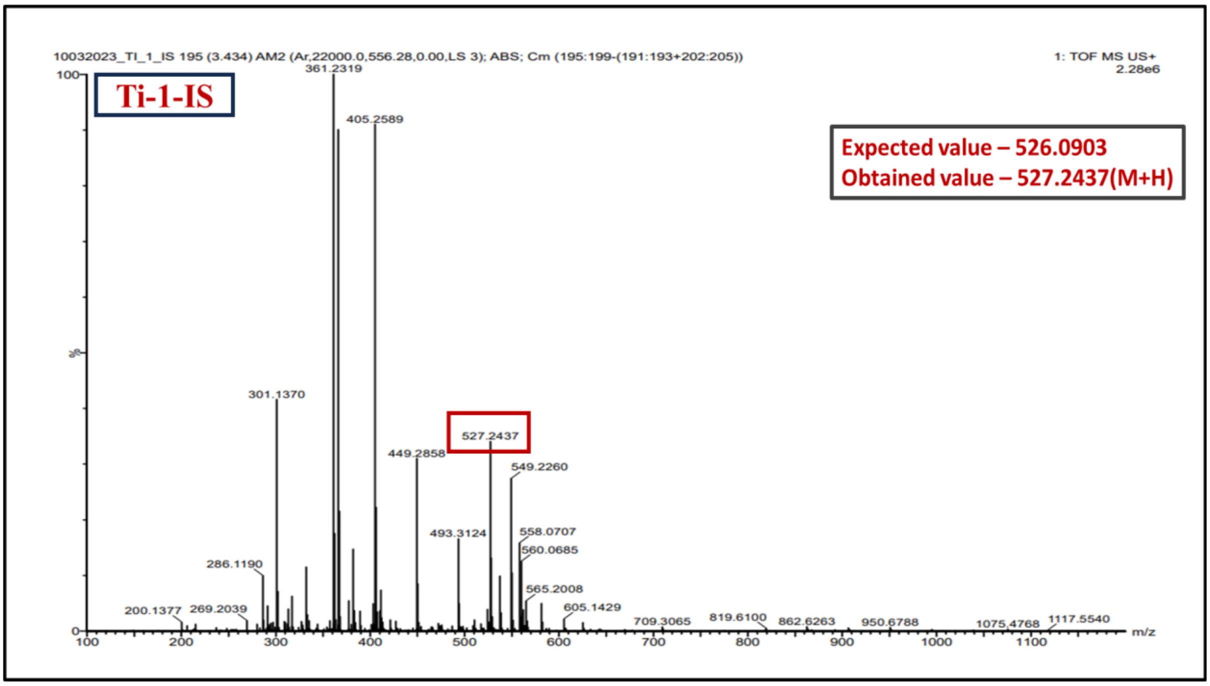

Figure.S28. ESI-MS spectrum of complex Ti-1-IS

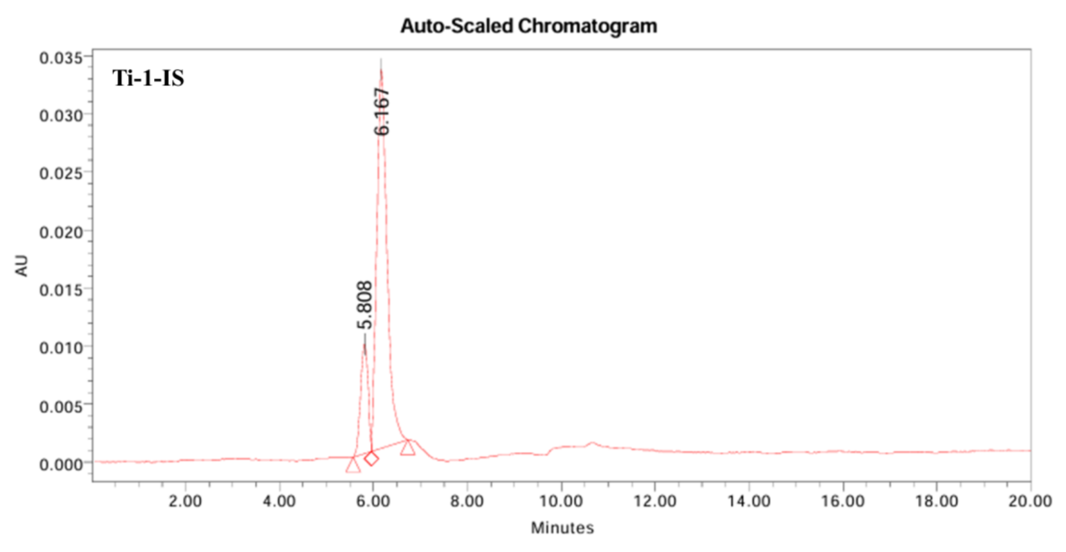

Peak Results

	Name	RT	Area	Height	Amount	Units
1		5.808	104329	9441		
2		6.167	496342	32625		

Figure.S29. HPLC spectrum of complex Ti-1-IS

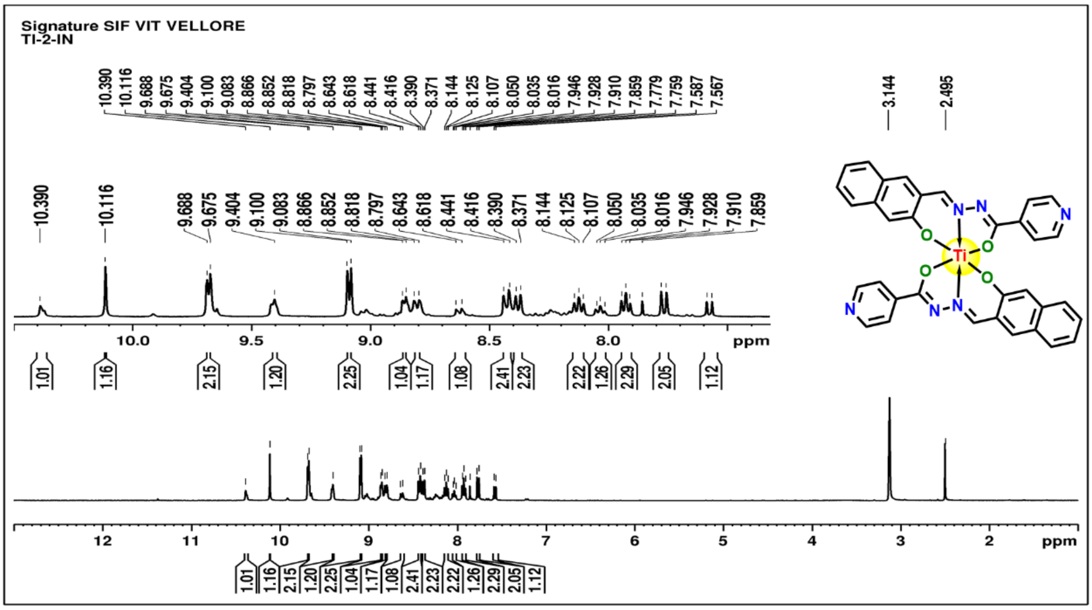

Figure.S30. [1]H NMR spectrum of complex Ti-2-IN (400 MHz, DMSO-d_6)

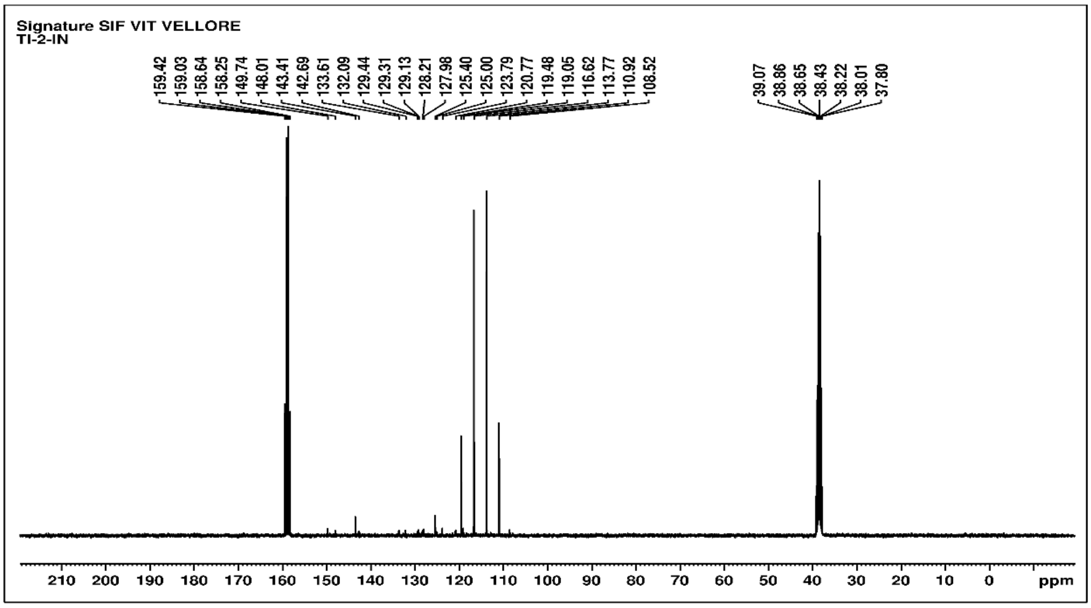

Figure.S31. ^{13}C **NMR spectrum of complex Ti-2-IN (400 MHz, DMSO-d$_6$)**

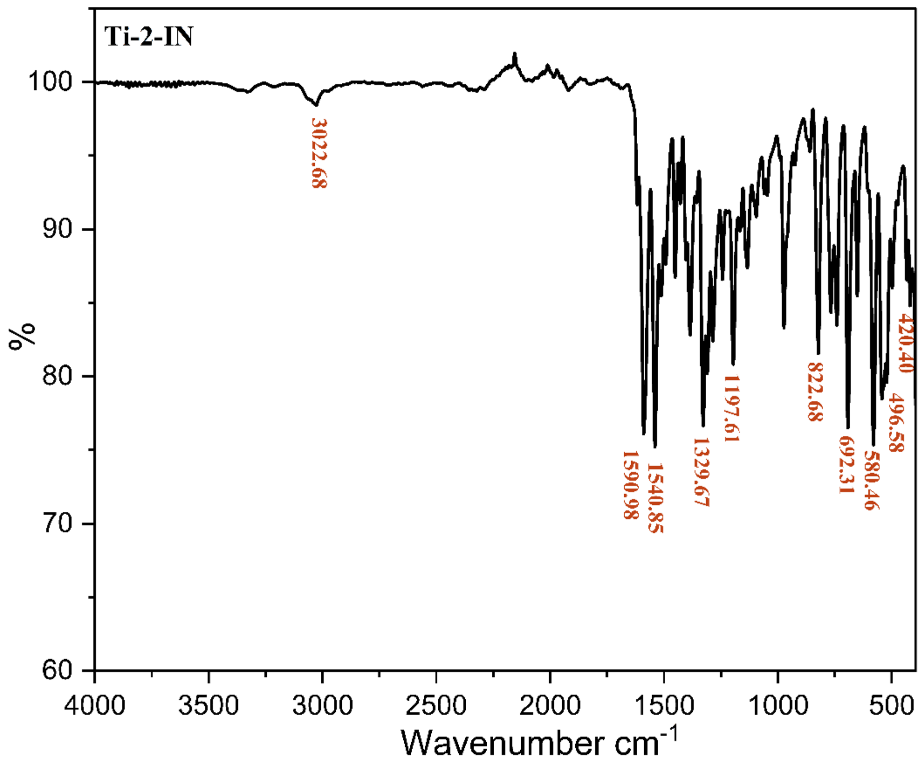

Figure.S32. FTIR spectrum of complex Ti-2-IN

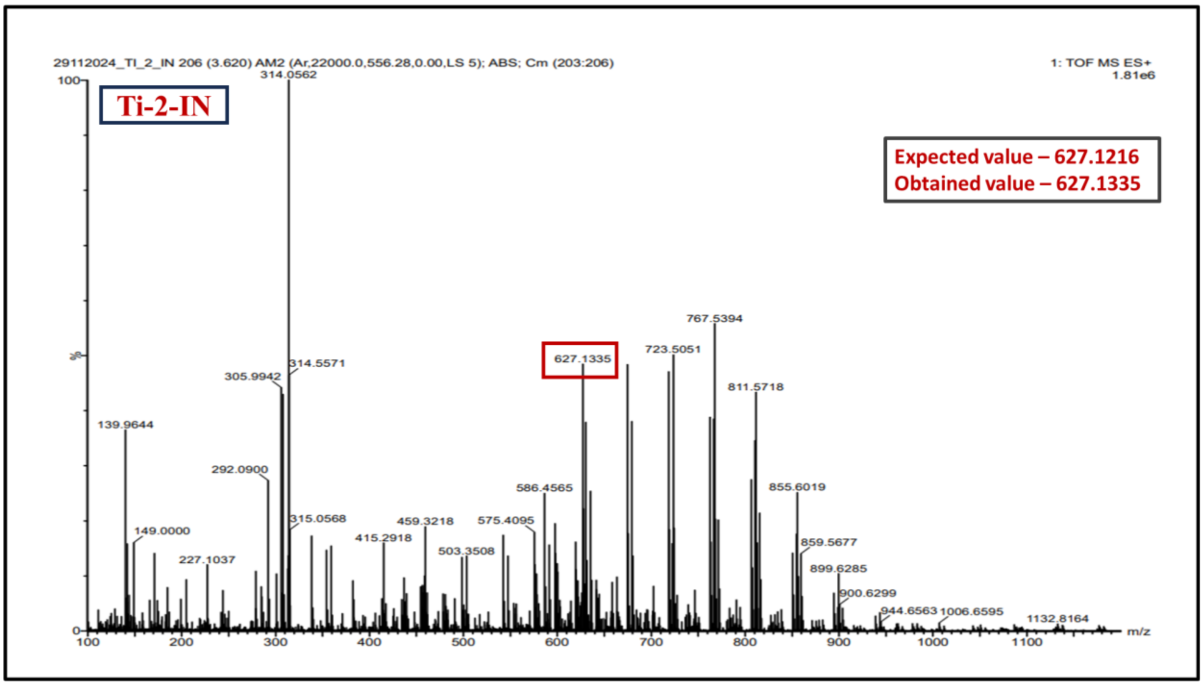

Figure.S33. ESI-MS spectrum of complex Ti-2-IN (400 MHz, DMSO-d_6)

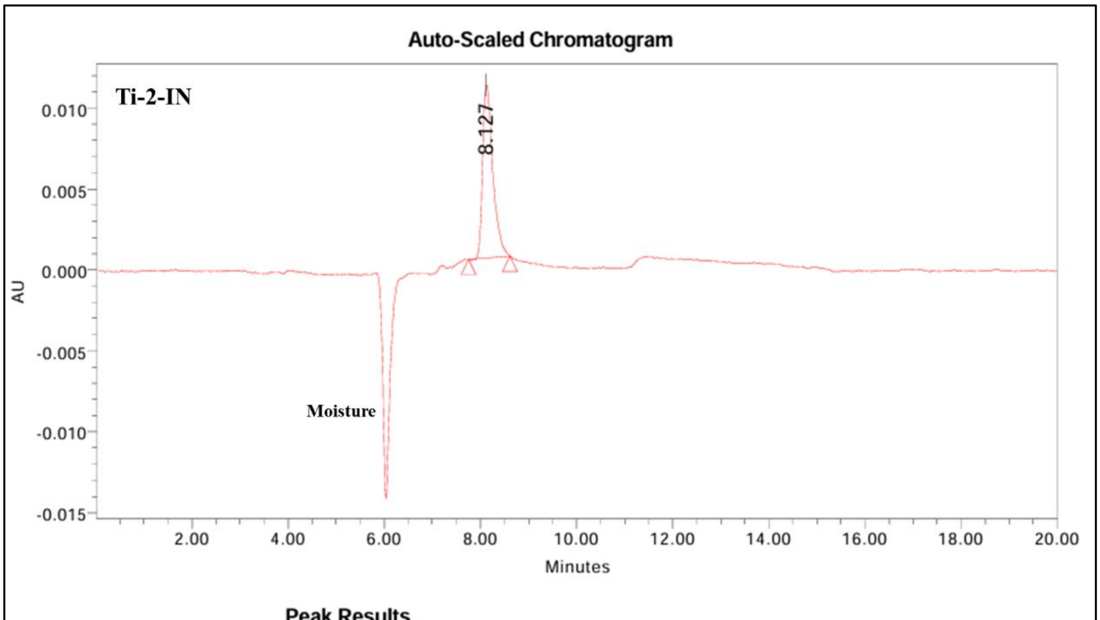

Peak Results

	Name	RT	Area	Height	Amount	Units
1		8.127	157767	10704		

Figure.S34. HPLC spectrum of complex Ti-2-IN

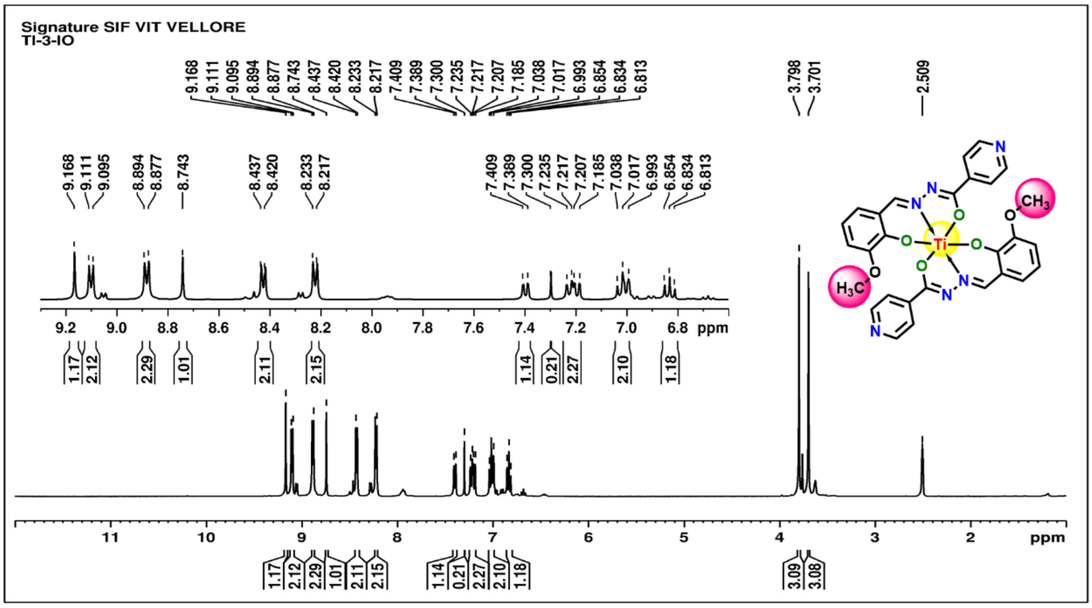

Figure.S35. ^{1}H NMR spectrum of complex Ti-3-IO (400 MHz, DMSO-d_6)

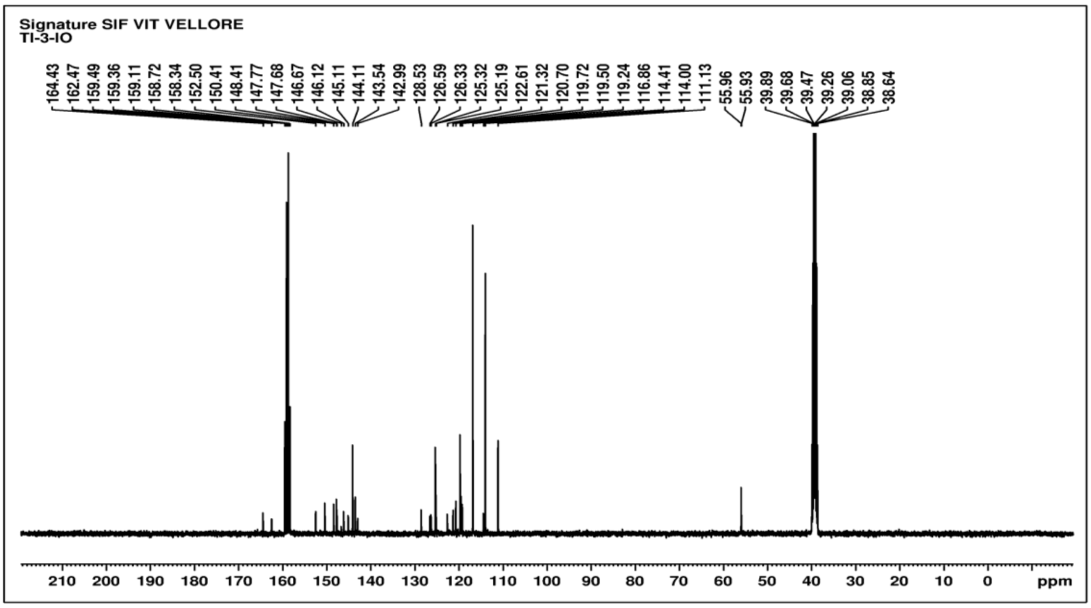

Figure.S36. ^{13}C NMR spectrum of complex Ti-3-IO (400 MHz, DMSO-d_6)

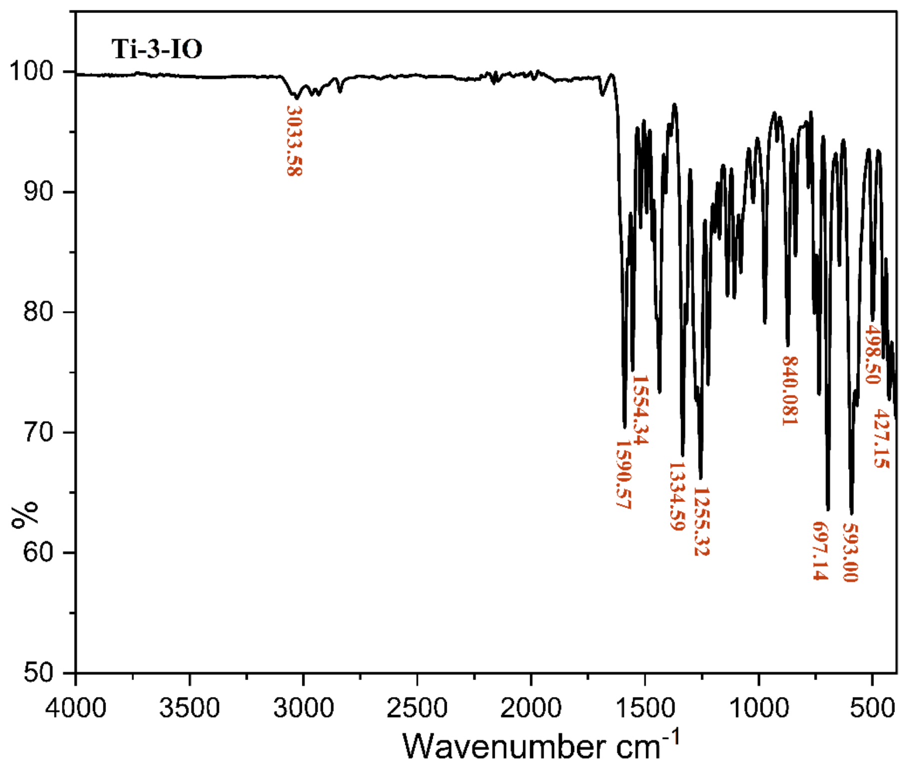

Figure.S37. FTIR spectrum of complex Ti-3-IO

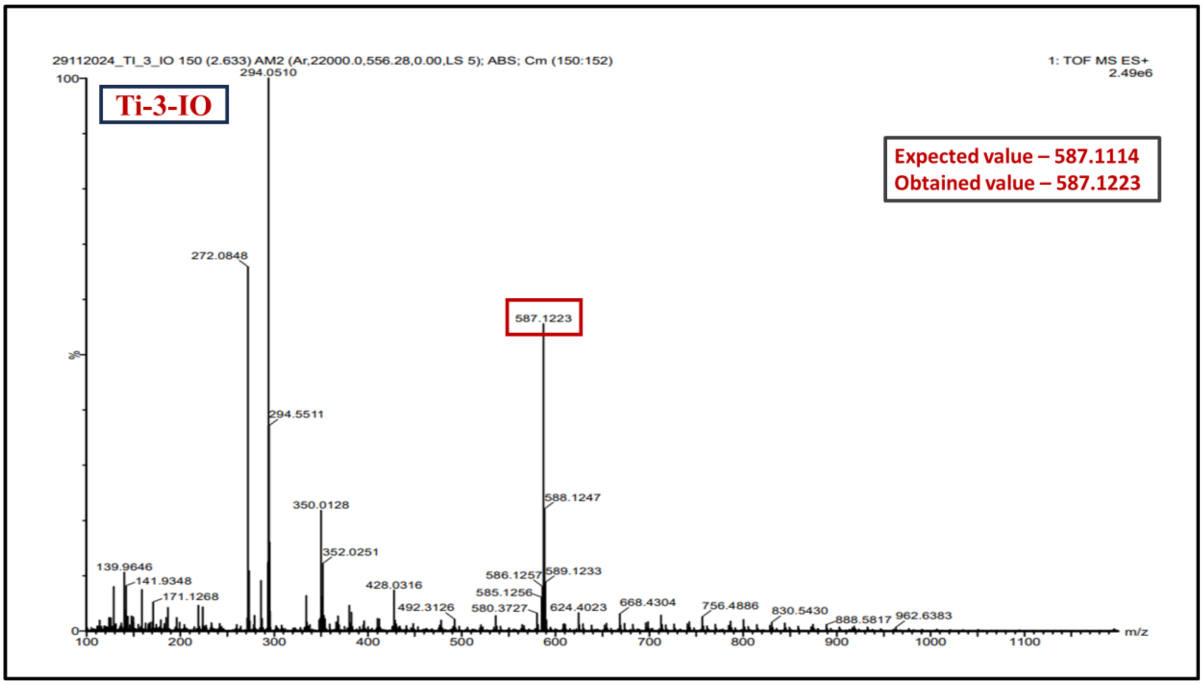

Figure.S38. ESI-MS spectrum of complex Ti-3-IO

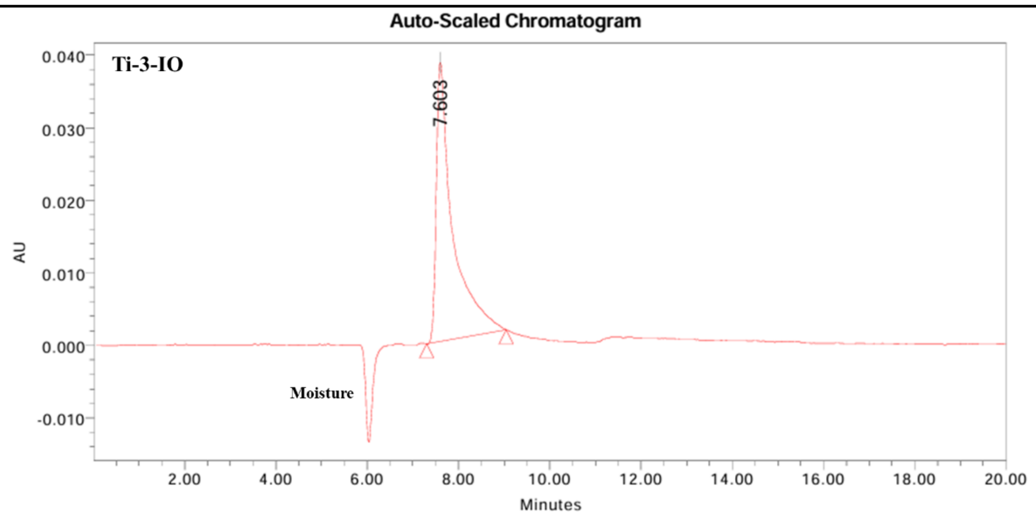

Peak Results

	Name	RT	Area	Height	Amount	Units
1		7.603	976997	38493		

Figure.S39. HPLC spectrum of complex Ti-3-IO

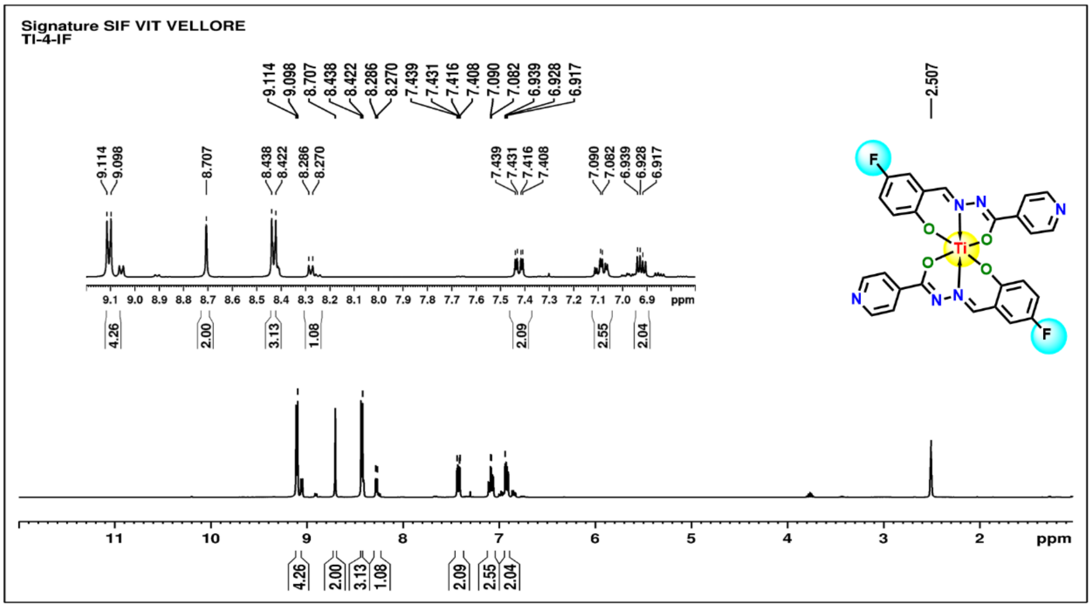

Figure.S40. ^{1}H NMR spectrum of complex Ti-4-IF(400 MHz, DMSO-d$_6$)

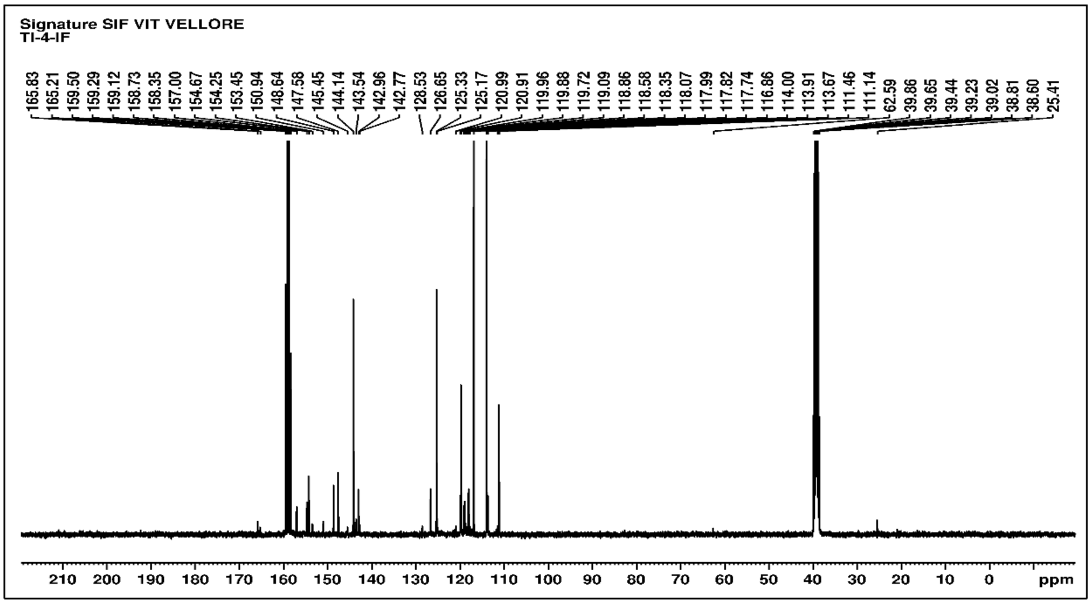

Figure.S41. ^{13}**C NMR spectrum of complex Ti-4-IF(400 MHz, DMSO-d$_6$)**

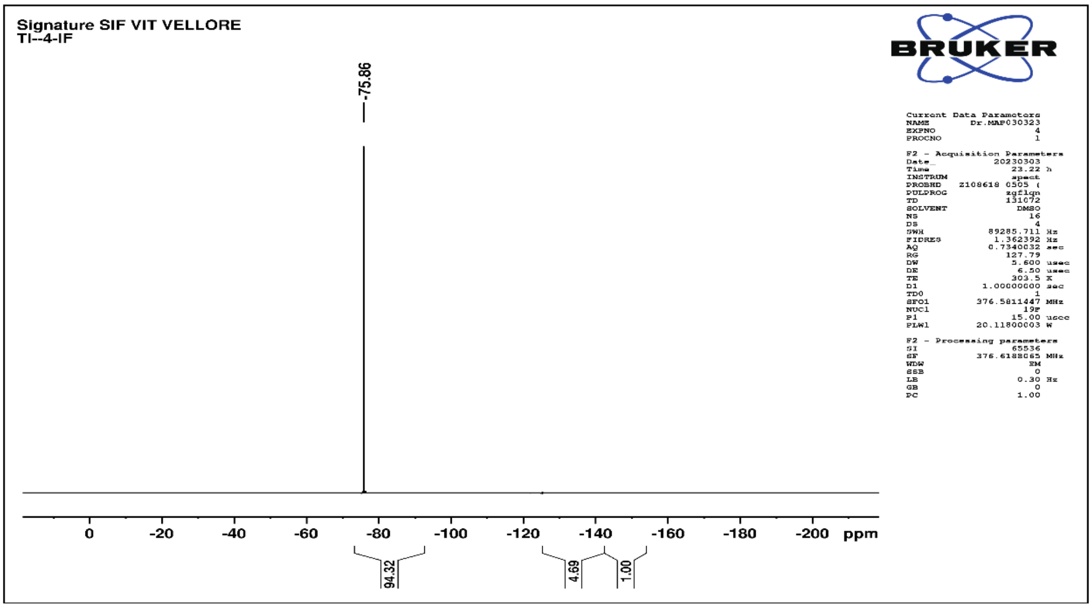

Figure.S42. ^{19}**F NMR spectrum of complex Ti-4-IF(400 MHz, DMSO-d$_6$)**

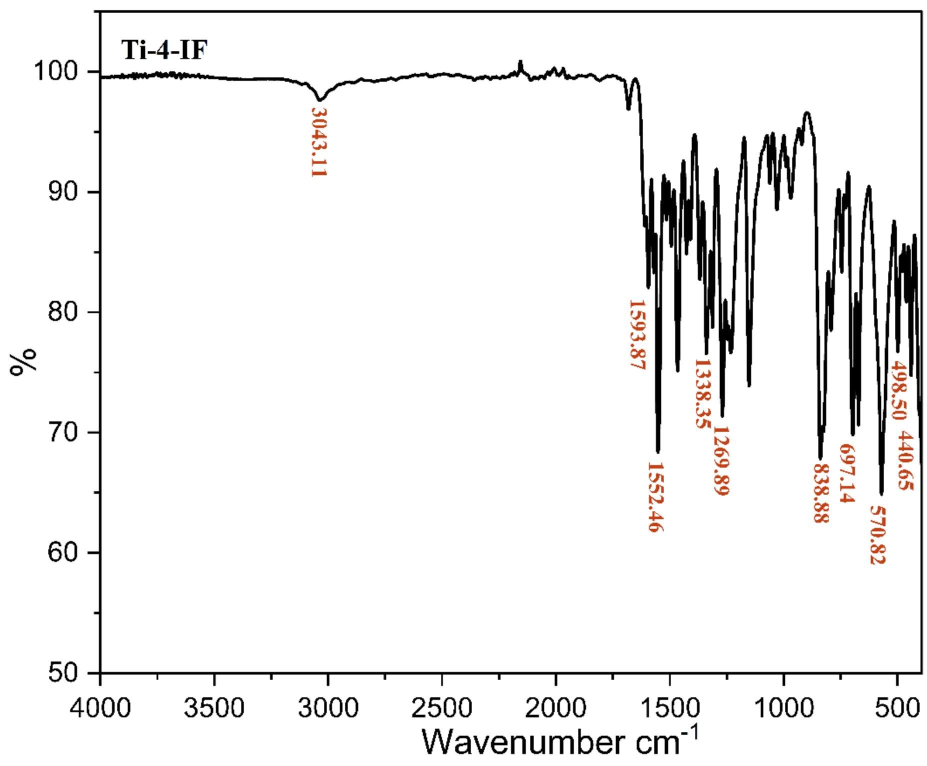

Figure.S43. FTIR spectrum of complex Ti-4-IF

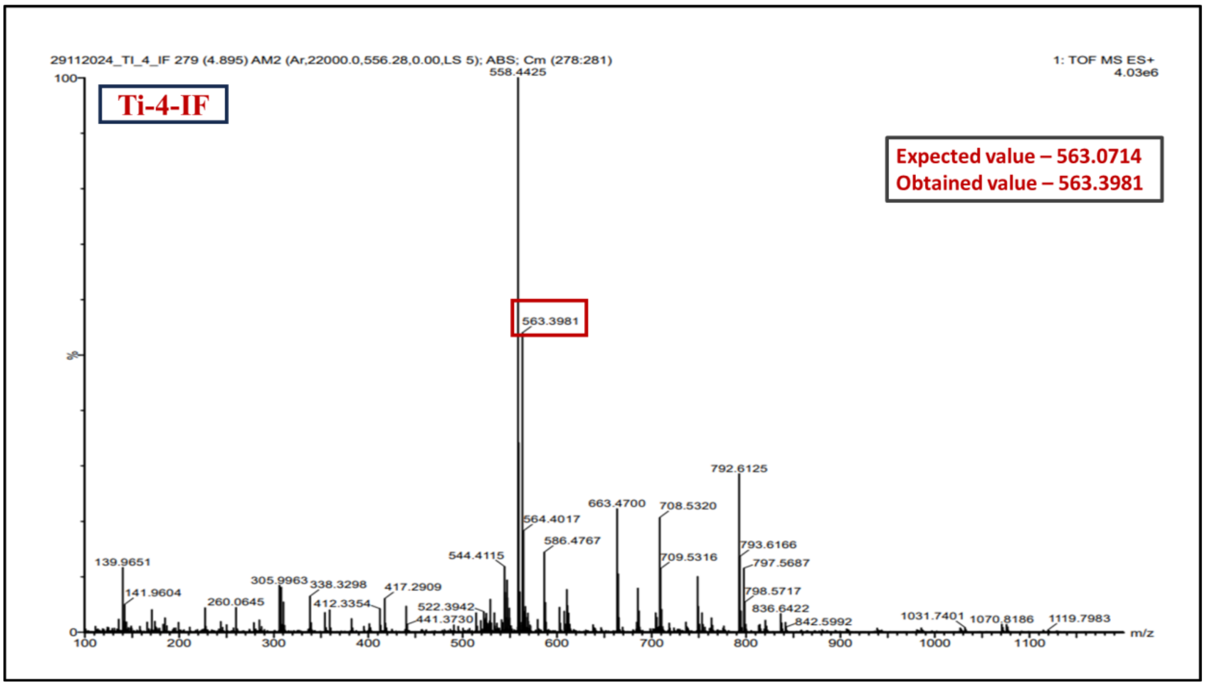

Figure.S44. ESI-MS spectrum of complex Ti-4-IF

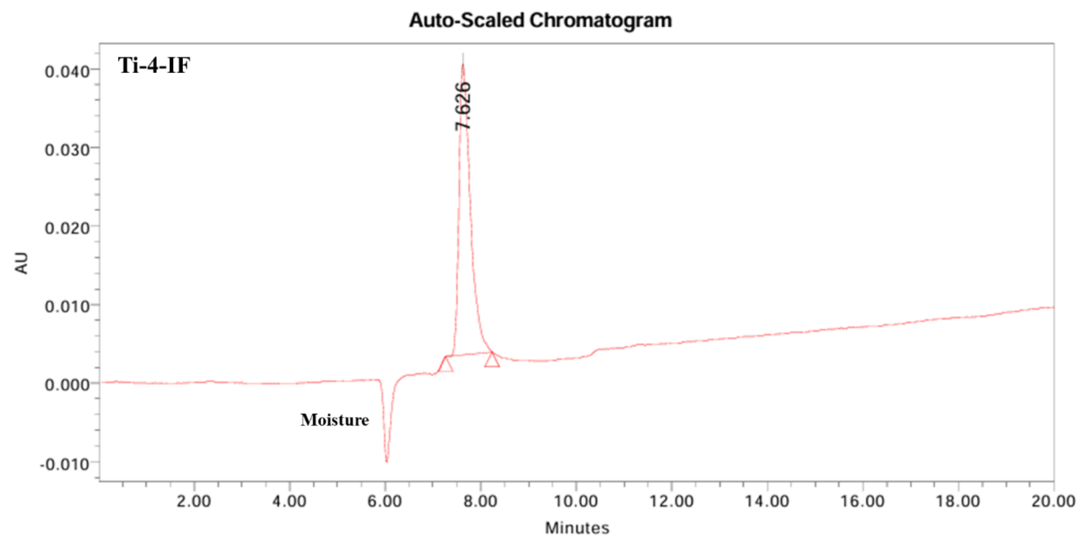

Peak Results

	Name	RT	Area	Height	Amount	Units
1		7.626	616721	37208		

Figure.S45. HPLC spectrum of complex Ti-4-IF

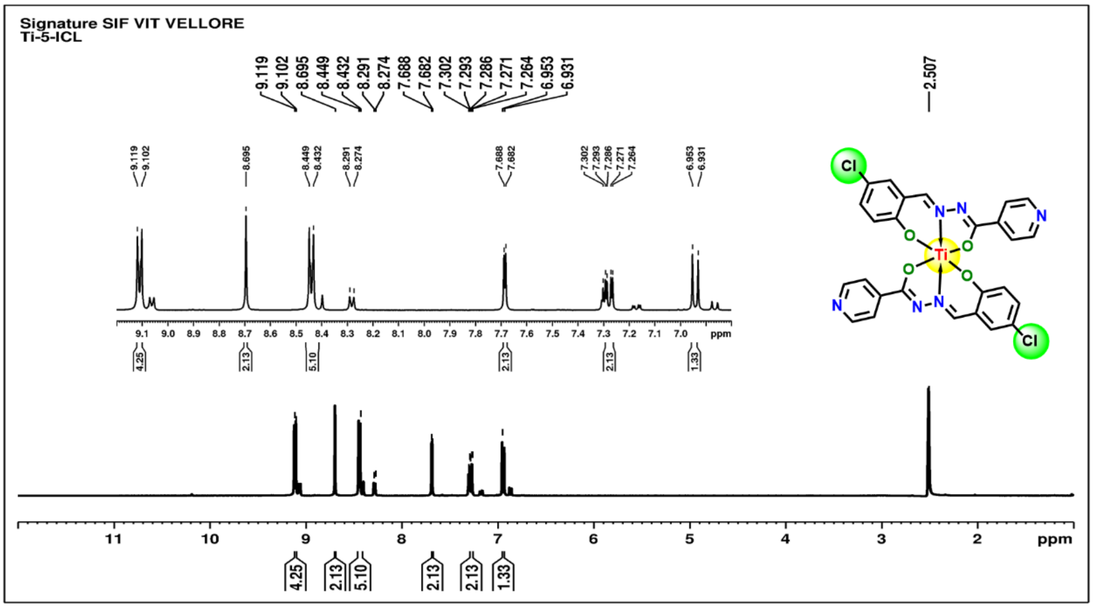

Figure.S46. ^{1}H NMR spectrum of complex Ti-5-ICl (400 MHz, DMSO-d_6)

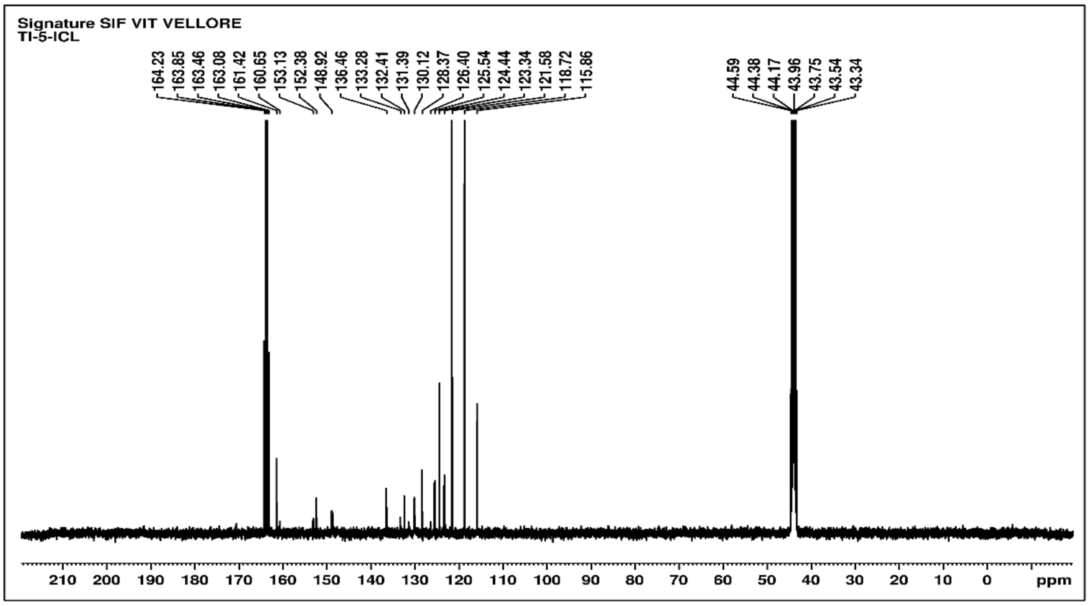

Figure.S47. ^{13}C NMR spectrum of complex Ti-5-ICl (400 MHz, DMSO-d_6)

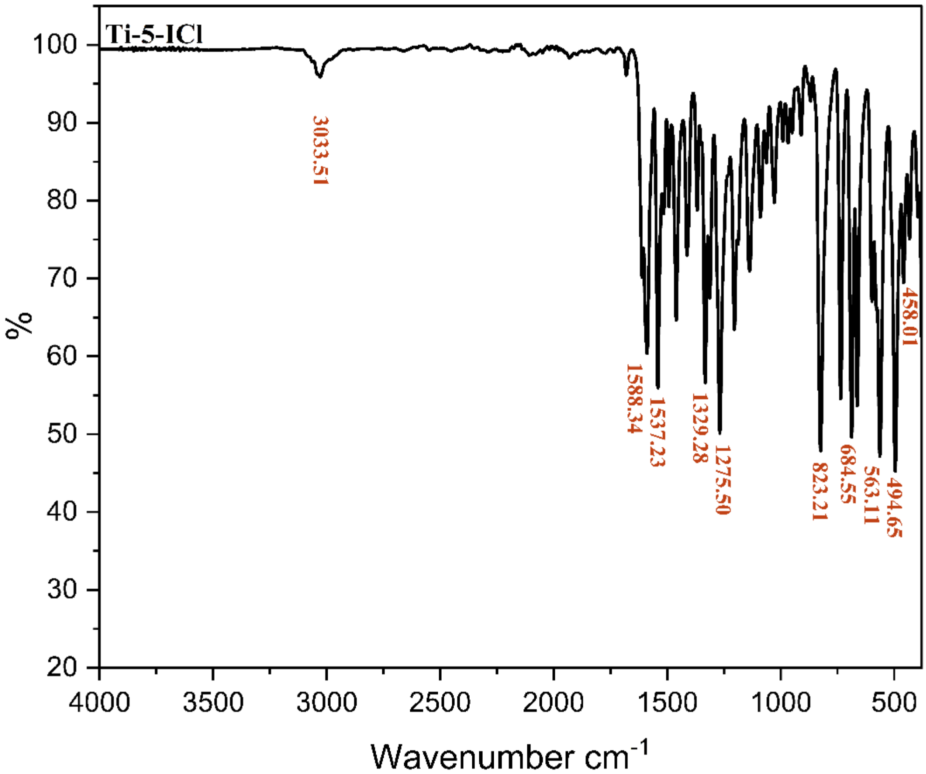

Figure.S48. FTIR spectrum of complex Ti-5-ICl

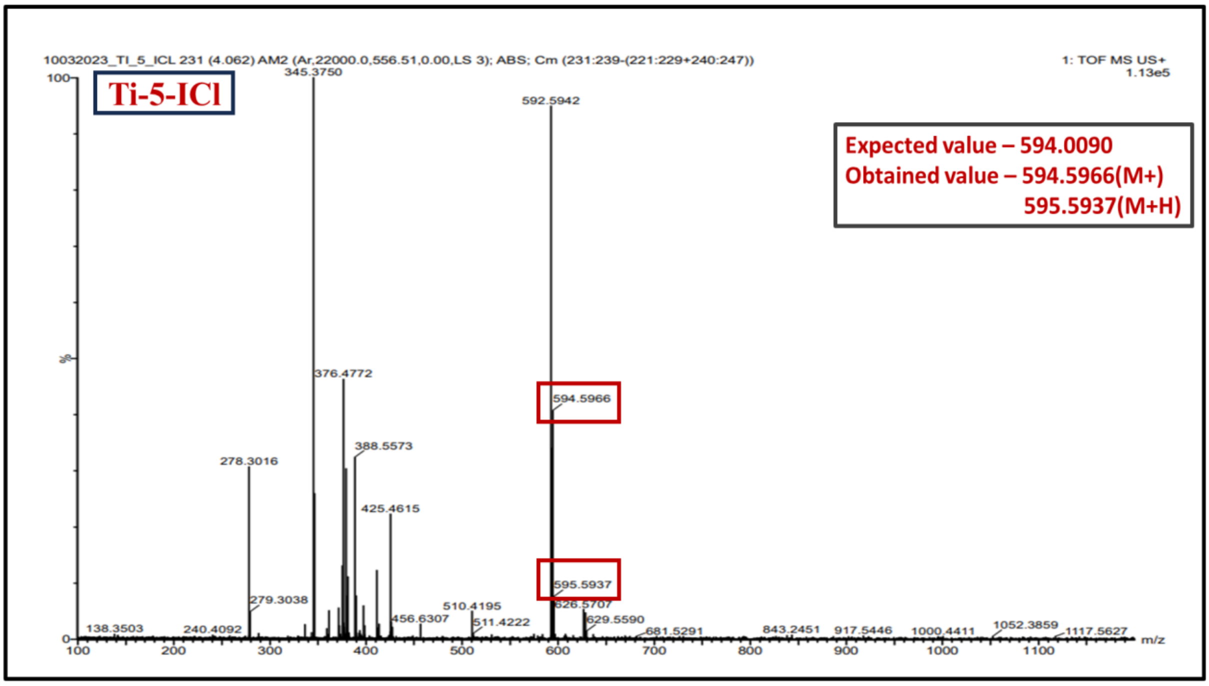

Figure.S49. ESI-MS spectrum of complex Ti-5-ICl

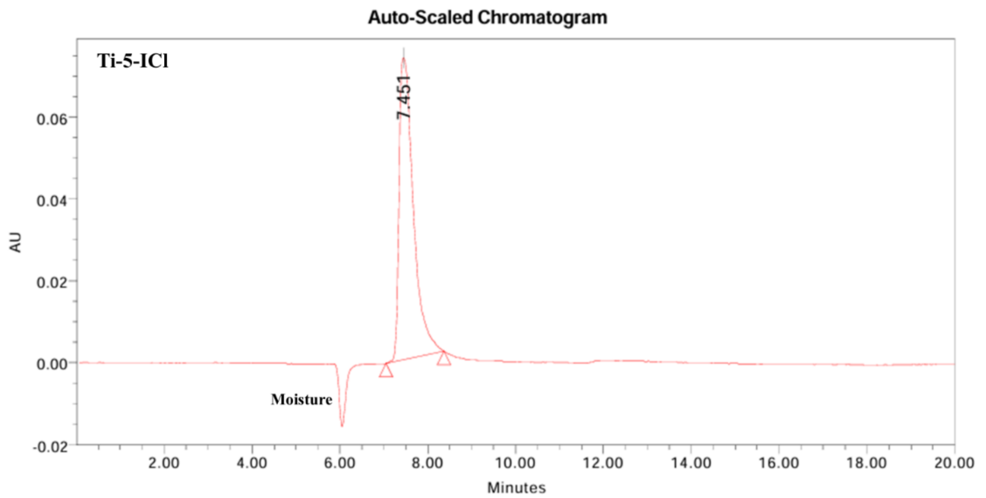

Peak Results

	Name	RT	Area	Height	Amount	Units
1		7.451	1666481	73690		

Figure.S50. HPLC spectrum of complex Ti-5-ICl

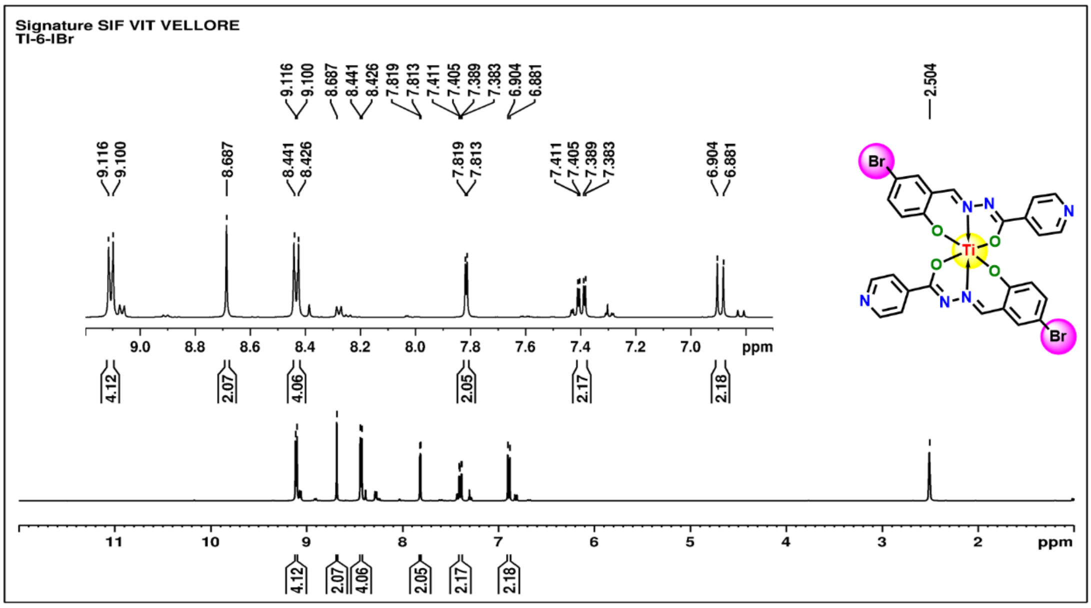

Figure.S51. ^{1}H NMR spectrum of complex Ti-6-IBr (400 MHz, DMSO-d_6)

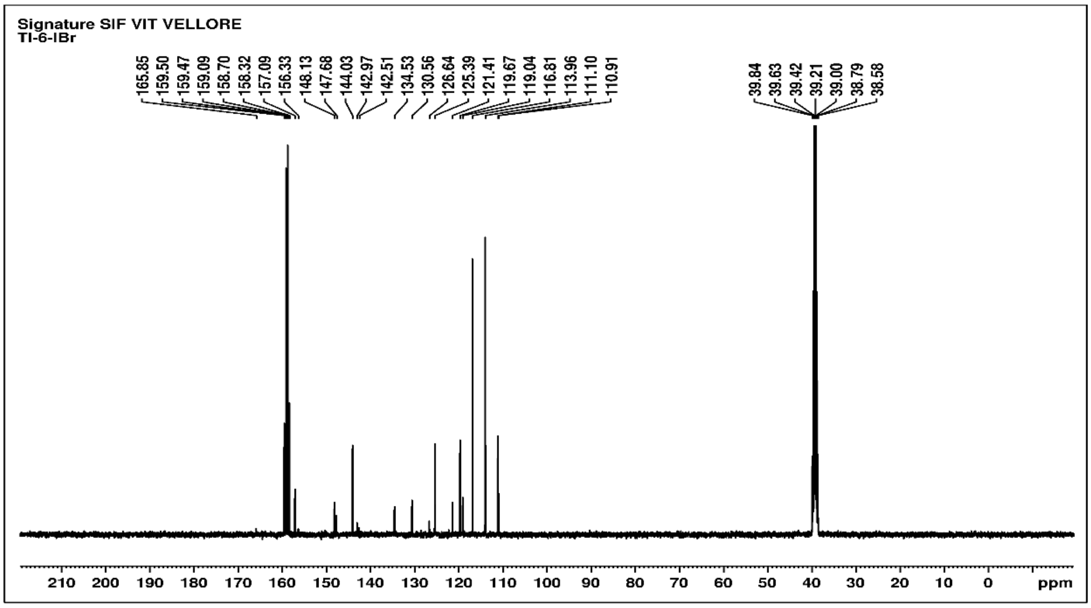

Figure.S52. ^{13}C NMR spectrum of complex Ti-6-IBr (400 MHz, DMSO-d_6)

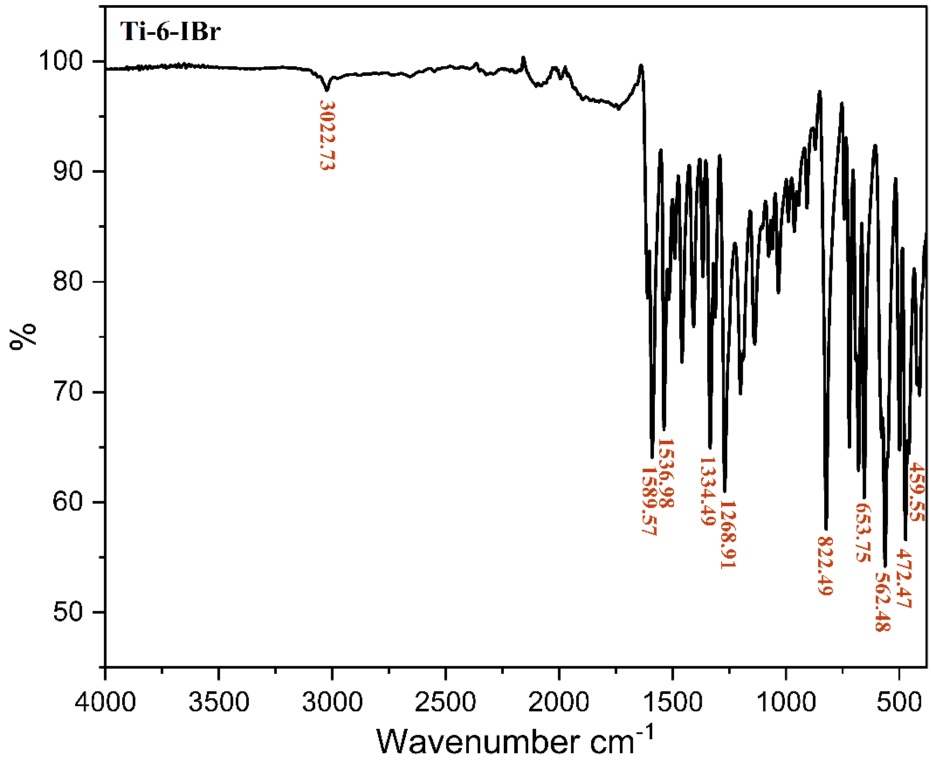

Figure.S53. FTIR spectrum of complex Ti-6-IBr

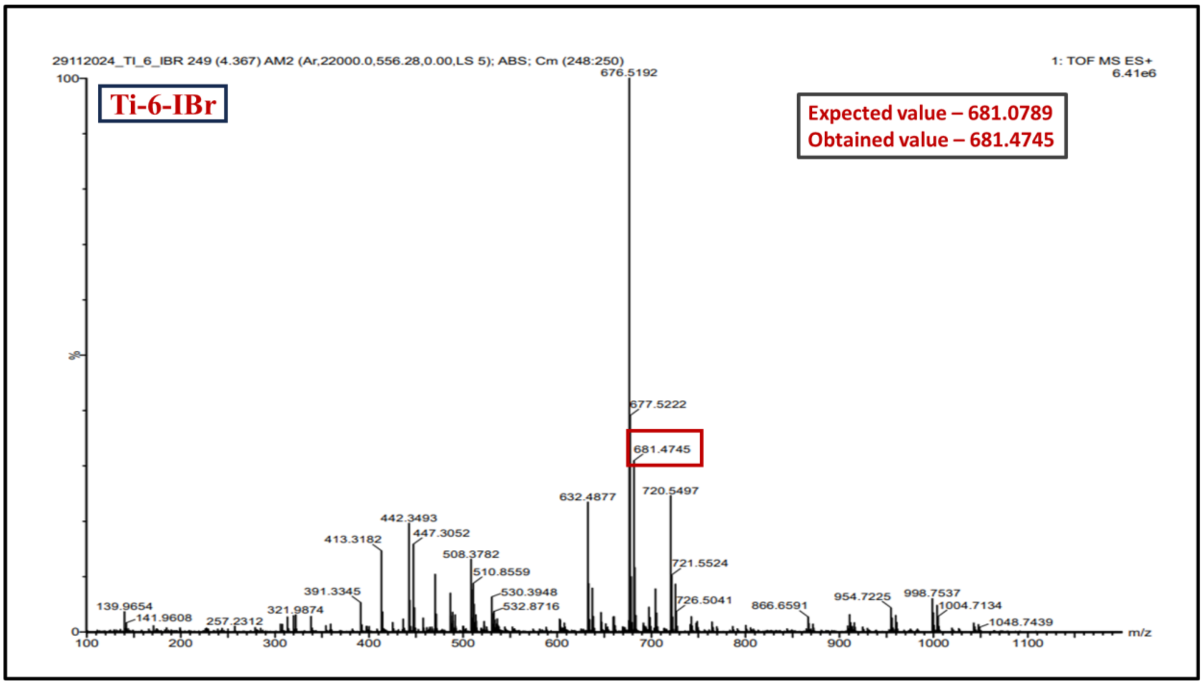

Figure.S54. ESI-MS spectrum of complex Ti-6-IBr

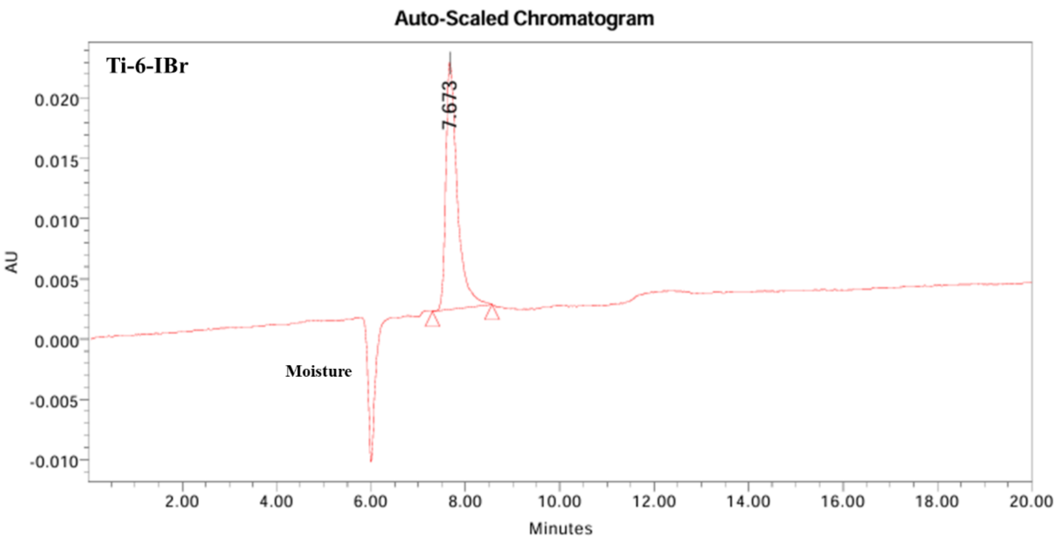

Peak Results

	Name	RT	Area	Height	Amount	Units
1		7.673	344930	20554		

Figure.S55. HPLC spectrum of complex Ti-6-IBr

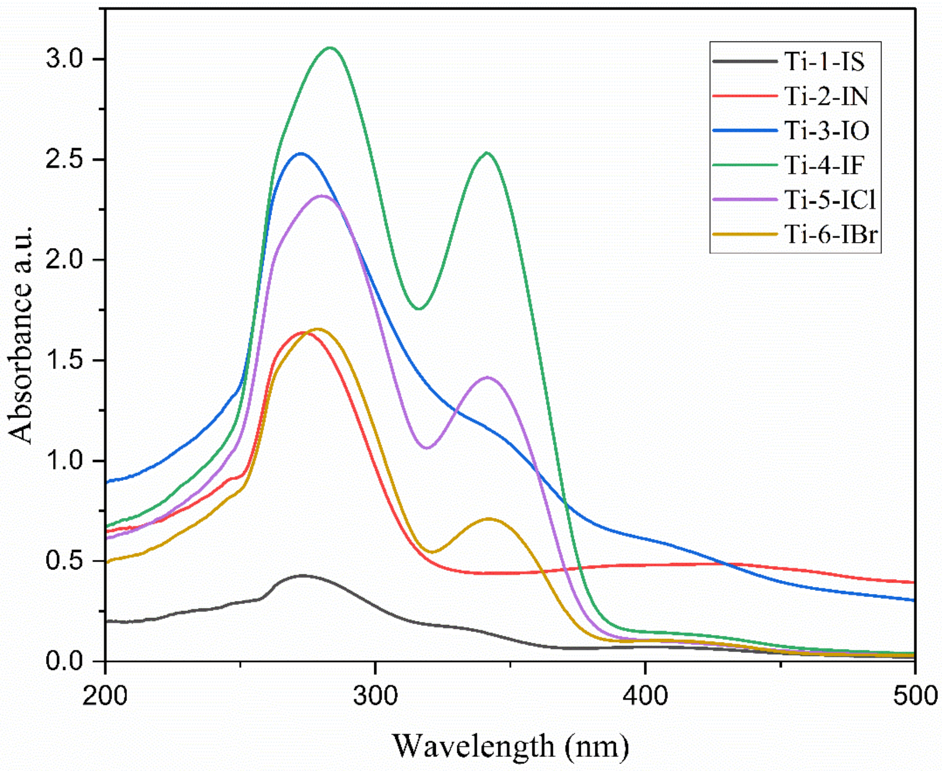

Fig.S56. UV-Vis Spectra of Ti(IV) complexes in DMSO: H_2O (1:9)

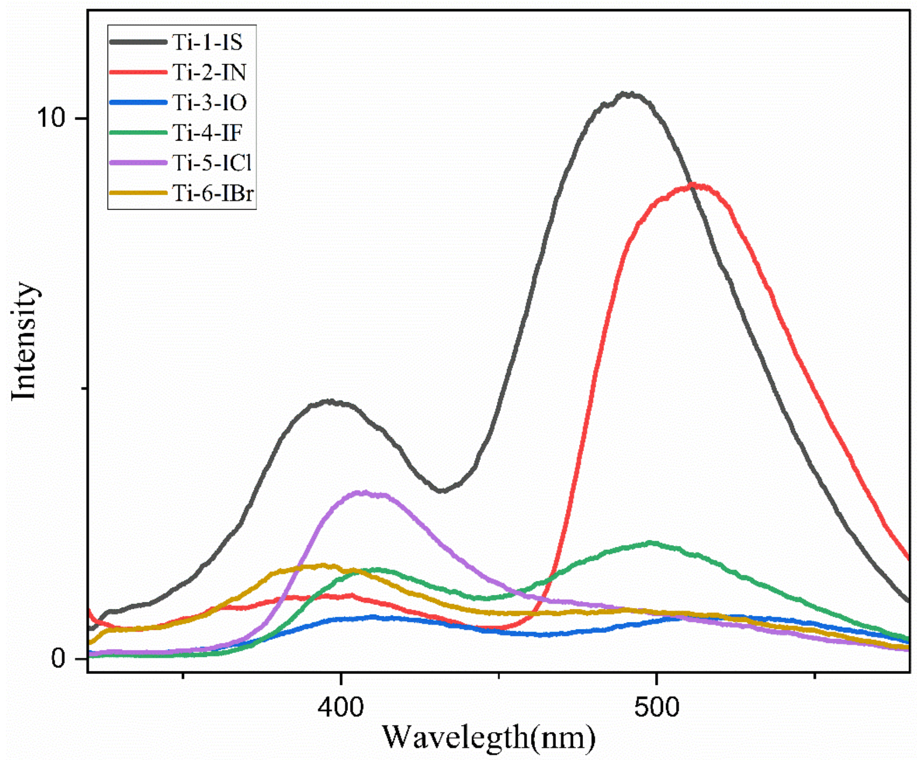

Fig.S57. Fluorescence Spectra of Ti(IV) complexes in DMSO: H_2O (1:9)

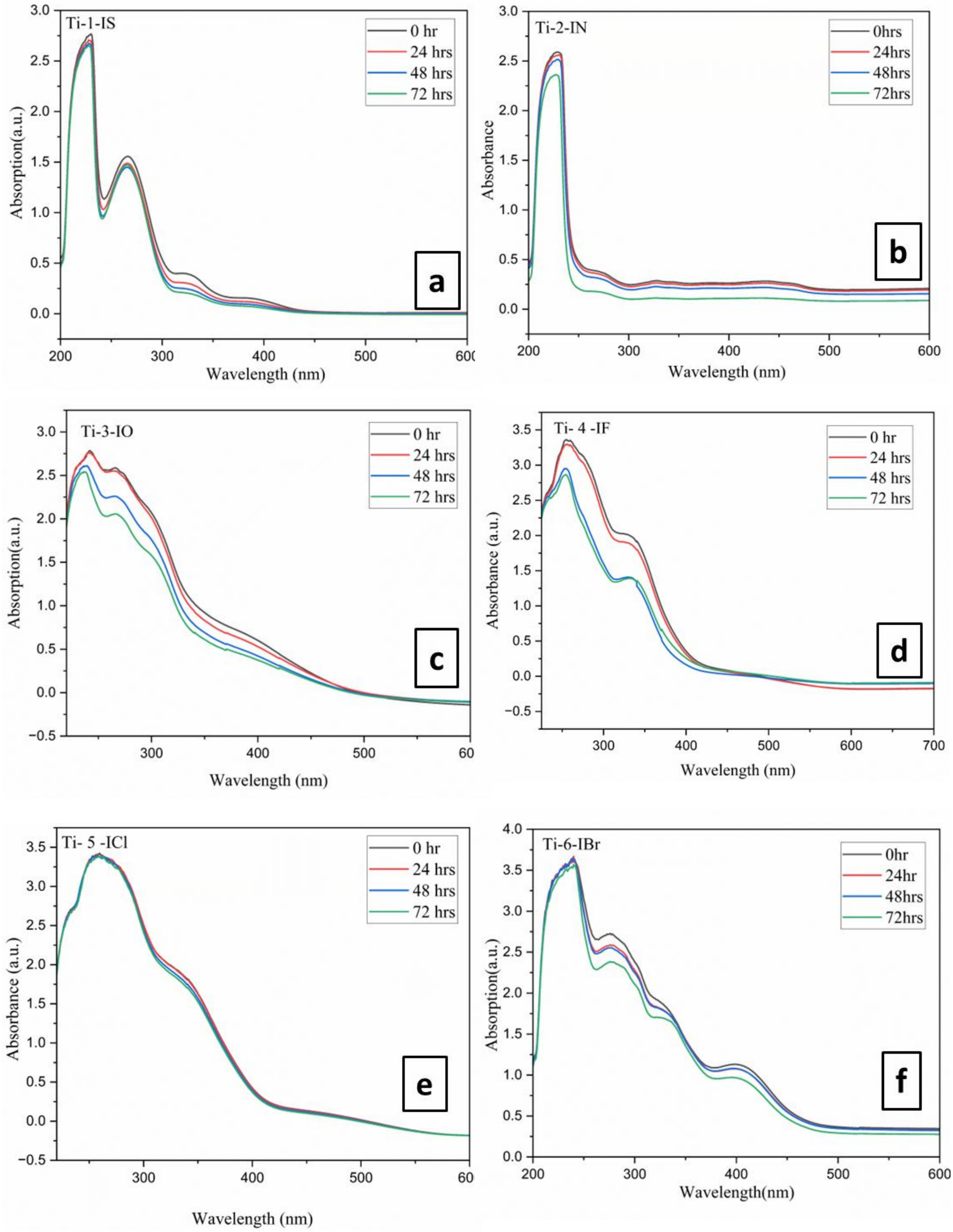

Fig.S58. UV-Vis stability study of Ti(IV) complexes in 1:9 DMSO: H_2O medium

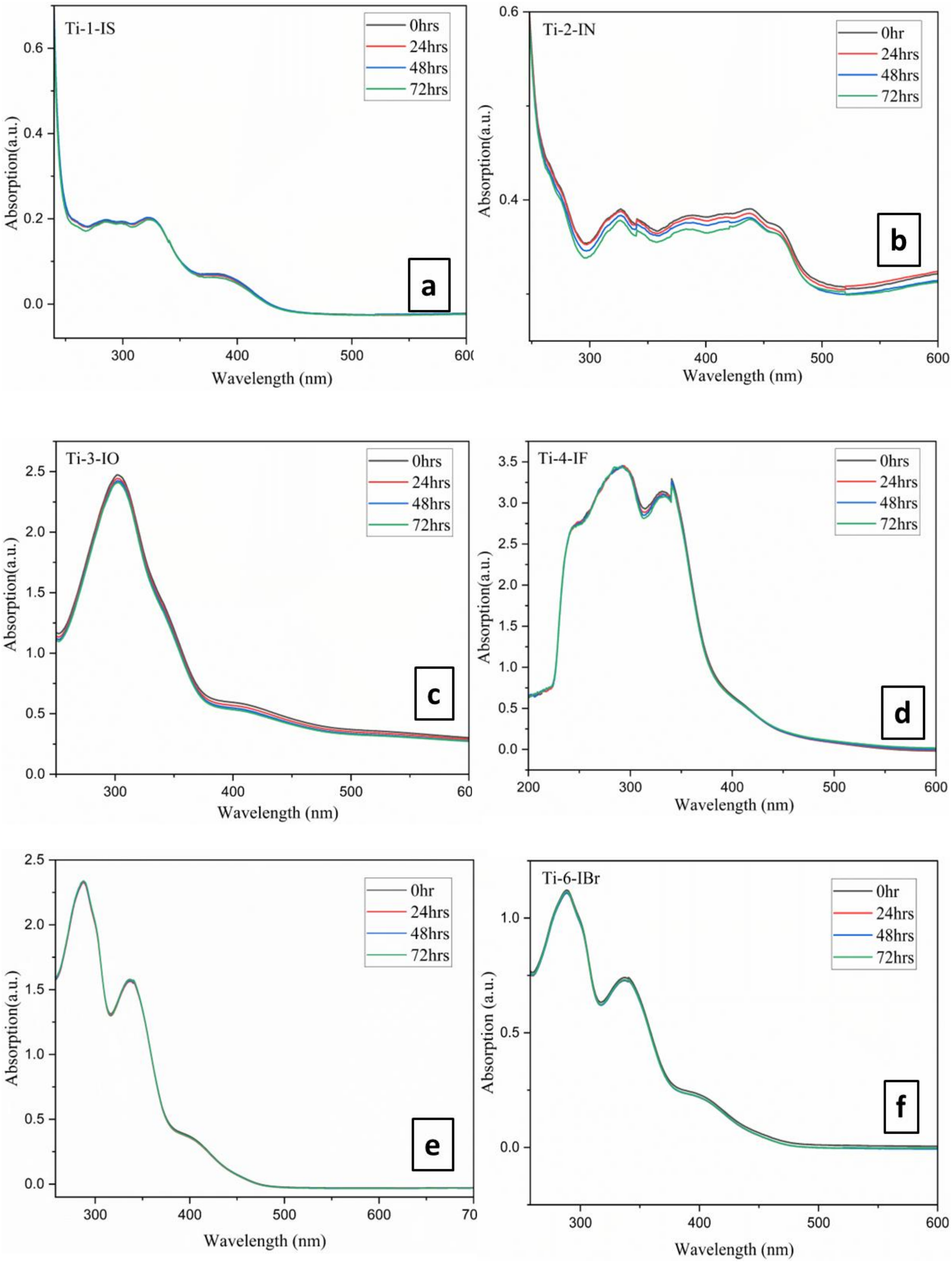

Fig.S59. UV-Vis stability study of Ti(IV) complexes in GSH medium

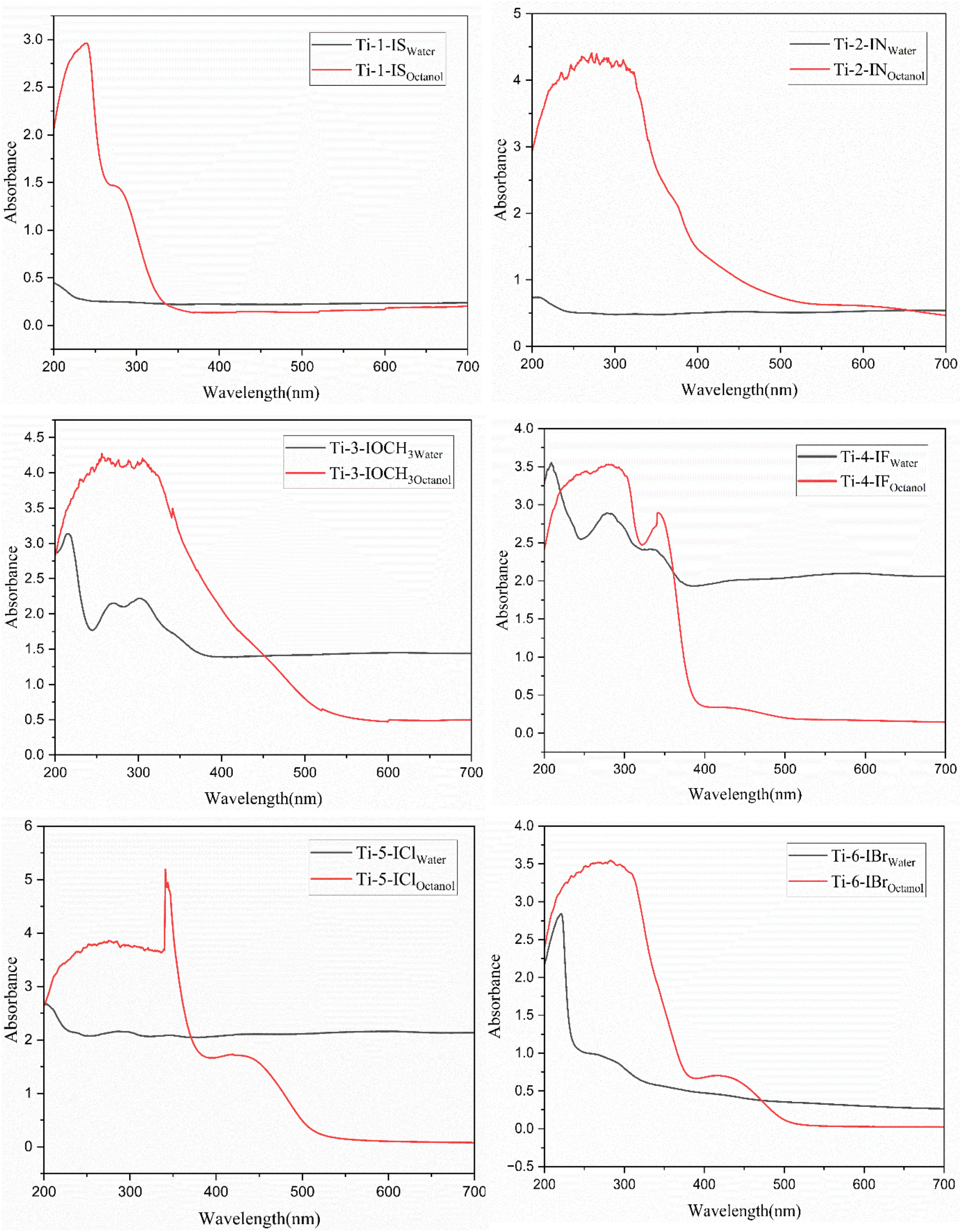

Fig. S60. UV-visible spectra of Ti(IV) complexes for Lipophilicity study of complexes in octanol: water

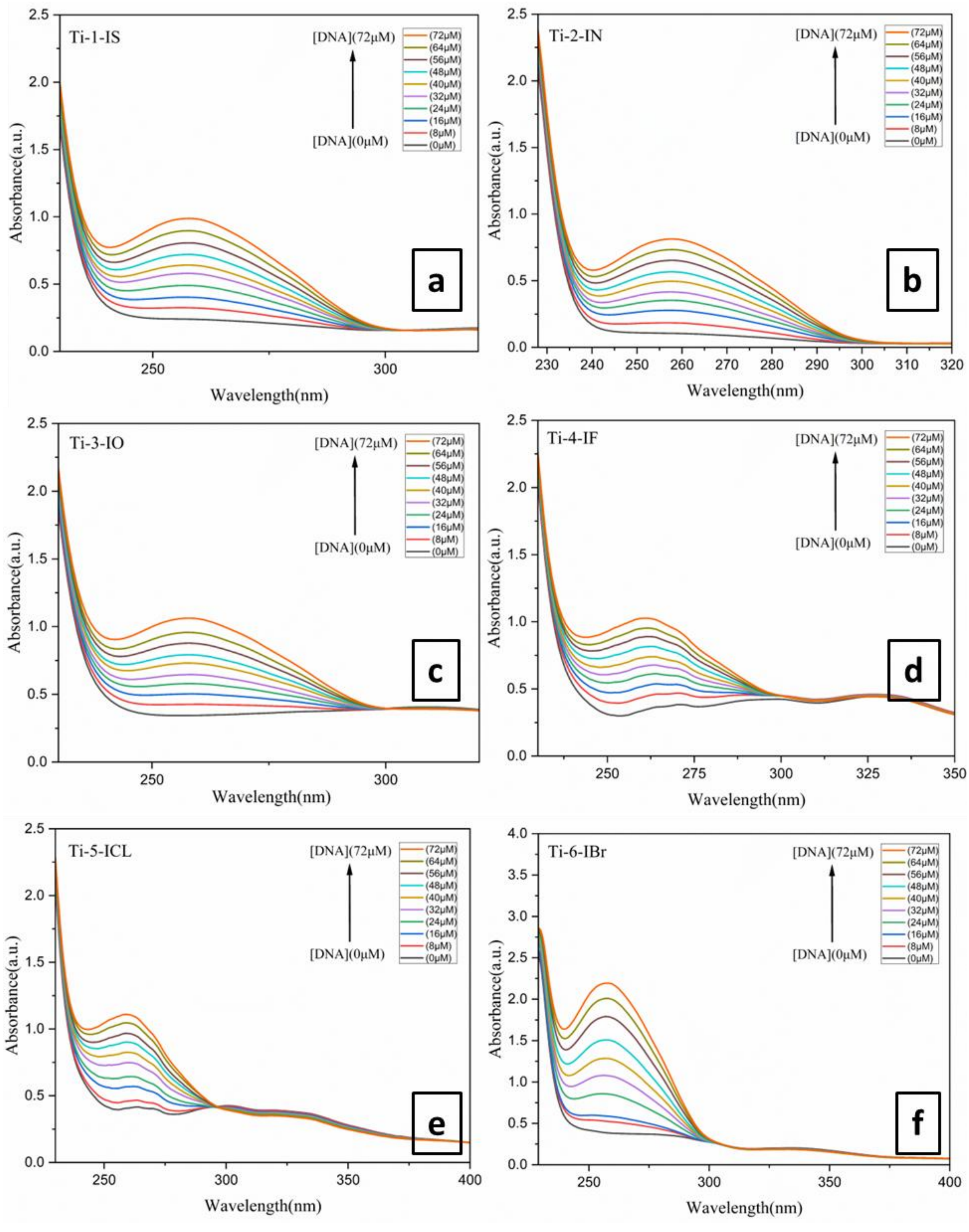

Fig.S61. UV-Visible spectra of DNA Binding studies of Ti(IV) complexes

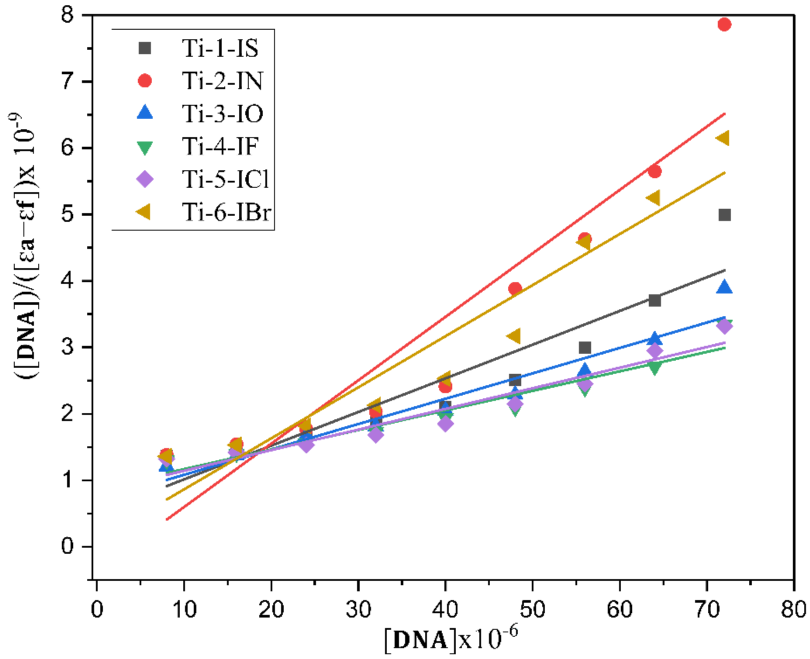

Fig.S62. Linear plots of DNA UV-binding studies of Ti(IV) complexes

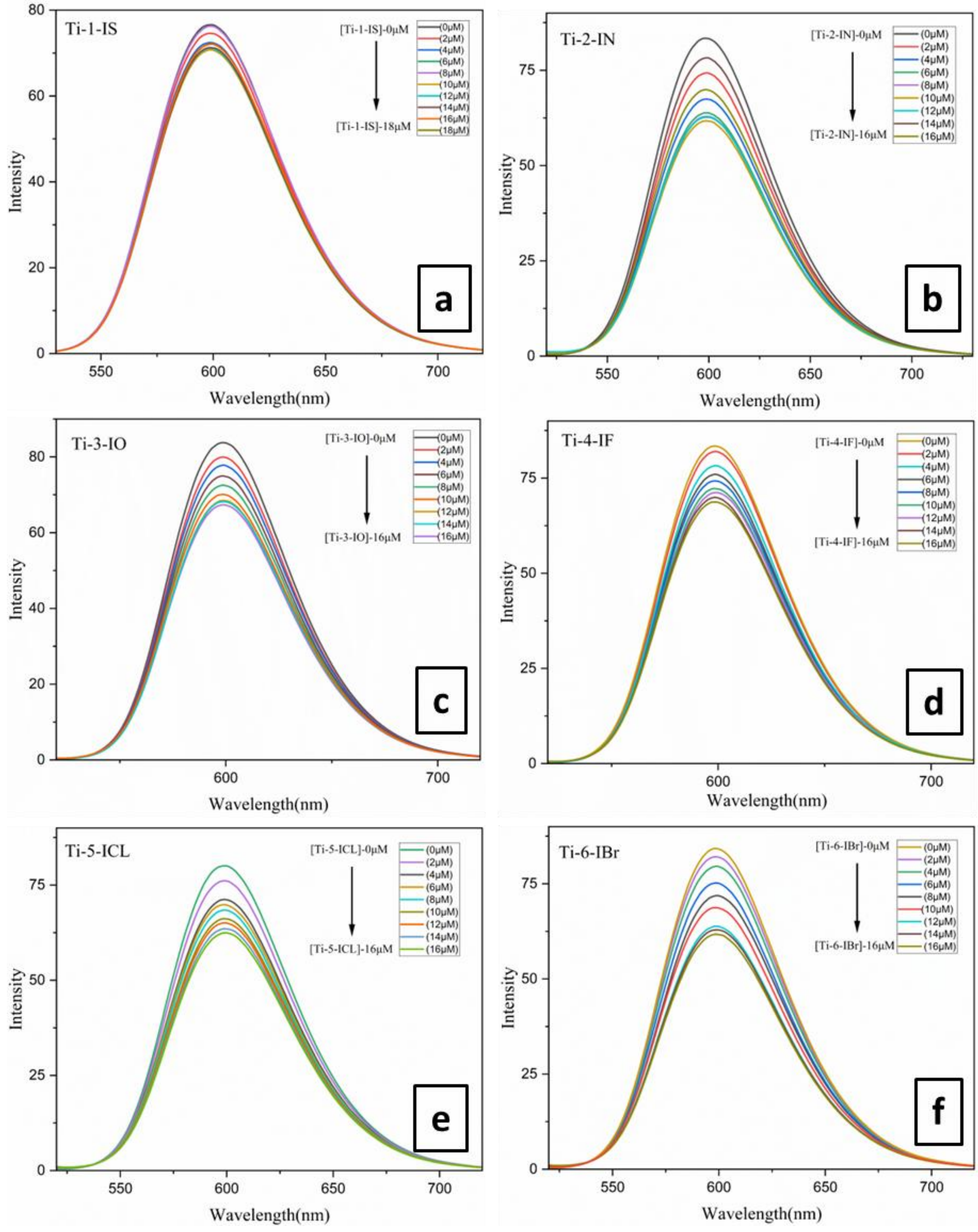

Fig.S63. Fluorescence quenching spectra of DNA with increasing concentration of Ti(IV) complexes

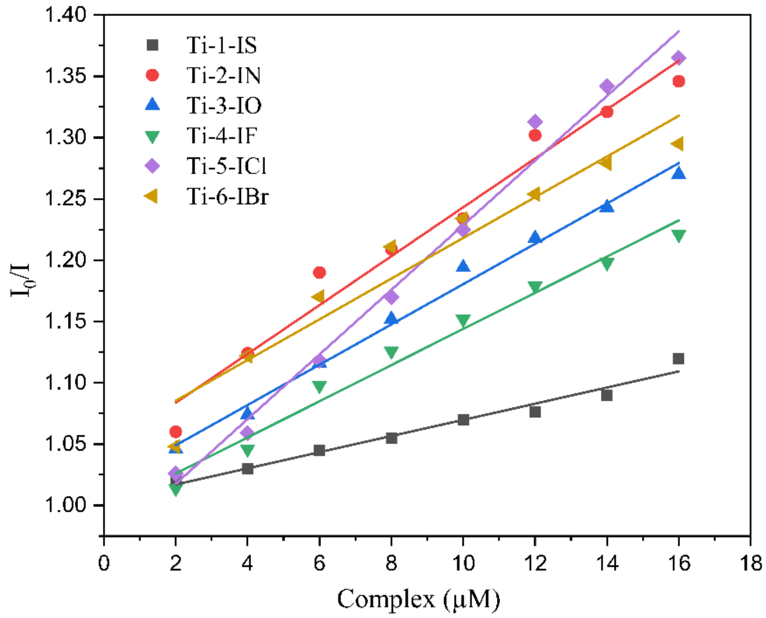

Fig.S64. Stern-Volmer plots of I_0/I vs. Ti(IV) complexes

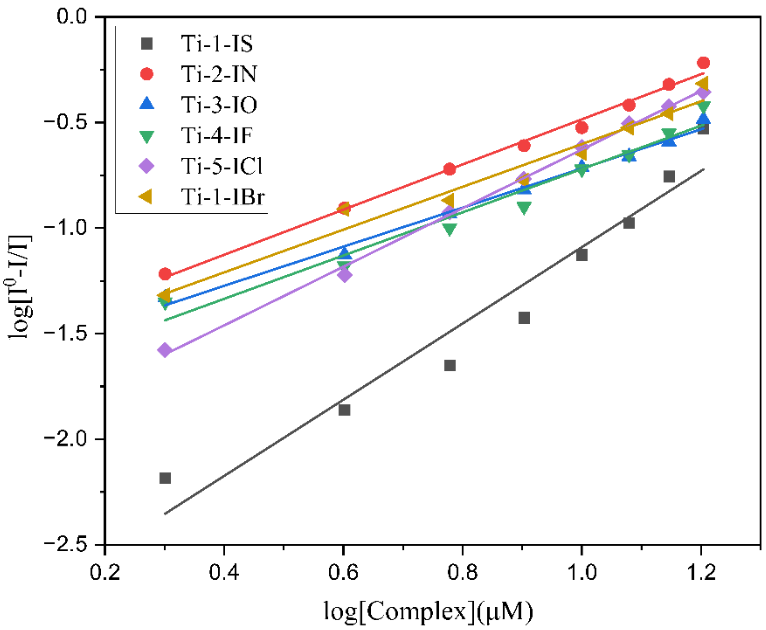

Fig.S65. Scatchard plot of log($[I_0$-I]/I) vs. log [Ti(IV) complexes]

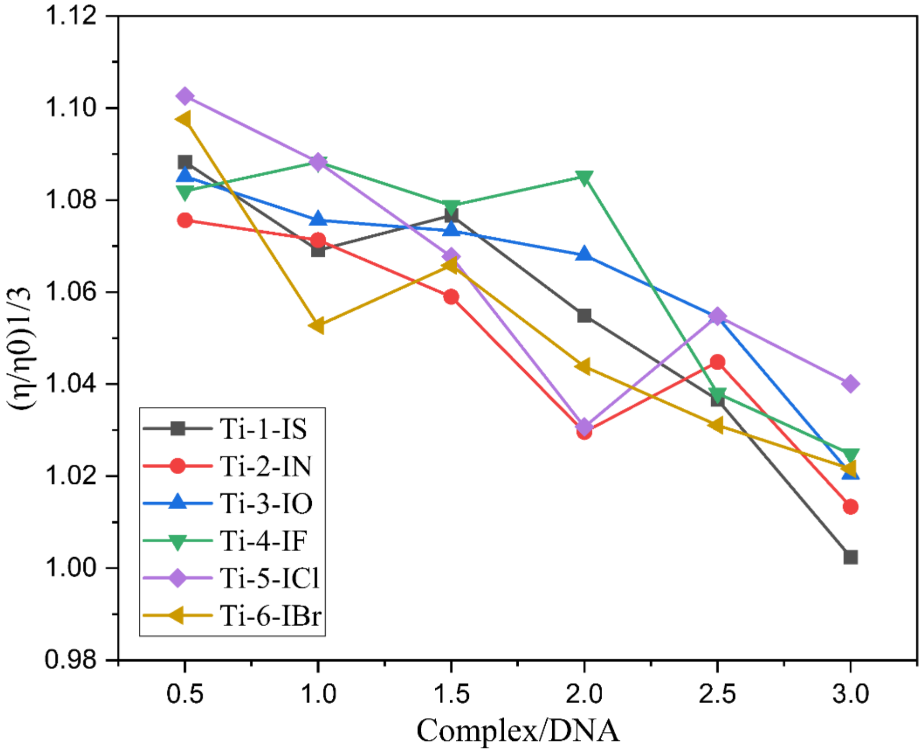

Fig.S66. Viscosity Studies of Ti(IV) complexes

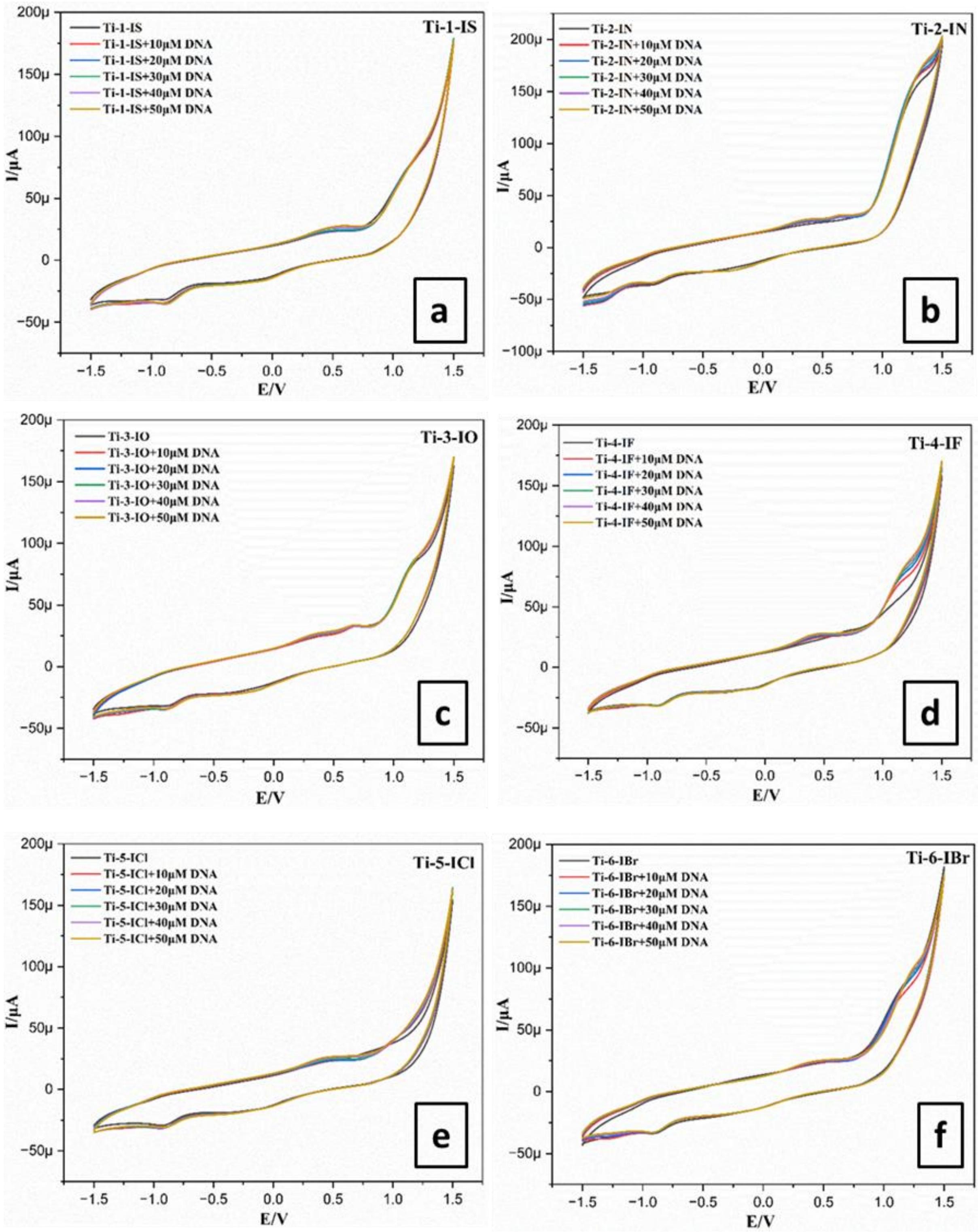

Fig.S67. Cyclic voltammetry DNA binding Studies of Ti(IV) complexes

Table S1: Oxidation and reduction peaks obtained from Cyclic Voltammograms of Ti(IV) complexes with CT-DNA(0–50 µM)

Complexes	Oxidation peak	Reduction peak
Ti-1-IS	-0.877, 0.533, 1.099	-0.860, -0.117, 1.327
Ti-2-IN	-1.328, -0.924, -0.233	-0.920, -0.335
Ti-3-IO	-0.892, -0.264	-0.900, -0.355, -0.665, 1.161
Ti-4-IF	-0.892, -0.417, 1.16	-0.892, -0.148, 0.859
Ti-5-ICl	-0.932, 0.425	-0.916, -0.218, 0.750
Ti-6-IBr	-0.908, 0.440, 1.239	-1.249, -0.908, -0.055

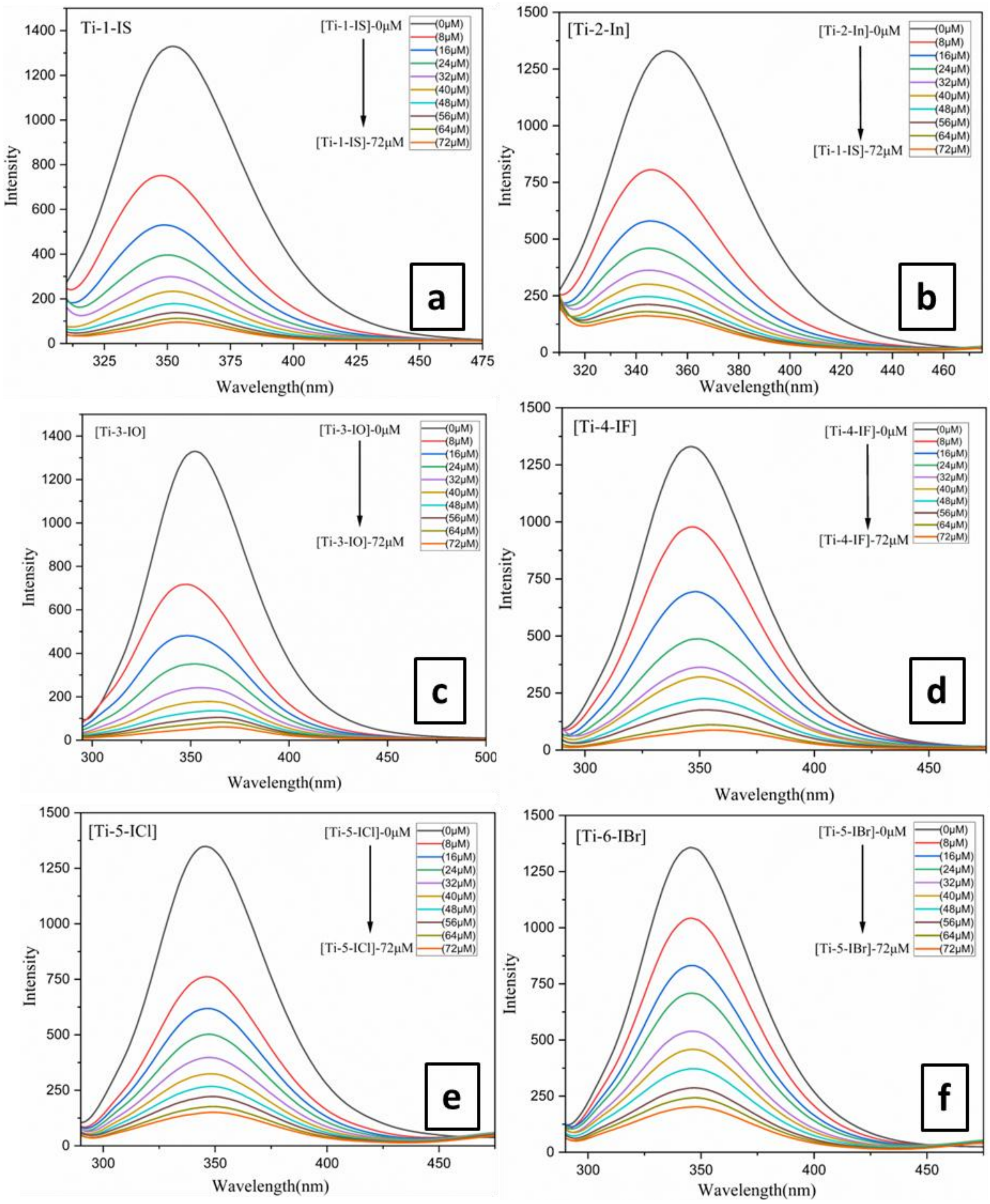

Fig.S68. Fluorescence quenching spectra of BSA with increasing concentration of Ti(IV) complexes

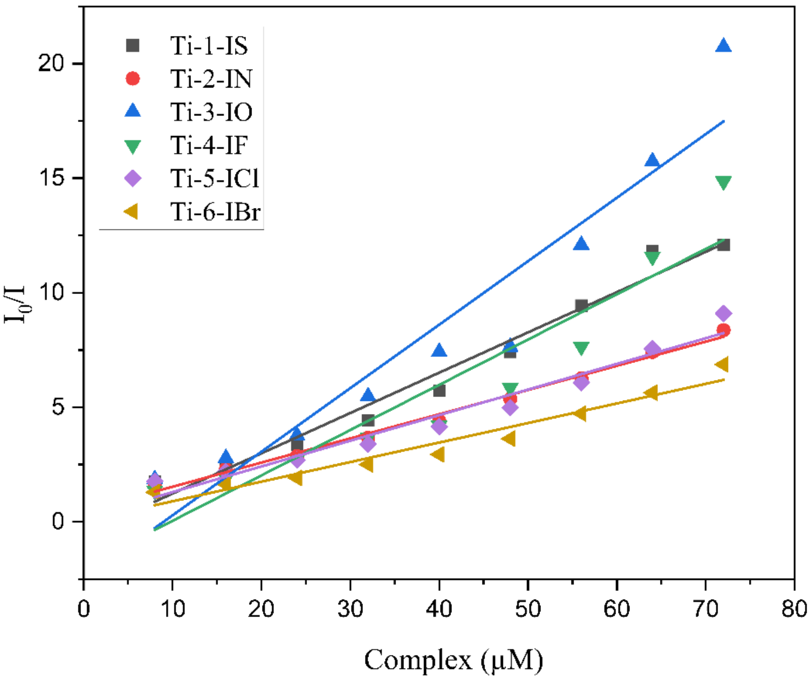

Fig.S69. Stern-Volmer plots of I_0/I vs. complex

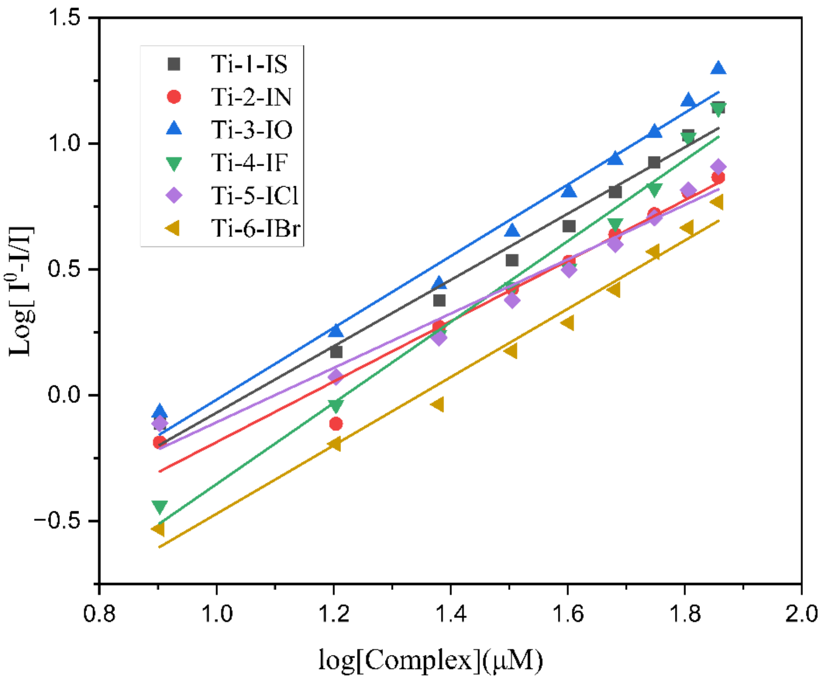

Fig.S70. Scatchard plot of log([I_0-I]/I) vs. log [complex]

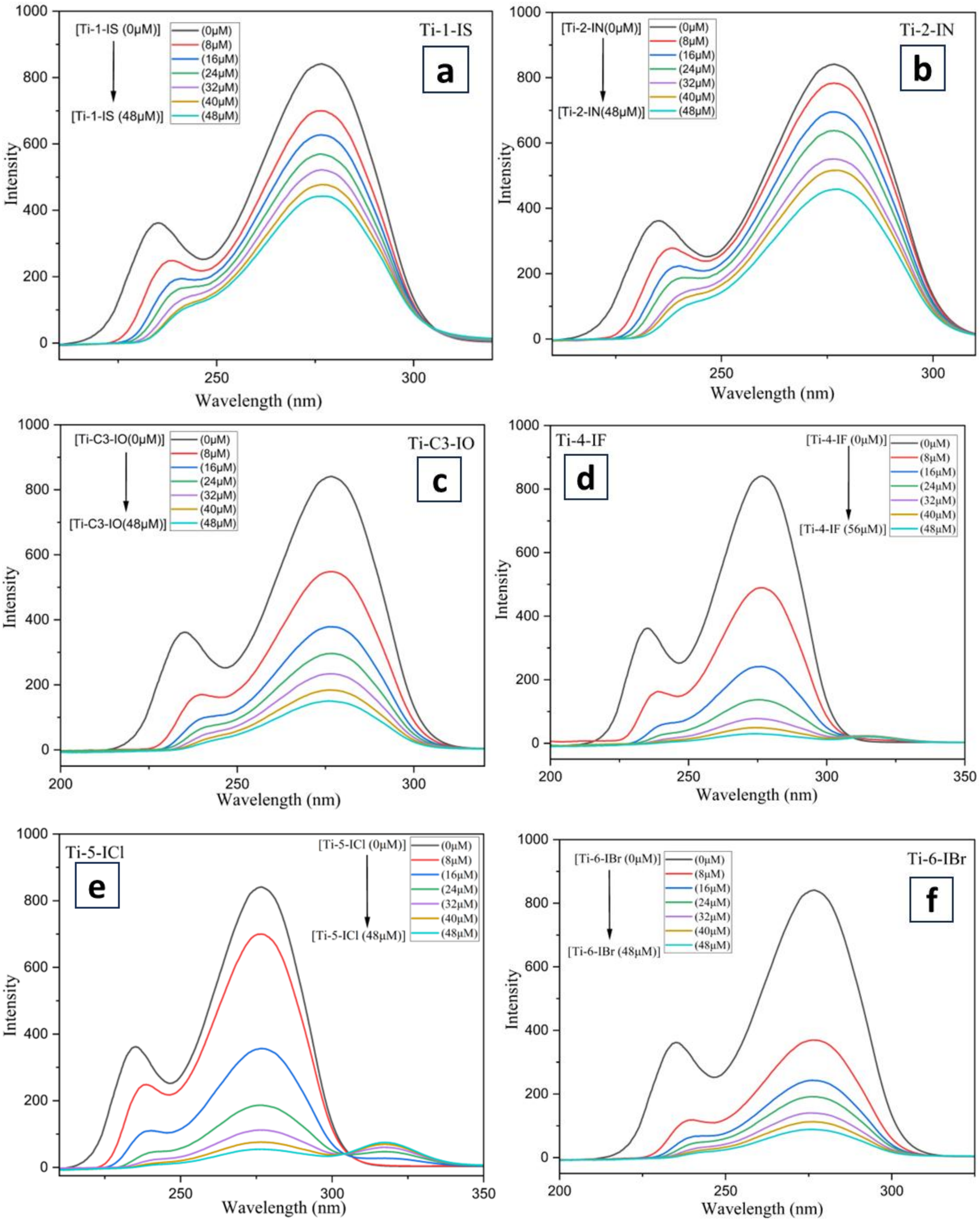

Fig.S71. Synchronous spectra of BSA with increasing concentration of Ti(IV) complexes at Δλ=15 nm

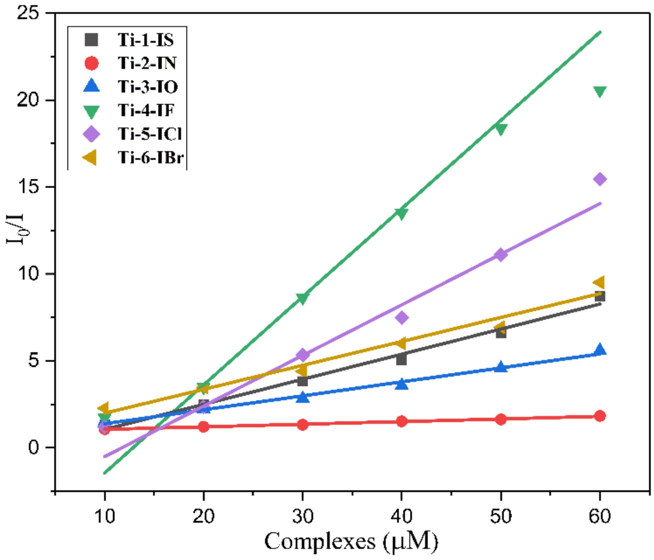

Fig.S72. Stern-Volmer plots of I_0/I vs. complex of Synchronous spectra of BSA with increasing concentration of Ti(IV) complexes at Δλ=15 nm

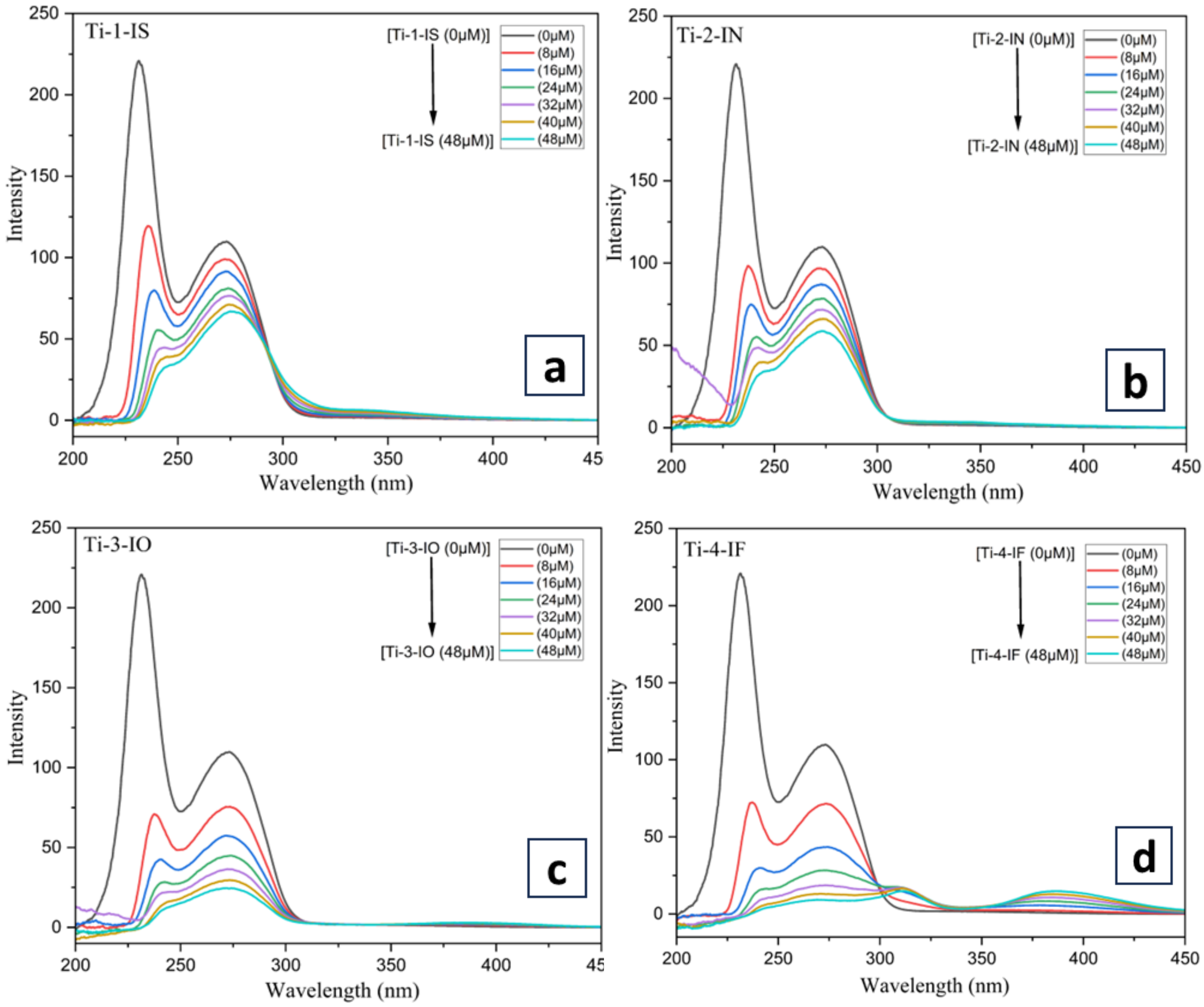

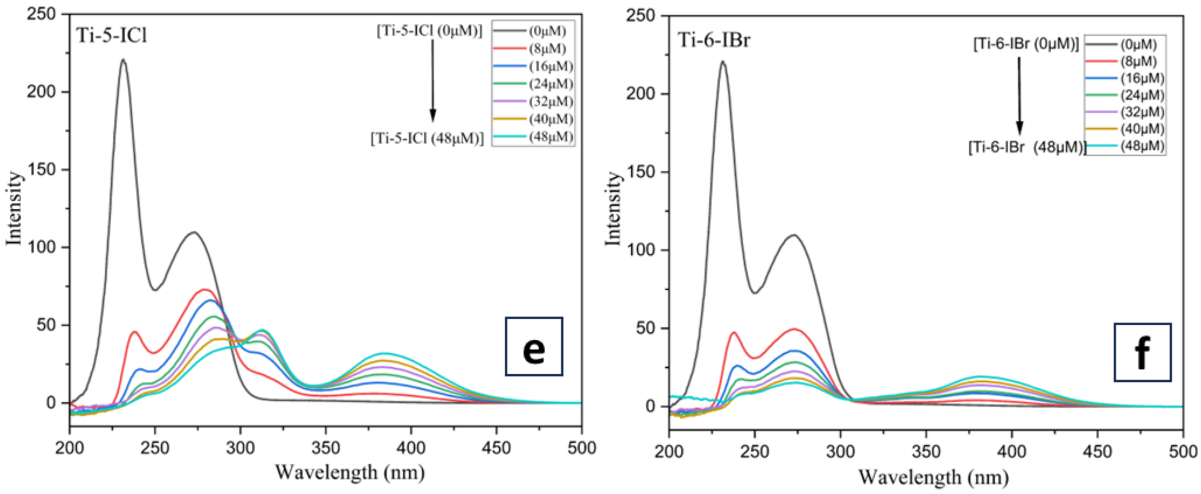

Fig.S73. Synchronous spectra of BSA with increasing concentration of Ti(IV) complexes at Δλ=60 nm

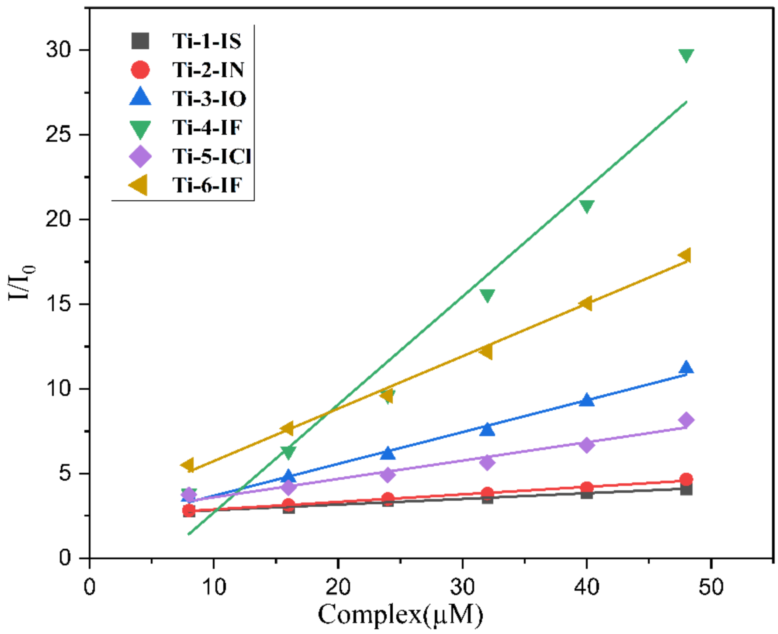

Fig.S74. Stern-Volmer plots of I_0/I vs. complex of Synchronous spectra of BSA with increasing concentration of Ti(IV) complexes at Δλ=60 nm

Table S2; Stern-Volmer plots of I_0/I vs. complex of Synchronous spectra of BSA with increasing concentration of Ru(II) complexes at Δλ=15 nm and 60nm

Complexes	Ka Δλ=15nm	Ka Δλ=60 nm
Ti-1-IS	0.1444	0.0334
Ti-2-IN	0.0150	0.0445
Ti-3-IO	0.0803	0.1882
Ti-4-IF	0.5071	0.6377
Ti-5-ICl	0.2911	0.1084
Ti-6-IBr	0.1376	0.3096

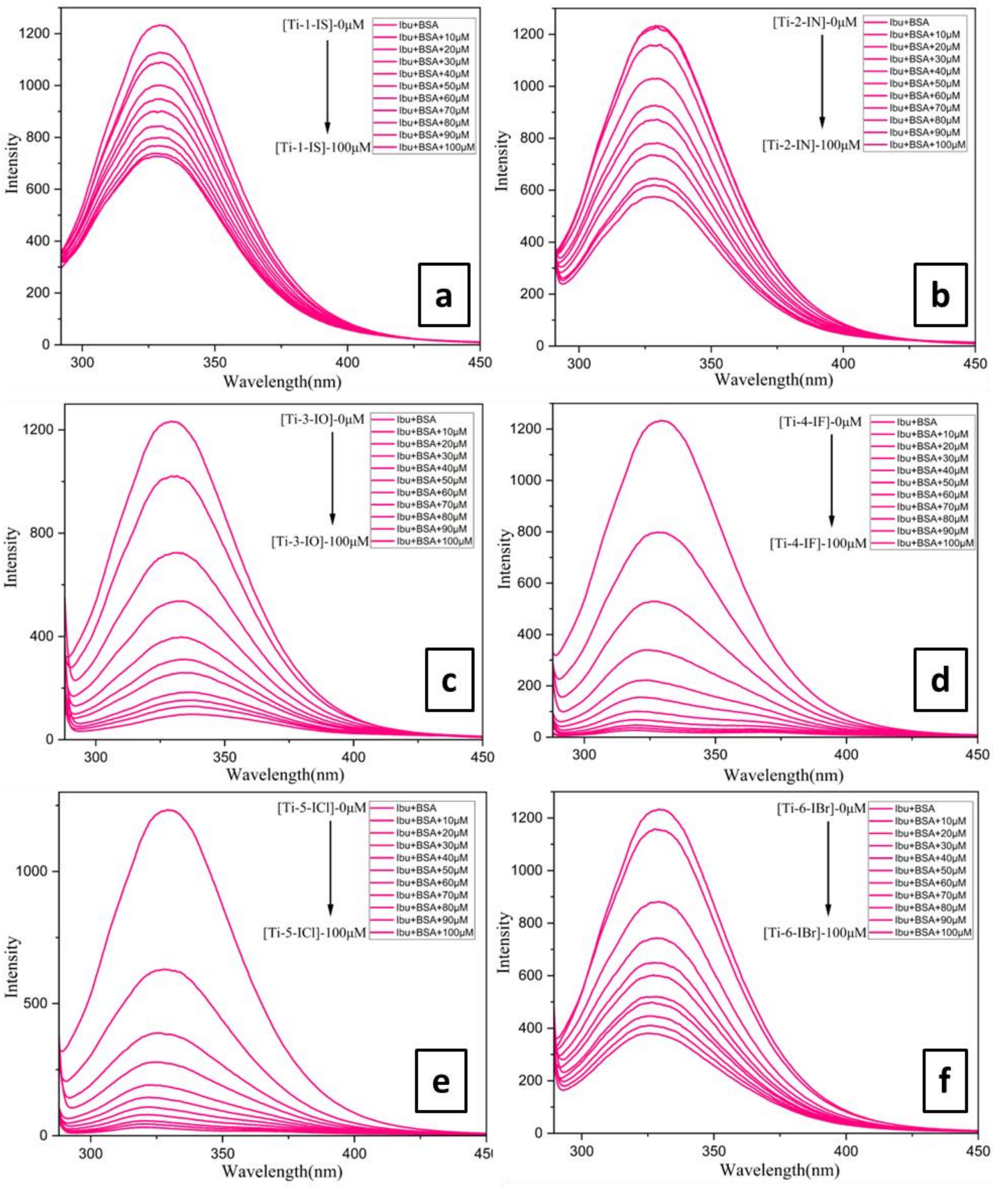

Fig.S75. Site marker fluorescence quenching studies of BSA+Ibuprofin with an increase in the concentration of Ti(IV) complexes

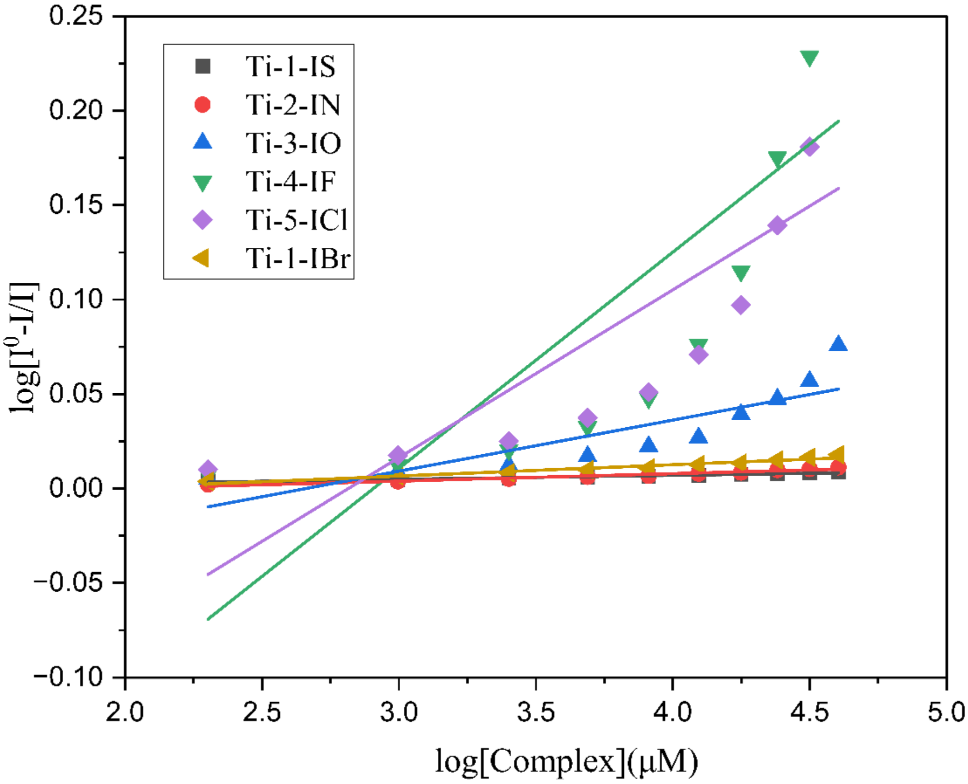

Fig.S76. Scatchard plot of log([I_0-I]/I) vs log [complex]of site marker fluorescence quenching studies of BSA+Ibuprofin

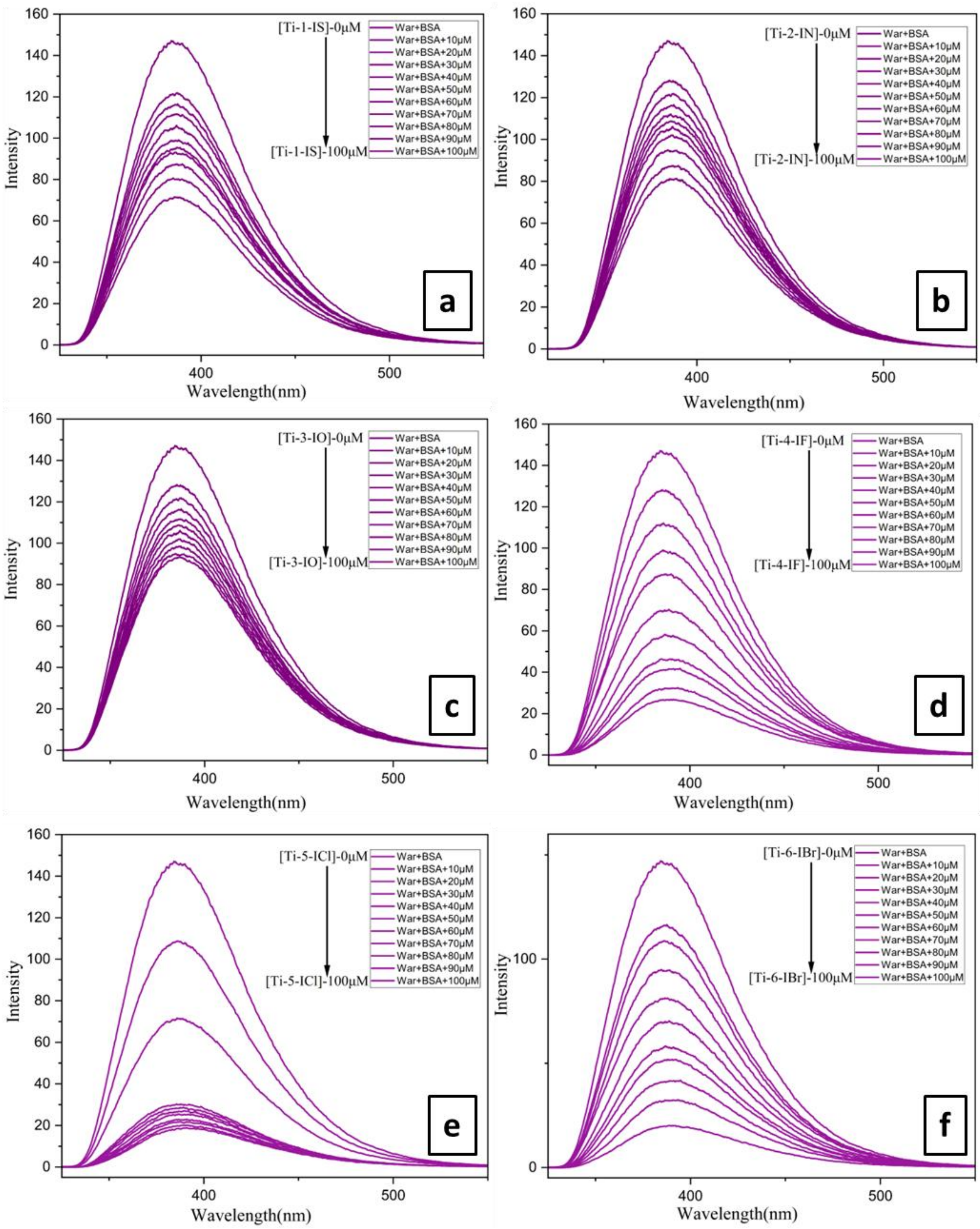

Fig.S77. Site marker fluorescence quenching studies of BSA+Warfarin with an increase in the concentration of Ti(IV) complexes

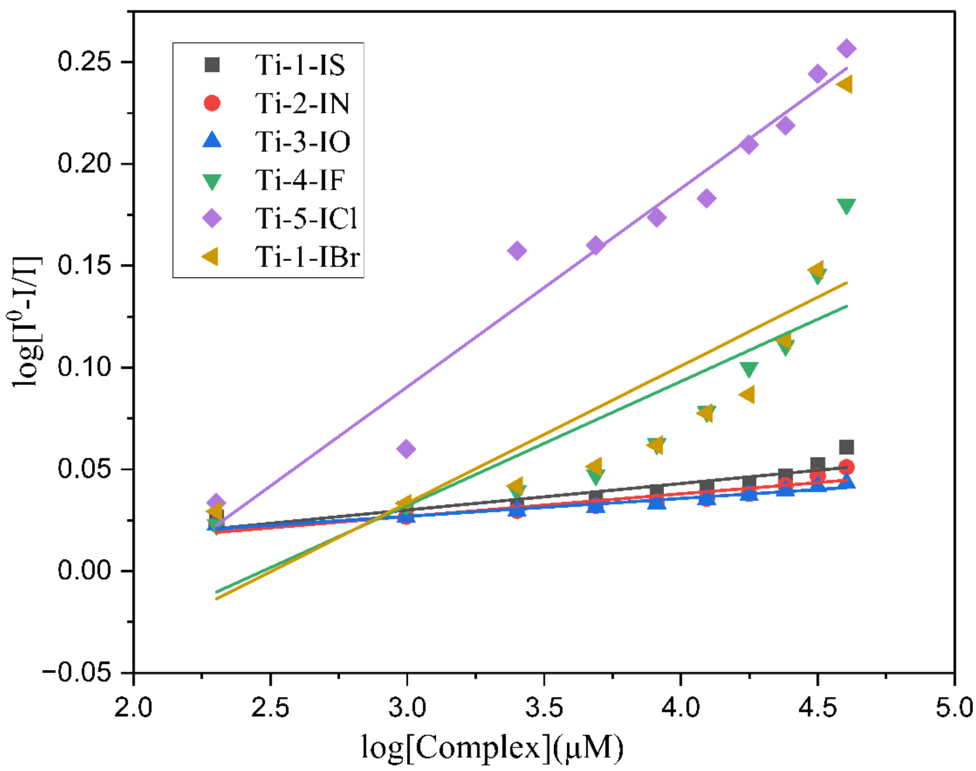

Fig.S78. Scatchard plot of log([I_0-I]/I) vs log [complex]of site marker fluorescence quenching studies of BSA+Warfarin

Table S3; The comparison of binding constants of the complexes Ti(IV) with BSA before and after the addition of site probe at 298 K. K_b binding constant [a]

COMPLEXES	BSA Kb [a] (× 10^4 M^{-1})	BSA+Ibuprofen Kb [a] (× 10^4 M^{-1})	BSA + Warfarin Kb [a] (× 10^4 M^{-1})
Ti-1-IS	**0.040**	0.034	0.048
Ti-2-IN	**0.047**	0.015	0.069
Ti-3-IO	**0.036**	0.050	0.058
Ti-4-IF	**0.011**	0.037	0.040
Ti-5-ICl	**0.065**	0.035	0.016
Ti-6-IBr	**0.014**	0.054	0.039

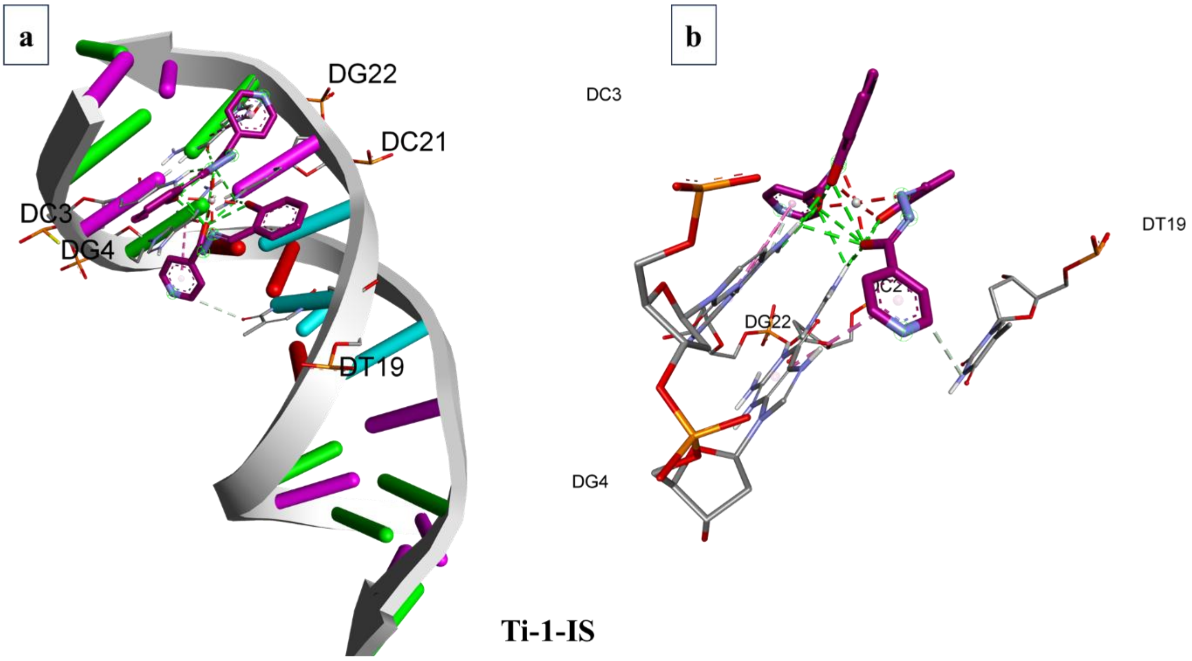

Fig.S79. Molecular docking of DNA with Ti-1-IS; purple color indicates carbon atoms, blue color indicates nitrogen, grey color indicates titanium(IV) ion, red color indicates oxygen atoms

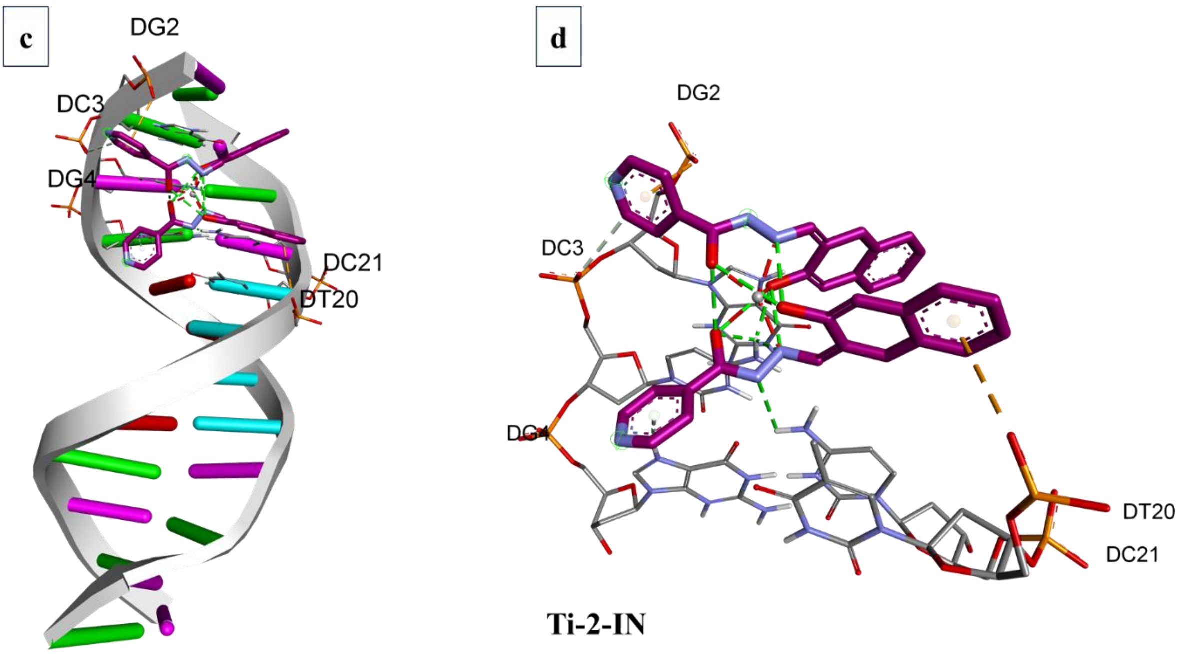

Fig.S80. Molecular docking of DNA with Ti-2-IN ; purple color indicates carbon atoms, blue color indicates nitrogen, grey color indicates titanium(IV) ion, red color indicates oxygen atoms

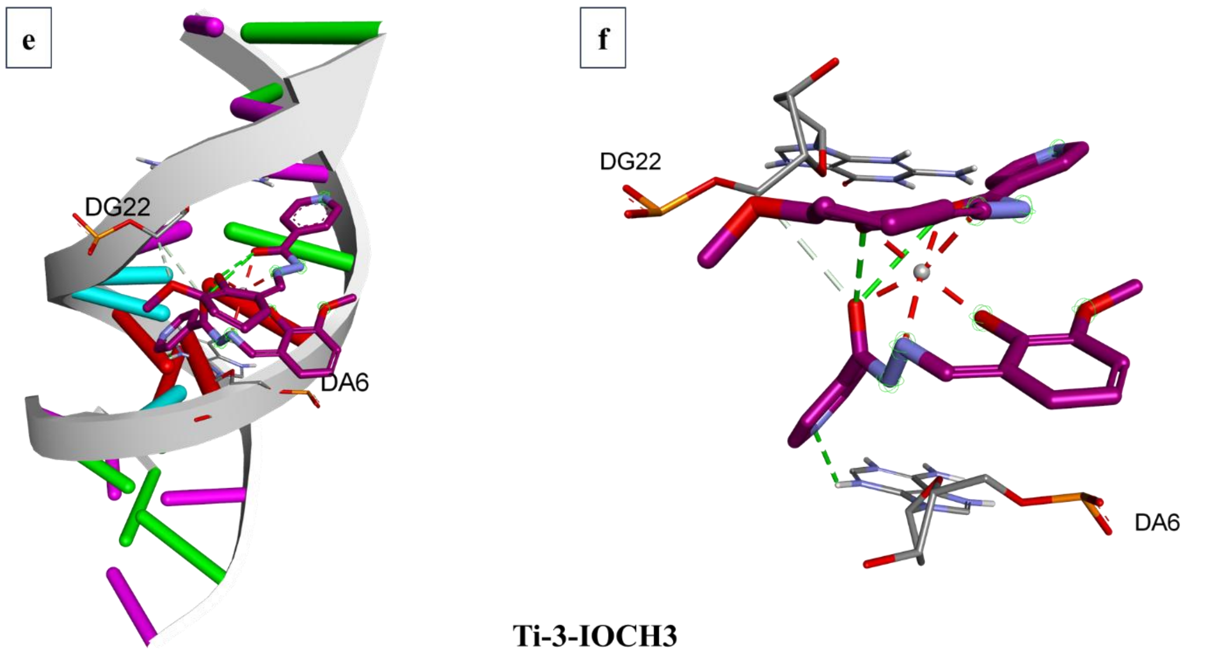

Ti-3-IOCH3

Fig.S81. Molecular docking of DNA with Ti-3-IO ; purple color indicates carbon atoms, blue color indicates nitrogen, grey color indicates titanium(IV) ion, red color indicates oxygen atoms

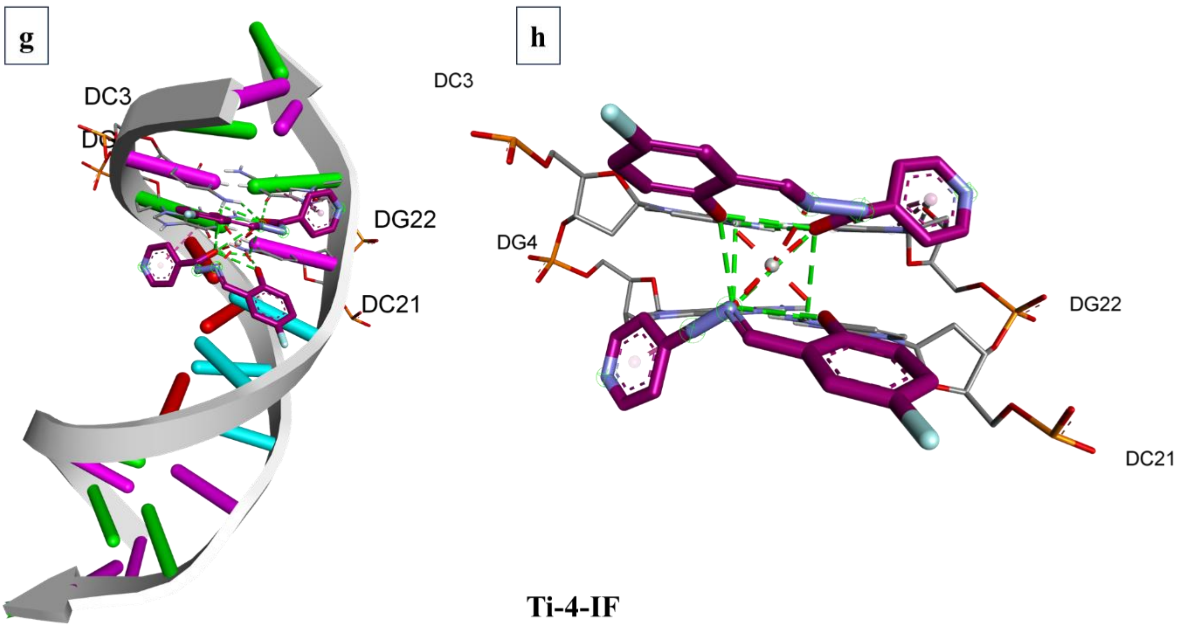

Ti-4-IF

Fig.S82. Molecular docking of DNA with Ti-4-IF ; purple color indicates carbon atoms, blue color indicates nitrogen, grey color indicates titanium(IV) ion, red color indicates oxygen atoms

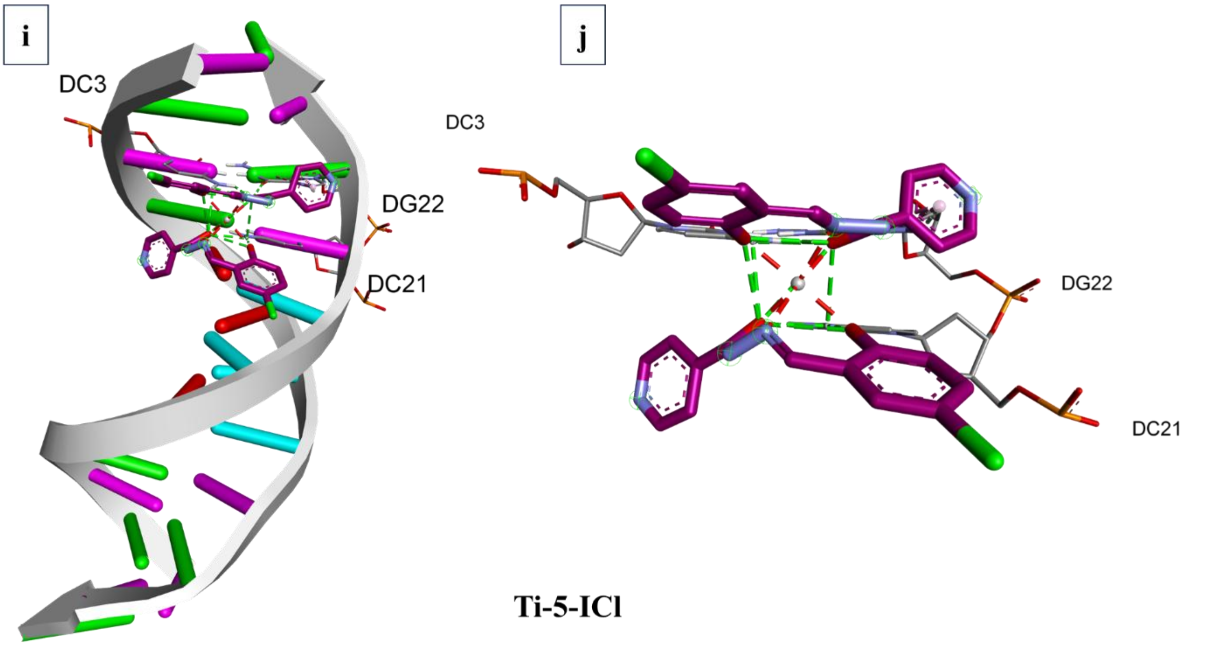

Fig.S83. Molecular docking of DNA with Ti-5-ICl ; purple color indicates carbon atoms, blue color indicates nitrogen, grey color indicates titanium(IV) ion, red color indicates oxygen atoms

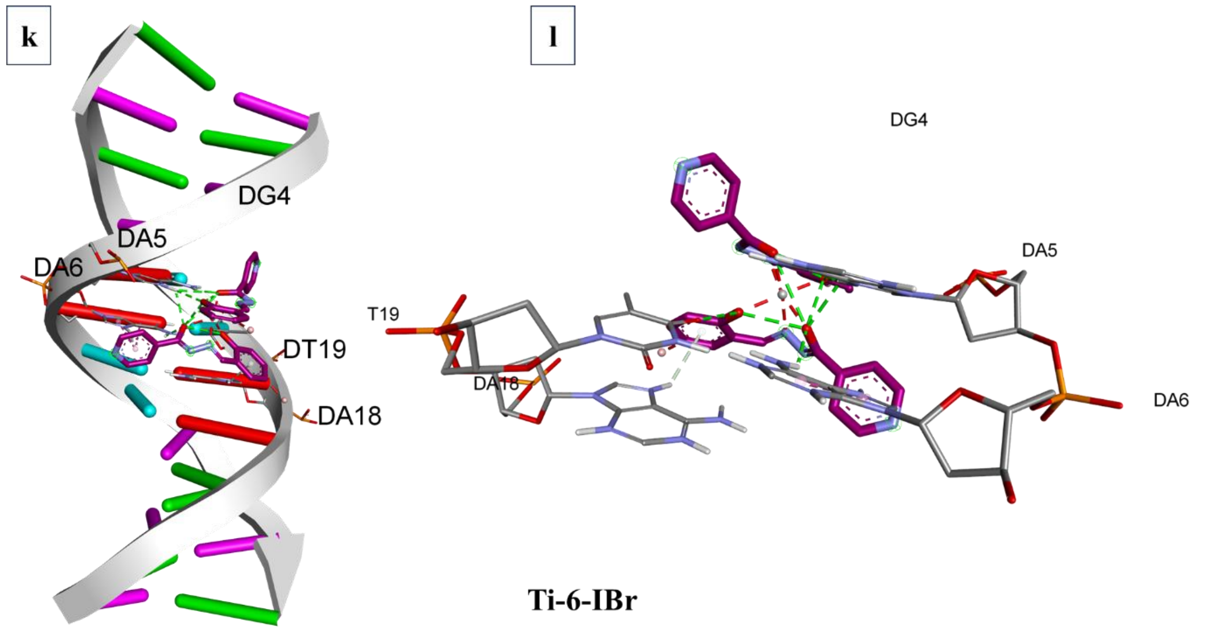

Fig.S84.Molecular docking of DNA with Ti-6-IBr ; purple color indicates carbon atoms, blue color indicates nitrogen, grey color indicates titanium(IV) ion, red color indicates oxygen atoms

Table S4; Docking scores and binding sites of DNA with Ti(IV) complexes

Complexes	Nucleotides	Docking scores in kcal/mol
Ti-1-IS	DC3, DG4, DT19, DC21, DG22	-9.3
Ti-2-IN	DG2, DG4, DC3, DC21, DT20	-10.3
Ti-3-IO	DA6, DG22	-8.4
Ti-4-IF	DC3, DG4, DC21, DG22	-9.7
Ti-5-ICl	DC21, DG22, DC3	-9.7
Ti-6-IBr	DG4,DA5,DA6,DA16, T19	-9.5

Table S5; Docking scores and binding sites of BSA with Ti(IV) complexes

Complexes	Amino acid residues	Docking scores in kcal/mol
Ti-1-IS	GLU182, ARG185, PRO117, LYS116, LEU115, LYS114, PRO516	-10.8
Ti-2-IN	SER109, LYS114, ARG427, GLU424, THR421, PRO420	-11.5
Ti-3-IO	PRO420, VAL423, ILE522, GLU424, SER109, PRO110, ARG144	-9.2
Ti-4-IF	GLU125, THR121, LEU122, LYS136, GLU140, LEU115, LYS116, ASP118	-9.8
Ti-5-ICl	ASP118, THR121, LEU122, GLU125, LYS132, LYS136, GLU140, PRO113, LEU115, LYS116, LEU115, LYS116	-9.9
Ti-6-IBr	THR121, GLU125, LYS132, LYS136, GLU140, LYS116, ASP118, LEU122	-9.7

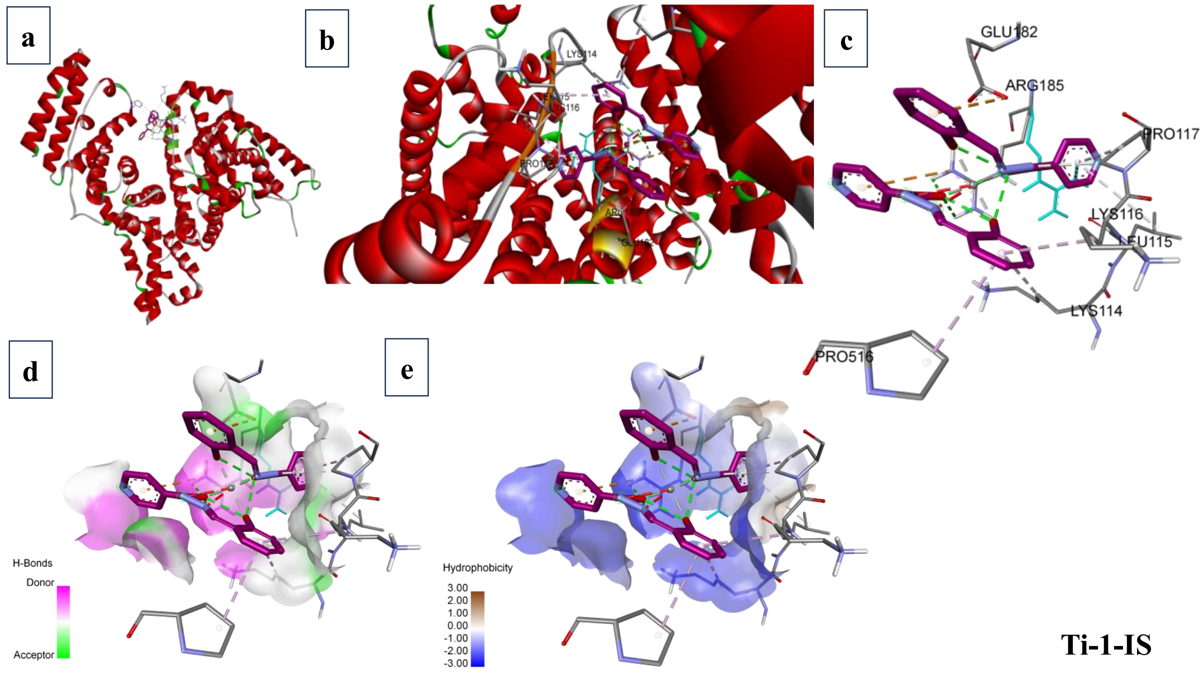

Fig.S85. Molecular docking of BSA with Ti-1-IS purple color indicates carbon atoms, blue color indicates nitrogen, grey color indicates titanium(IV) ion, red color indicates oxygen atoms

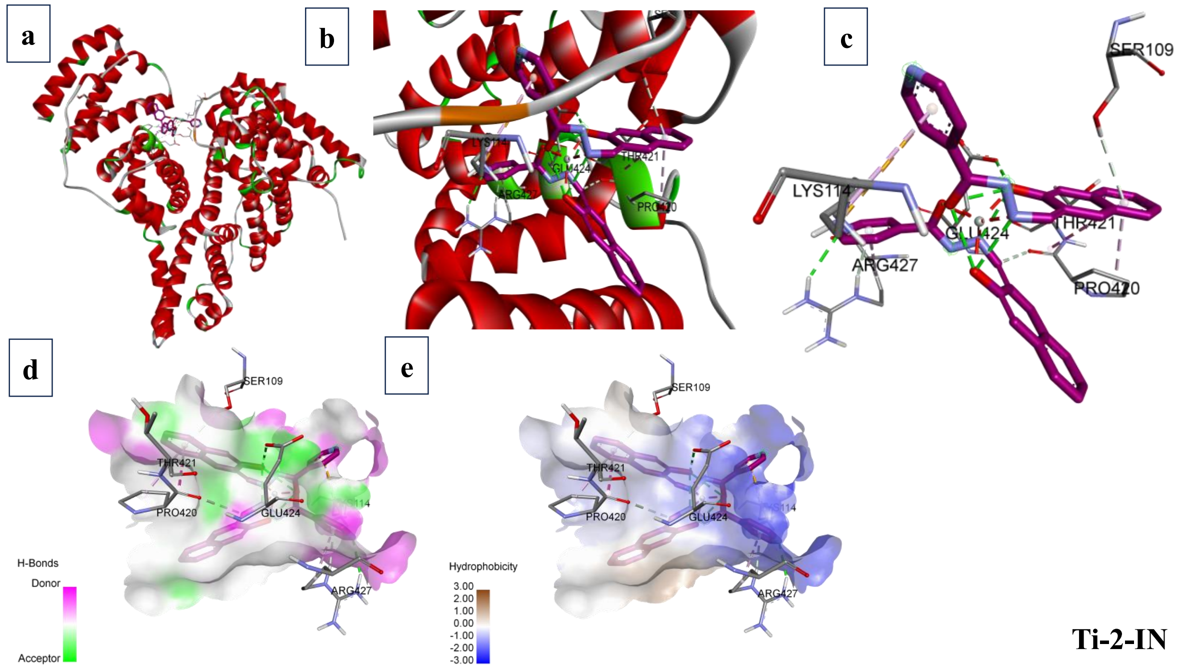

Fig.S86. Molecular docking of BSA with Ti-2-IN purple color indicates carbon atoms, blue color indicates nitrogen, grey color indicates titanium(IV) ion, red color indicates oxygen atoms

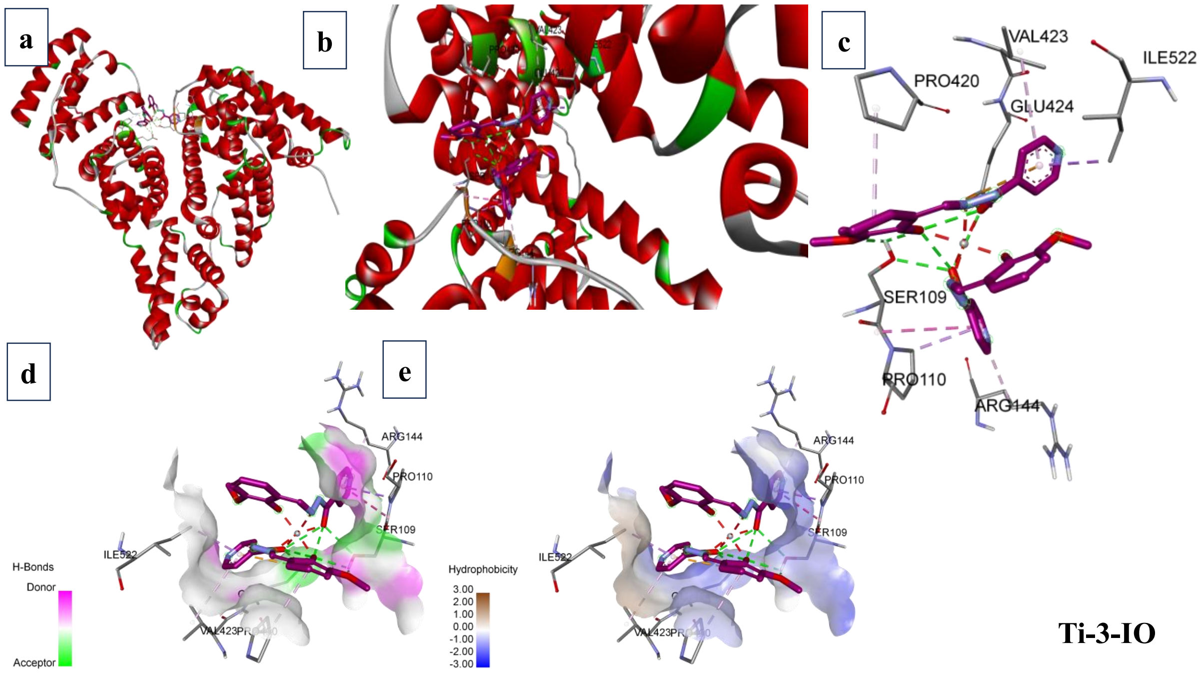

Fig.S87. Molecular docking of BSA with Ti-3-IO purple color indicates carbon atoms, blue color indicates nitrogen, grey color indicates titanium(IV) ion, red color indicates oxygen atoms

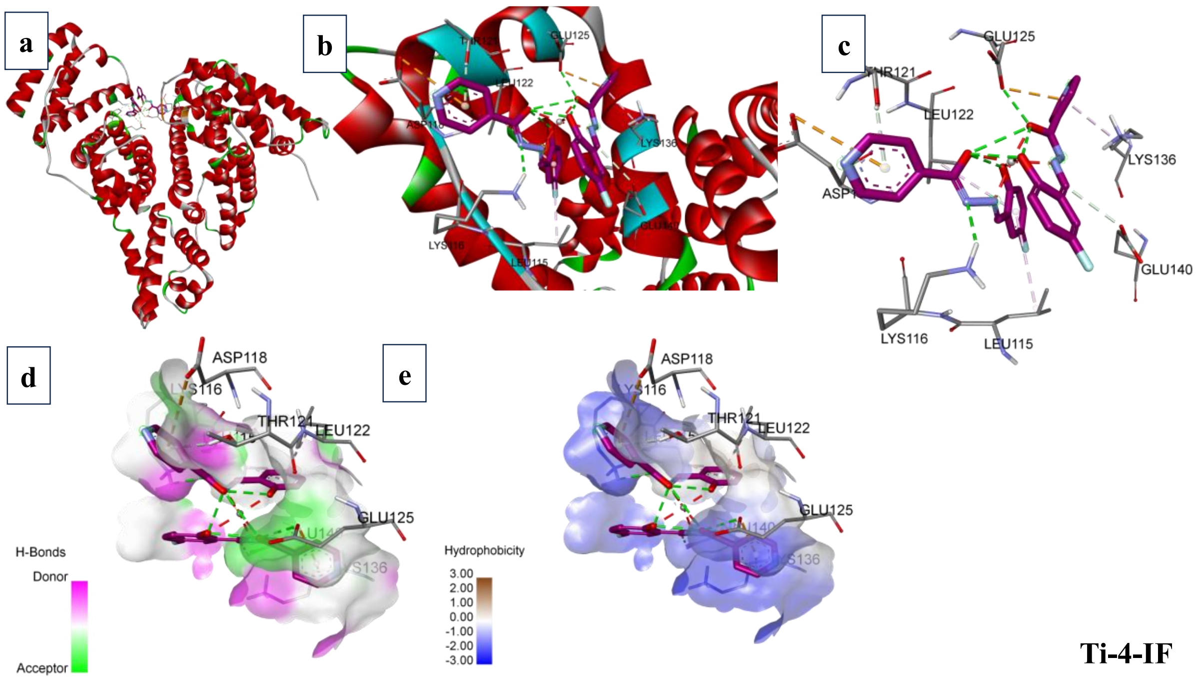

Fig.S88. Molecular docking of BSA with Ti-4-IF purple color indicates carbon atoms, blue color indicates nitrogen, grey color indicates titanium(IV) ion, red color indicates oxygen atoms

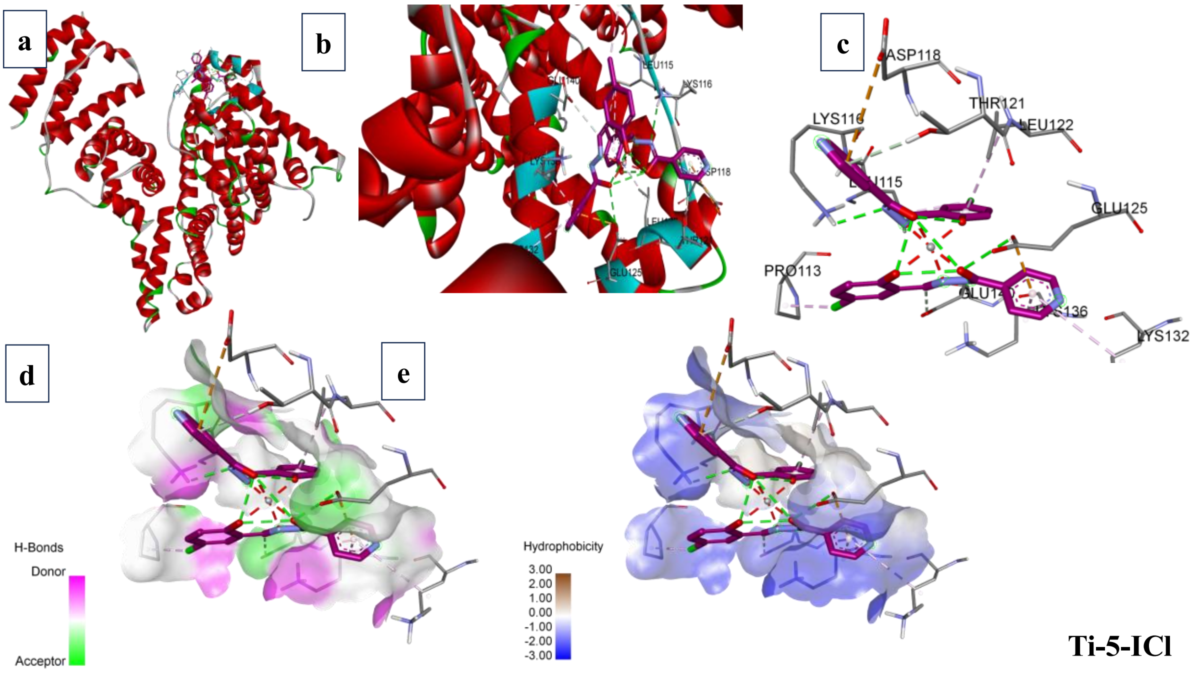

Ti-5-ICl

Fig.S89. Molecular docking of BSA with Ti-5-ICl purple color indicates carbon atoms, blue color indicates nitrogen, grey color indicates titanium(IV) ion, red color indicates oxygen atoms

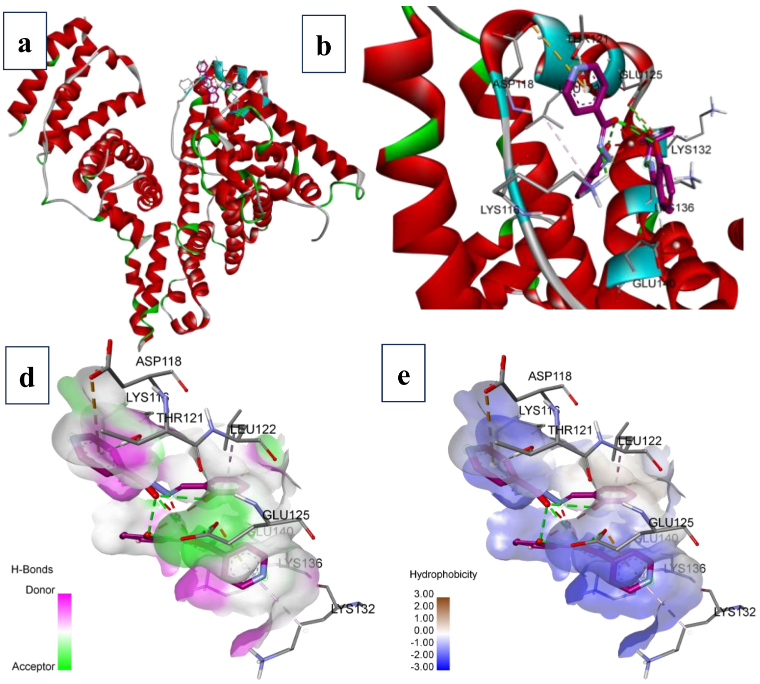

Ti-6-IBr

Fig.S90. Molecular docking of BSA with Ti-6-IBr purple color indicates carbon atoms, blue color indicates nitrogen, grey color indicates titanium(IV) ion, red color indicates oxygen atoms

Table S6; Bond length (Å) of Ti(IV) complexes

S. NO	Code	O-Ti	N-Ti	O-Ti
1	**Ti-1-IS**	1.997	2.886	2.032
2	**Ti-2-IN**	1.997	2.887	2.031
3	**Ti-3-IO**	2.031	2.882	2.032
4	**Ti-4-IF**	1.998	2.885	2.030
5	**Ti-5-ICl**	2.001	2.886	2.031
6	**Ti-6-IBr**	2.000	2.885	2.029

Table S7; Comparison of experimental and theoretical excitation spectral details

Code	Experimental	Theoretical Prediction			
	Abs (nm)	Abs. max (nm)	Oscillator strength (f)	Transition	Orbital Contribution
Ti-1-IS	339	389	0.325	$S_0 \rightarrow S9$	H→L+4 82%, H-3→L 3%,
Ti-2-IN	341	378	0.233	$S_0 \rightarrow S_{10}$	H→L+4 46%, H-3→L 19%,
Ti-3-IO	340	412	0.298	$S_0 \rightarrow S_{12}$	H→L+3 68%, H-3→L 12%,
Ti-4-IF	343	406	0.282	$S_0 \rightarrow S_{10}$	H→L+5 48%, H-4→L 26%,
Ti-5-ICl	345	443	0.316	$S_0 \rightarrow S_{11}$	H→L+3 55%, H→L+4 21%,
Ti-6-IBr	343	625	0.238	$S_0 \rightarrow S_{10}$	H→L+5 78%, H-4→L 6%,

*H – HOMO, L - LUMO

H→L+4 83%, H-4→L+2 4%

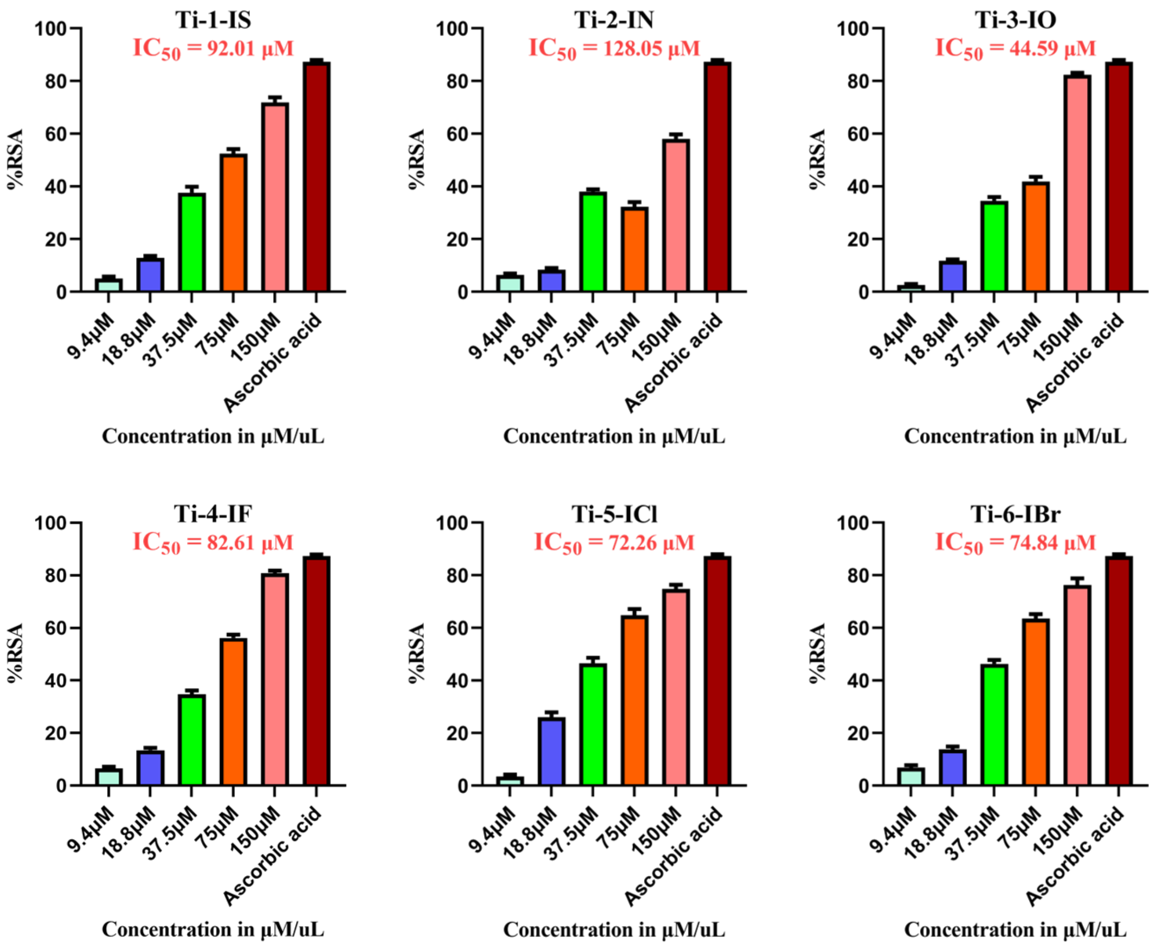

Fig.S91. DPPH assay of Ti(IV) complexes

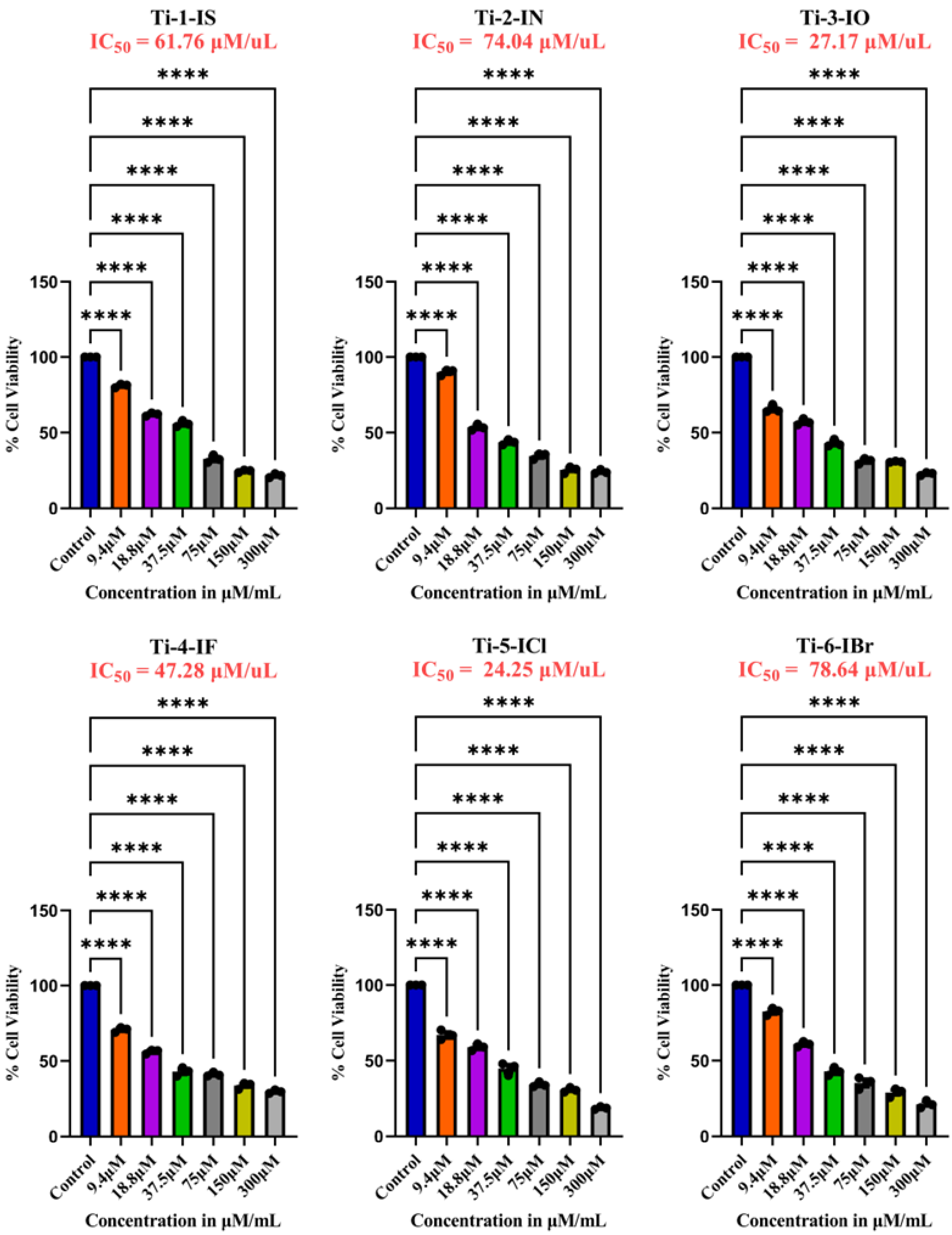

Fig.S92. MTT assay of Ti(IV) complexes on HeLa cell line

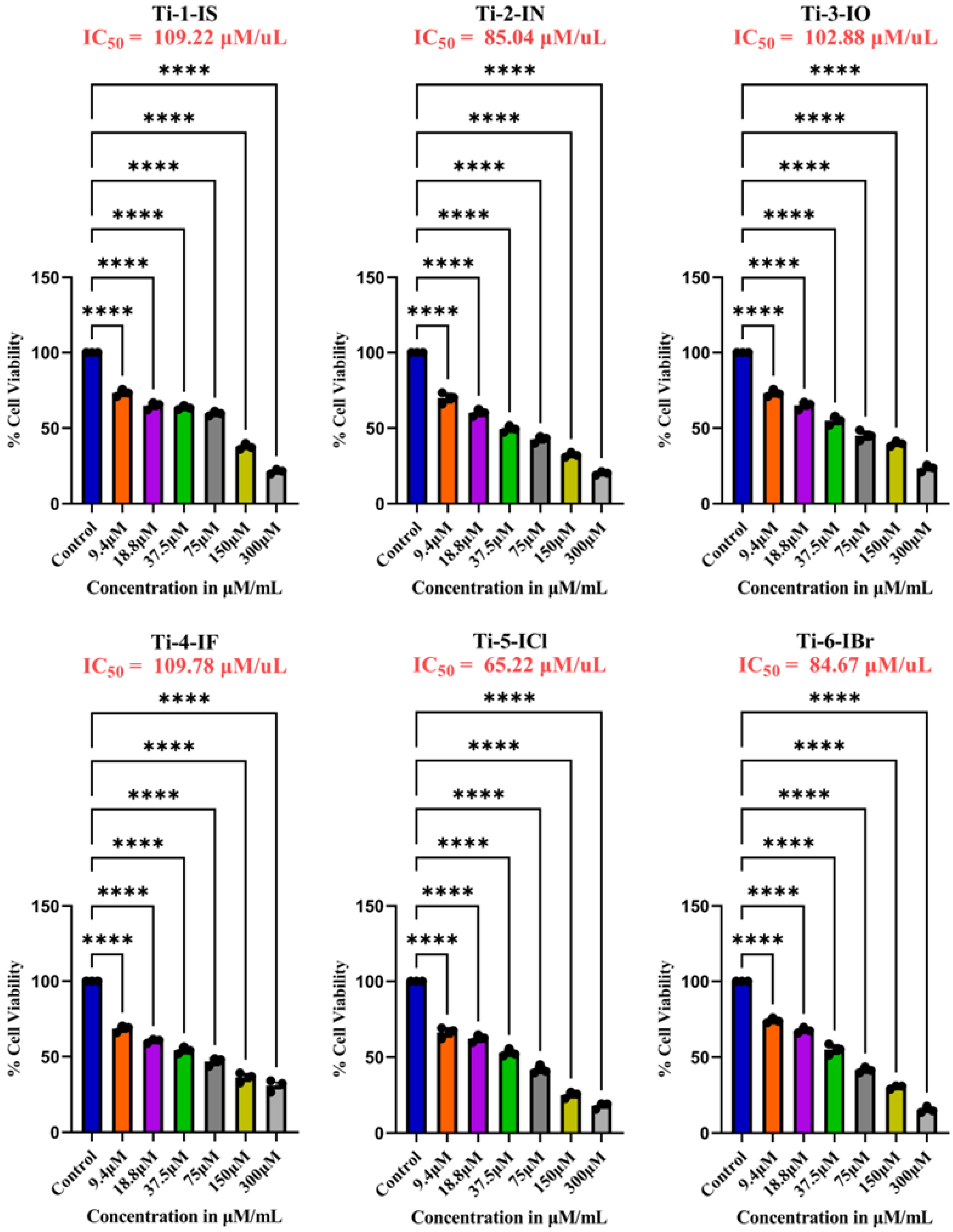

Fig.S93. MTT assay of Ti(IV) complexes on MCF7 cell line

References:

1. Subramaniyan, Mahabarathi, et al. "New bioactive titanium (IV) derivatives with their DFT, molecular docking, DNA/BSA interaction, antioxidant and in-vitro investigations." *Inorganica Chimica Acta* 571 (2024): 122191.
2. Thanigachalam, Sathish, et al. "Bioactive O^ N^ O^ Schiff base appended homoleptic titanium (iv) complexes: DFT, BSA/CT-DNA interactions, molecular docking and antitumor activity against HeLa and A549 cell lines." *RSC advances* 14.19 (2024): 13062-13082.
3. Dorairaj, Dorothy Priyanka, et al. "Ru (II)-p-Cymene complexes of furoylthiourea ligands for anticancer applications against breast cancer cells." *Inorganic Chemistry* 62.30 (2023): 11761-11774.
4. Haribabu, Jebiti, et al. "Michael addition-driven synthesis of cytotoxic palladium (ii) complexes from chromone thiosemicarbazones: investigation of anticancer activity through in vitro and in vivo studies." *New Journal of Chemistry* 47.33 (2023): 15748-15759.
5. Arunachalam, Abirami, et al. "Synthesis and Structure of Naphthoyl Thiourea-Based Binuclear Ruthenium (II) Arene Complexes: Studies on Anticancer Activity and Apoptotic Mechanism." *ChemBioChem*: e202500057.
6. Monika, Sankar, et al. "Binuclear Ruthenium (II) Complexes Featuring Arylthiourea Ligands: Synthesis, Crystal Structure and Anticancer Assessment." *Applied Organometallic Chemistry* 39.5 (2025): e70146.
7. Kar, Binoy, et al. "2-Aryl-1 H-imidazo [4, 5-f][1, 10] phenanthroline-Based Binuclear Ru (II)/Ir (III)/Re (I) Complexes as Mitochondria Targeting Cancer Stem Cell Therapeutic Agents#." *Journal of Medicinal Chemistry* 67.13 (2024): 10928-10945.
8. Das, Utpal, et al. "Exploring the phototoxicity of GSH-resistant 2-(5, 6-dichloro-1 H-benzo [d] imidazol-2-yl) quinoline-based Ir (III)-PTA complexes in MDA-MB-231 cancer cells." *Dalton Transactions* 53.14 (2024): 6459-6471.